

UC Riverside

UC Riverside Electronic Theses and Dissertations

Title

Gauge Extensions of the Standard Model: Uncovering Dark Symmetry and Neutrino Mass Among Extended Structure

Permalink

<https://escholarship.org/uc/item/9wk2v5c7>

Author

Kownacki, Corey

Publication Date

2018

Peer reviewed|Thesis/dissertation

UNIVERSITY OF CALIFORNIA
RIVERSIDE

Gauge Extensions of the Standard Model: Uncovering Dark Symmetry and
Neutrino Mass Among Extended Structure

A Dissertation submitted in partial satisfaction
of the requirements for the degree of

Doctor of Philosophy

in

Physics

by

Corey M Kownacki

December 2018

Dissertation Committee:

Dr. Ernest Ma, Chairperson

Dr. Jose Wudka

Dr. Philip Tanedo

Copyright by
Corey M Kownacki
2018

The Dissertation of Corey M Kownacki is approved:

Committee Chairperson

University of California, Riverside

Acknowledgments

I would first like to thank my advisor, Dr. Ernest Ma, for his inspiring lectures and for providing me with continual project guidance. I would also like to thank Dr. Philip Tanedo for serving as my co-advisor, for his helpful life advice, and for allowing me to ramble at him about machine learning. I thank Dr. Jose Wudka for his careful and conceptual perspective, especially invaluable to me during my first few years of journal club. Thanks again to my committee for taking the time to review my dissertation.

Next, I would like to thank those collaborators that I have worked with previously that were instrumental to my learning: Dr. M. Zakeri, Dr. O. Popov, and Dr. S. Fraser. Thanks also to my friends from Pheno, PiTP, and Riverside. A special thanks to Lydia, not just for tolerating my particle physics memes, but for making happy memories so easy to come by.

This thesis is based on works published previously in collaboration with E. Ma, S. Fraser, O. Popov, M. Zakeri, and N. Pollard.

ABSTRACT OF THE DISSERTATION

Gauge Extensions of the Standard Model: Uncovering Dark Symmetry and Neutrino Mass
Among Extended Structure

by

Corey M Kownacki

Doctor of Philosophy, Graduate Program in Physics
University of California, Riverside, December 2018
Dr. Ernest Ma, Chairperson

Though it appears to describe the world well to at least the electroweak scale, the Standard Model is becoming increasingly inadequate: it can fit fermionic masses but offers no explanation for the observed hierarchy; it provides no mechanism for generating neutrinos mass; and lastly, but perhaps most significantly, it is absent any dark matter candidate. Myriad extensions exist that are able to accommodate these problems individually including the many models that resort to ad hoc symmetries to protect dark matter. Here, extensions are motivated by generalizations of symmetries contained in the Standard Model (such as B-L) or symmetries introduced to enhance Standard Model structure. In the first part we study generalizations of U(1) gauge extensions such as B-L and I3R. For generalized B-L, we allow families to transform differently from one another and study the resulting flavor-changing neutral current constraints. In the next project, to incorporate dark matter to the puzzle, we then implement the scotogenic mechanism to generate neutrino mass via the Type II seesaw with interesting collider signatures coming from the double charged scalar. The next extension is a U(1) family symmetry that is also a dark symmetry, in both cases coupling

exclusively to right-handed objects. We then push to explore Alternative Left-Right models both individually and as low-energy subgroups of the unified trinification and quartification models. We uncover naturally emerging dark symmetries for certain breaking patterns and investigate phenomenological signatures that arise from dark matter and glueball-like states of leptonic color. Obtaining gauge coupling unification at one-loop imposes further constraints on the possible symmetry breaking patterns as well as permissible low-energy particle content.

Contents

List of Figures	x
List of Tables	xi
1 Introduction	1
1.1 The Standard Model of Particle Interactions	1
I U(1) Extensions of Generalized Symmetries	4
2 Generalized Gauge U(1) Family Symmetry for Quarks and Leptons	5
2.1 Introduction	5
2.2 Basic structure of Model A	8
2.3 Scalar sector of Model A	10
2.4 Gauge sector of Model A	11
2.5 Flavor-changing interactions	12
2.6 Lepton sector of Model A	14
2.7 Basic structure of Model B	15
2.8 Lepton sector of Model B	16
2.9 Application to LHC anomalies	17
2.10 Conclusions	17
3 Type II Radiative Seesaw Model of Neutrino Mass with Dark Matter	18
3.1 Introduction	18
3.2 Type II Radiative Seesaw Neutrino Masses	20
3.3 Doubly Charged Higgs Production and Decay	23
3.4 Dark Matter Properties	26
3.5 Conclusions	29
4 Gauge $U(1)$ Dark Symmetry and Radiative Light Fermion Masses	30
4.1 Introduction	30
4.2 New Gauge $U(1)_D$ Symmetry	32
4.3 Radiative Masses for Neutrinos and the First and Second Families	34

4.4	Tree-Level Flavor-Changing Neutral Couplings	36
4.5	Z_D Gauge Boson	37
4.6	Scalar Sector	38
4.7	Relevance to the Diphoton Excess	39
4.8	Dark Matter	41
4.9	Conclusions	41
 II Alternative Left-Right Models Containing Dark Symmetry with Unification		42
5	Dark Gauge U(1) Symmetry for an Alternative Left-Right Model	43
5.1	Introduction	43
5.2	Model	44
5.3	Gauge sector	47
5.4	Fermion sector	49
5.5	Scalar sector	50
5.6	Present phenomenological constraints	52
5.7	Dark sector	53
5.8	Conclusions	58
6	Quartified Leptonic Color, Bound States, and Future Electron-Positron Collider	60
6.1	Introduction	61
6.2	The BMW model	62
6.3	Gauge coupling unification and the leptonic color confinement scale	64
6.4	Thermal history of stickons	65
6.5	Formation and decay of stickballs	66
6.6	Revelation of leptonic color at future e^-e^+ colliders	67
6.7	Conclusions	72
7	Dark Revelations of the $[SU(3)]^3$ and $[SU(3)]^4$	74
7.1	Introduction	75
7.2	Dark Symmetries in $[SU(3)]^3$	76
7.3	Gauge Boson Masses in (B)	81
7.4	Dark Symmetries in $[SU(3)]^4$	82
7.5	Conclusions	85
8	Alternative $[SU(3)]^4$ Model of Leptonic Color and Dark Matter	87
8.1	Introduction	87
8.2	Fermion Content and Dark Symmetry	89
8.3	Symmetry Breaking Pattern	91
8.4	Renormalization-Group Running of Gauge Couplings	92
8.5	Low-Energy Particle Content	96
8.6	Gauge Sector	98

8.7	Scalar Sector	100
8.8	Dark Matter Interactions	102
8.9	Leptonic Color in the Early Universe	103
8.10	Leptonic Color at Future e^-e^+ Colliders	105
8.11	Conclusions	109
9	Conclusions	111
	Bibliography	113

List of Figures

3.1	One-loop Z_2 scotogenic neutrino mass.	20
3.2	LHC Production cross section of $\xi^{++}\xi^{--}$ at 13 TeV.	24
3.3	Number of $e^\pm e^\pm \mu^\mp \mu^\mp 2s_1 2s_1^*$ events for 13 TeV at luminosity 100 fb^{-1}	27
3.4	Allowed values of λ_{12} plotted against m_{s_1} from relic abundance assuming $\lambda_{11} = 0$	28
4.1	One-loop neutrino mass from trilinear couplings.	32
4.2	One-loop neutrino mass from trilinear and quadrilinear couplings.	33
4.3	One-loop electron mass.	33
4.4	One-loop muon mass.	34
4.5	One-loop u quark mass.	35
4.6	One-loop d quark mass.	35
5.1	Relic-abundance constraints on λ_0 and f_0 for $m_\zeta = 150 \text{ GeV}$ and various values of m_{χ_0}	55
6.1	Moose diagram of $[SU(3)]^4$ quartification.	62
8.1	Evolution of α_i^{-1} as a function of energy scale.	94
8.2	Dark scalar annihilation to hemions.	103

List of Tables

1.1	Fermion assignments under the Standard Model	2
2.1	Fermion assignments under $U(1)_F$	6
2.2	Examples of models satisfying Eq. (5).	7
2.3	Two new models satisfying Eq. (5).	8
3.1	Events observed by CMS at 8 TeV with integrated luminosity 19.5 fb^{-1}	25
4.1	Particle content of proposed model of gauge $U(1)$ dark symmetry.	31
5.1	Particle content of proposed model of dark gauge $U(1)$ symmetry.	45
5.2	Particle content of proposed model under $(T_{3R} + S) \times Z_2$	46
6.1	Particle content of proposed model.	63
6.2	Partial decay widths of the hemionium Ω	71
8.1	Particle content of proposed model.	96
8.2	Partial decay widths of the hemionium Ω	108

Chapter 1

Introduction

This thesis is divided into four parts. First, the Standard Model will be briefly introduced. The second part will discuss $U(1)$ extensions of generalized symmetries. The third part will consider more general gauge extensions that link left-right symmetry with dark matter. The final part contains the conclusion and bibliography.

1.1 The Standard Model of Particle Interactions

The Standard Model, at a basic level, is a description of fundamental particles and their interactions under the gauge group $SU(3)_C \times SU(2)_L \times U(1)_Y$. Particles are divided into two categories: the integer-spin, force-carrying particles, called bosons, and half-integer-spin particles called fermions. Based on their interactions, the latter are further divided into quarks and leptons.

$$\textit{Quarks} : (u, d) (c, s) (t, b), \quad \textit{Leptons} : (e, \nu_e) (\mu, \nu_\mu) (\tau, \nu_\tau) \quad (1.1)$$

Quarks and leptons are compactly organized according to their respective transformations under fundamental interactions.

Table 1.1: Fermion assignments under the Standard Model

Particle	$SU(3)_C$	$SU(2)_L$	$U(1)_Y$
$Q_{iL} = (u, d)_{iL}$	3	2	1/6
u_{iR}	3	1	2/3
d_{iR}	3	1	-1/3
$L_{iL} = (\nu, l)_{iL}$	1	2	-1/2
l_{iR}	1	1	-1

In Table 1.1, integers greater than 1 (here 2 and 3, read as "doublet" and "triplet") are a short-hand to describe the representation in which the particles transform under the corresponding gauge group. The remaining numbers signify particles' charge eigenvalues.

The table shows that the electron e_L transforms differently than the electron e_R . In fact, all listed fermions transform differently than their opposite chirality counterparts; they are not the same fermions. They are separate degrees of freedom. This is further apparent since particles of different handedness belong to distinct representations of the Poincare group. Then, in general, they may also belong to unrelated representations of a gauge group.

Though persistent in electroweak gauge interactions, left-right distinctions are blurred when the distinguishing symmetry is spontaneously broken. In the Standard Model

$$SU(3)_C \times SU(2)_L \times U(1)_Y \rightarrow SU(3)_C \times U(1)_Y \quad (1.2)$$

This breaking is induced by the higgs mechanism whereby

$$\phi_0 = (-1/\sqrt{2})(h + iA) \rightarrow \langle \phi_0 \rangle = 246 GeV \quad (1.3)$$

The higgs mixes left and right-handed fermions into physical particles with a mass proportional to the scale of breaking.

$$f_{ij}(\bar{\nu}_{Li}, \bar{l}_{Li}) \phi l_{Rj} + h.c. \quad (1.4)$$

This mass eigenstate of e_L and e_R is the electron.

Examining the Yukawa couplings, there are two important features that deserve attention. First, since the couplings f_{ij} are proportional to the mass, there is a large disparity in magnitudes between the three families. Although nature might simply choose these fine-tuned values arbitrarily, one might instead hope to find a more complete theory that describes such low energy behavior. This fermion mass hierarchy problem is a small motivation for work in the next part of this thesis.

Second, f_{ij} can link any left-handed and right-handed gauge-invariant-product-pair from the three families; there is no reason a priori it should couple diagonally. One can then redefine the fermion fields to be the mass eigenstate fields through appropriate chiral rotations. Regardless, the gauge interaction eigenstates of those fermions is fixed. This discrepancy may lead to flavor-violating currents. Of these, flavor-changing neutral currents are highly constrained in the Standard Model, potentially providing powerful constraints on models that alter the mass generation mechanism.

Part I

U(1) Extensions of Generalized Symmetries

Chapter 2

Generalized Gauge U(1) Family

Symmetry for Quarks and Leptons

If the standard model of quarks and leptons is extended to include three singlet right-handed neutrinos, then the resulting fermion structure admits an infinite number of anomaly-free solutions with just one simple constraint. Well-known examples satisfying this constraint are $B - L$, $L_\mu - L_\tau$, $B - 3L_\tau$, etc. We derive this simple constraint, and discuss two new examples which offer some insights to the structure of mixing among quark and lepton families, together with their possible verification at the Large Hadron Collider.

2.1 Introduction

In the standard model of particle interactions, there are three families of quarks and leptons. Under its $SU(3)_C \times SU(2)_L \times U(1)_Y$ gauge symmetry, singlet right-handed neutrinos ν_R do not transform. They were thus not included in the minimal standard model

which only has three massless left-handed neutrinos. Since neutrinos are now known to be massive, ν_R should be considered as additions to the standard model. In that case, the model admits a possible new family gauge symmetry $U(1)_F$, with charges $n_{1,2,3}$ for the quarks and $n'_{1,2,3}$ for the leptons as shown in Table 1.

Table 2.1: Fermion assignments under $U(1)_F$.

Particle	$SU(3)_C$	$SU(2)_L$	$U(1)_Y$	$U(1)_F$
$Q_{iL} = (u, d)_{iL}$	3	2	1/6	n_i
u_{iR}	3	1	2/3	n_i
d_{iR}	3	1	-1/3	n_i
$L_{iL} = (\nu, l)_{iL}$	1	2	-1/2	n'_i
l_{iR}	1	1	-1	n'_i
ν_{iR}	1	1	0	n'_i

To constrain $n_{1,2,3}$ and $n'_{1,2,3}$, the requirement of gauge anomaly cancellation is imposed. The contributions of color triplets to the $[SU(3)]^2 U(1)_F$ anomaly sum up to

$$[SU(3)]^2 U(1)_F : \frac{1}{2} \sum_{i=1}^3 (2n_i - n_i - n_i); \quad (2.1)$$

and the contributions of $Q_{iL}, u_{iR}, d_{iR}, L_{iL}, l_{iR}$ to the $U(1)_Y [U(1)_F]^2$ anomaly sum up to

$$U(1)_Y [U(1)_F]^2 : \sum_{i=1}^3 \left[6 \left(\frac{1}{6} \right) - 3 \left(\frac{2}{3} \right) - 3 \left(-\frac{1}{3} \right) \right] n_i^2 + \left[2 \left(-\frac{1}{2} \right) - (-1) \right] n_i'^2. \quad (2.2)$$

Both are automatically zero, as well as the $[U(1)_F]^3$ anomaly because all fermions couple to $U(1)_F$ vectorially. The contributions of the $SU(2)_L$ doublets to the $[SU(2)]^2 U(1)_F$ anomaly sum up to

$$[SU(2)]^2 U(1)_F : \frac{1}{2} \sum_{i=1}^3 (3n_i + n'_i); \quad (2.3)$$

and the contributions to the $[U(1)_Y]^2 U(1)_F$ anomaly sum up to

$$\begin{aligned}
[U(1)_Y]^2 U(1)_F & : \sum_{i=1}^3 \left[6 \left(\frac{1}{6} \right)^2 - 3 \left(\frac{2}{3} \right)^2 - 3 \left(-\frac{1}{3} \right)^2 \right] n_i + \left[2 \left(-\frac{1}{2} \right)^2 - (-1)^2 \right] n'_i \\
& = \sum_{i=1}^3 \left(-\frac{3}{2} n_i - \frac{1}{2} n'_i \right). \tag{2.4}
\end{aligned}$$

Both are zero if

$$\sum_{i=1}^3 (3n_i + n'_i) = 0. \tag{2.5}$$

There are many specific examples of models which satisfy this condition as shown in Table 2. If there are four families, then $n_{1,2,3} = 1/3$, $n_4 = -1$, and $n'_{1,2,3} = 1$, $n'_4 = -3$,

Table 2.2: Examples of models satisfying Eq. (5).

n_1	n_2	n_3	n'_1	n'_2	n'_3	Model
1/3	1/3	1/3	-1	-1	-1	$B - L$ [1]
0	0	0	0	1	-1	$L_\mu - L_\tau$ [2, 3, 4, 5]
1/3	1/3	1/3	0	0	-3	$B - 3L_\tau$ [6, 7, 8, 9]
1/3	1/3	1/3	3	-3	-3	Ref. [10]
1	1	-2	1	1	-2	Ref. [11]
a	a	$-2a$	0	-1	1	Ref. [12]

would also satisfy Eq. (5). This may then be considered [13] as the separate gauging of B and L .

In this paper, we discuss two new examples which offer some insights to the structure of mixing among quarks and lepton families. Both have nontrivial connections between quarks and leptons. Their structures are shown in Table 3. In both cases, with only one Higgs doublet with zero charge under $U(1)_F$, quark and lepton mass matrices are diagonal except for the first two quark families. This allows for mixing among them, but not with the third family. It is a good approximation to the 3×3 quark mixing matrix, to the extent

Table 2.3: Two new models satisfying Eq. (5).

n_1	n_2	n_3	n'_1	n'_2	n'_3	Model
1	1	0	0	-2	-4	A
1	1	-1	0	-1	-2	B

that mixing with the third family is known to be suppressed. In the lepton sector, mixing also comes from the Majorana mass matrix of ν_R which depends on the choice of singlets with vacuum expectation values which break $U(1)_F$. Adding a second Higgs doublet with nonzero $U(1)_F$ charge will allow mixing of the first two families of quarks with the third in both cases. As for the leptons, this will not affect Model A, but will cause mixing in the charged-lepton and Dirac neutrino mass matrices in Model B. Flavor-changing neutral currents are predicted, with interesting phenomenological consequences.

2.2 Basic structure of Model A

Consider first the structure of the 3×3 quark mass matrix \mathcal{M}_d linking $(\bar{d}_L, \bar{s}_L, \bar{b}_L)$ to (d_R, s_R, b_R) . Using

$$\Phi_1 = (\phi_1^+, \phi_1^0) \sim (1, 2, 1/2; 0), \quad (2.6)$$

with $\langle \phi_1^0 \rangle = v_1$, it is clear that \mathcal{M}_d is block diagonal with a 2×2 submatrix which may be rotated on the left to become

$$\mathcal{M}_d = \begin{pmatrix} c_L & -s_L & 0 \\ s_L & c_L & 0 \\ 0 & 0 & 1 \end{pmatrix} \begin{pmatrix} m'_d & 0 & 0 \\ 0 & m'_s & 0 \\ 0 & 0 & m'_b \end{pmatrix} \quad (2.7)$$

where $s_L = \sin \theta_L$ and $c_L = \cos \theta_L$. We now add a second Higgs doublet

$$\Phi_2 = (\phi_2^+, \phi_2^0) \sim (1, 2, 1/2; 1), \quad (2.8)$$

with $\langle \phi_2^0 \rangle = v_2$, so that

$$\mathcal{M}_d = \begin{pmatrix} c_L & -s_L & 0 \\ s_L & c_L & 0 \\ 0 & 0 & 1 \end{pmatrix}, \begin{pmatrix} m'_d & 0 & m'_{db} \\ 0 & m'_s & m'_{sb} \\ 0 & 0 & m'_b \end{pmatrix} \quad (2.9)$$

is obtained. At the same time, \mathcal{M}_u is of the form

$$\mathcal{M}_u = \begin{pmatrix} m'_u & 0 & 0 \\ 0 & m'_c & 0 \\ m'_{ut} & m'_{ct} & m'_t \end{pmatrix} \begin{pmatrix} c_R & s_R & 0 \\ -s_R & c_R & 0 \\ 0 & 0 & 1 \end{pmatrix}, \quad (2.10)$$

where it has been rotated on the right. Because of the physical mass hierarchy $m_u \ll m_c \ll m_t$, the diagonalization of Eq. (10) will have very small deviations from unity on the left. Hence the unitary matrix diagonalizing Eq. (9) on the left will be essentially the experimentally observed quark mixing matrix V_{CKM} which has three angles and one phase. Now \mathcal{M}_d of Eq. (9) has exactly seven parameters, the three diagonal masses m'_d, m'_s, m'_b , the angle θ_L , the off-diagonal mass m'_{sb} which can be chosen real, and the off-diagonal mass m'_{db} which is complex. With the input of the three quark mass eigenvalues m_d, m_s, m_b and V_{CKM} , these seven parameters can be determined.

Consider the diagonalization of the real mass matrix

$$\begin{pmatrix} a & 0 & s_1 c \\ 0 & b & s_2 c \\ 0 & 0 & c \end{pmatrix} = V_L \begin{pmatrix} a(1 - s_1^2/2) & 0 & 0 \\ 0 & b(1 - s_2^2/2) & 0 \\ 0 & 0 & c(1 + s_1^2/2 + s_2^2/2) \end{pmatrix} V_R^\dagger, \quad (2.11)$$

where $s_{1,2} \ll 1$ and $a \ll b \ll c$ have been assumed. We obtain

$$V_L = \begin{pmatrix} 1 - s_1^2/2 & -s_1 s_2 b^2 / (b^2 - s_1^2 c^2 - a^2) & s_1 \\ s_1 s_2 a^2 / (b^2 + s_2^2 c^2 - a^2) & 1 - s_2^2/2 & s_2 \\ -s_1 & -s_2 & 1 - s_1^2/2 - s_2^2/2 \end{pmatrix}, \quad (2.12)$$

and

$$V_R^\dagger = \begin{pmatrix} 1 & s_1 s_2 ab / (b^2 - a^2) & -s_1 a/c \\ -s_1 s_2 ab / (b^2 - a^2) & 1 & -s_2 b/c \\ s_1 a/c & s_2 b/c & 1 \end{pmatrix}. \quad (2.13)$$

Hence

$$V_{CKM} = \begin{pmatrix} c_L & -s_L & 0 \\ s_L & c_L & 0 \\ 0 & 0 & 1 \end{pmatrix} \begin{pmatrix} e^{i\alpha} & 0 & 0 \\ 0 & 1 & 0 \\ 0 & 0 & 1 \end{pmatrix} V_L, \quad (2.14)$$

where α is the phase transferred from m'_{db} .

Comparing the above with the known values of V_{CKM} [14], we obtain

$$s_1 = 0.00886, \quad s_2 = 0.0405, \quad s_L = -0.2253, \quad e^{i\alpha} = -0.9215 + i0.3884, \quad (2.15)$$

with $m_d = m'_d$, $m_s = m'_s$, $m_b = m'_b$ to a very good approximation.

2.3 Scalar sector of Model A

In addition to $\Phi_{1,2}$, we add a scalar singlet

$$\sigma \sim (1, 1, 0; 1), \quad (2.16)$$

then the Higgs potential containing $\Phi_{1,2}$ and σ is given by

$$\begin{aligned}
V &= m_1^2 \Phi_1^\dagger \Phi_1 + m_2^2 \Phi_2^\dagger \Phi_2 + m_3^2 \bar{\sigma} \sigma + [\mu \sigma \Phi_2^\dagger \Phi_1 + H.c.] \\
&+ \frac{1}{2} \lambda_1 (\Phi_1^\dagger \Phi_1)^2 + \frac{1}{2} \lambda_2 (\Phi_2^\dagger \Phi_2)^2 + \frac{1}{2} \lambda_3 (\bar{\sigma} \sigma)^2 + \lambda_{12} (\Phi_1^\dagger \Phi_1) (\Phi_2^\dagger \Phi_2) \\
&+ \lambda'_{12} (\Phi_1^\dagger \Phi_2) (\Phi_2^\dagger \Phi_1) + \lambda_{13} (\Phi_1^\dagger \Phi_1) (\bar{\sigma} \sigma) + \lambda_{23} (\Phi_2^\dagger \Phi_2) (\bar{\sigma} \sigma).
\end{aligned} \tag{2.17}$$

Let $\langle \phi_{1,2}^0 \rangle = v_{1,2}$ and $\langle \sigma \rangle = u$, then the minimum of V is determined by

$$0 = v_1(m_1^2 + \lambda_1 v_1^2 + (\lambda_{12} + \lambda'_{12})v_2^2 + \lambda_{13}u^2) + \mu v_2 u, \tag{2.18}$$

$$0 = v_2(m_2^2 + \lambda_2 v_2^2 + (\lambda_{12} + \lambda'_{12})v_1^2 + \lambda_{23}u^2) + \mu v_1 u, \tag{2.19}$$

$$0 = u(m_3^2 + \lambda_3 u^2 + \lambda_{13}v_1^2 + \lambda_{23}v_2^2) + \mu v_1 v_2. \tag{2.20}$$

For m_2^2 large and positive, a solution exists with $v_2^2 \ll v_1^2 \ll u^2$, i.e.

$$u^2 \simeq \frac{-m_3^2}{\lambda_3}, \quad v_1^2 \simeq \frac{-m_1^2 - \lambda_{13}u^2}{\lambda_1}, \quad v_2 \simeq \frac{-\mu v_1 u}{m_2^2 + \lambda_{23}u^2}. \tag{2.21}$$

Hence the scalar particle spectrum of Model A consists of a Higgs boson h very much like that of the SM with $m_h^2 \simeq 2\lambda_1 v_1^2$, a heavy Higgs boson which breaks $U(1)_F$ with $m_\sigma^2 \simeq 2\lambda_3 u^2$, and a heavy scalar doublet very much like Φ_2 with $m^2(\phi_2^+, \phi_2^0) \simeq m_2^2 + \lambda_{23}u^2$.

2.4 Gauge sector of Model A

With the scalar structure already considered, the $Z - Z_F$ mass-squared matrix is given by

$$\mathcal{M}_{Z, Z_F}^2 = \begin{pmatrix} g_Z^2(v_1^2 + v_2^2)/4 & -g_Z g_F v_2^2/2 \\ -g_Z g_F v_2^2/2 & g_F^2(u^2 + v_2^2) \end{pmatrix}. \tag{2.22}$$

The $Z - Z_F$ mixing is then $(g_Z/2g_F)(v_2^2/u^2)$. For $v_2 \sim 10$ GeV and $u \sim 1$ TeV, this is about 10^{-4} , well within the experimentally allowed range.

Since Z_F couples to quarks and leptons according to $n_{1,2,3}$ and $n'_{1,2,3}$, its branching fractions to e^-e^+ and $\mu^-\mu^+$ are given by $2n'_{1,2}{}^2/(12\sum n_i^2+3\sum n_i'^2)$. Since $n'_1=0$, we need consider only the branching fraction $Z_F\rightarrow\mu^-\mu^+$ to compare against data. For Model A, it is about 2/21. The $c_{u,d}$ coefficients used in the experimental search [15, 16] of Z_F are then

$$c_u=c_d=2g_F^2(2/21). \quad (2.23)$$

For $g_F=0.13$, a lower bound of about 4.0 TeV on m_{Z_F} is obtained from the Large Hadron Collider (LHC) based on the preliminary 13 TeV data by comparison with the published data from the 7 and 8 TeV runs. Note however that if $Z_F\rightarrow e^-e^+$ is ever observed, this particular model is ruled out.

2.5 Flavor-changing interactions

Whereas the SM Z boson does not mediate any flavor-changing interactions, the heavy Z_F does because it distinguishes families. For quarks,

$$\mathcal{L}_{Z_F}=g_F Z_F^\mu(\bar{u}'\gamma_\mu u'+\bar{c}'\gamma_\mu c'+\bar{d}'\gamma_\mu d'+\bar{s}'\gamma_\mu s'). \quad (2.24)$$

Using Eqs. (12) and (13) to express the above in terms of mass eigenstates for the d sector, and keeping only the leading flavor-changing terms, we find

$$\mathcal{L}'_{Z_F}=g_F Z_F^\mu[s_1(\bar{d}_L\gamma_\mu b_L+\bar{b}_L\gamma_\mu d_L)+s_2(\bar{s}_L\gamma_\mu b_L+\bar{b}_L\gamma_\mu s_L)-s_1s_2(\bar{d}_L\gamma_\mu s_L+\bar{s}_L\gamma_\mu d_L)]. \quad (2.25)$$

From the experimental values of the $B^0-\bar{B}^0$, $B_S^0-\bar{B}_S^0$, and K_L-K_S mass differences, severe constraints on $g_F^2/m_{Z_F}^2$ are obtained, coming from the operators

$$(\bar{d}_L\gamma_\mu b_L)^2+H.c., \quad (\bar{s}_L\gamma_\mu b_L)^2+H.c., \quad (\bar{d}_L\gamma_\mu s_L)^2+H.c. \quad (2.26)$$

respectively. Using typical values of quark masses and hadronic decay and bag parameters [17], we estimate the various Wilson coefficients to find their contributions as follows:

$$\Delta M_B = 4.5 \times 10^{-2} s_1^2 (g_F^2/m_{Z_F}^2) \text{ GeV}^3, \quad (2.27)$$

$$\Delta M_{B_s} = 6.4 \times 10^{-2} s_2^2 (g_F^2/m_{Z_F}^2) \text{ GeV}^3, \quad (2.28)$$

$$\Delta M_K = 1.9 \times 10^{-3} s_1^2 s_2^2 (g_F^2/m_{Z_F}^2) \text{ GeV}^3. \quad (2.29)$$

Using Eq. (15) and assuming that the above contributions are no more than 10% of their experimental values [14], we find the lower limits on m_{Z_F}/g_F to be 10.2, 9.5, 0.84 TeV respectively. This is easily satisfied for $m_{Z_F} > 4.0$ TeV with $g_F = 0.13$ from the LHC bound discussed in the previous section.

In the scalar sector, since $\Phi_{1,2}$ both contribute to \mathcal{M}_d , the neutral scalar field orthogonal to the SM Higgs field will also mediate flavor-changing interactions. The Yukawa interactions are

$$\mathcal{L}_Y = \frac{h_1}{\sqrt{2}v_1} (m'_d \bar{d}'_L d'_R + m'_s \bar{s}'_L s'_R + m'_b \bar{b}'_L b'_R) + \frac{h_2}{\sqrt{2}v_2} (m'_{db} \bar{d}'_L b'_R + m'_{sb} \bar{s}'_L b'_R). \quad (2.30)$$

Extracting again the leading flavor-changing terms, we obtain

$$\begin{aligned} \mathcal{L}'_Y = & \left(\frac{h_2}{\sqrt{2}v_2} - \frac{h_1}{\sqrt{2}v_1} \right) (s_1 m_b \bar{d}'_L b'_R + s_2 m_b \bar{s}'_L b'_R - s_1 s_2 m_s \bar{d}'_L s'_R - s_1 s_2 m_d \bar{s}'_L d'_R \\ & - s_1 s_2^2 m_d \bar{b}'_L d'_R - s_2^3 m_s \bar{b}'_L s'_R), \end{aligned} \quad (2.31)$$

where the physical scalar $(v_1 h_2 - v_2 h_1)/\sqrt{v_1^2 + v_2^2} = H + iA$ is a complex field, with $m_H \simeq m_A$.

Assuming negligible mixing between H or A with the SM h (identified as the 125

GeV particle observed at the LHC), we consider the following effective operators [18]:

$$\frac{s_1^2 m_b^2}{8v_2^2} \left(\frac{1}{m_H^2} - \frac{1}{m_A^2} \right) (\bar{d}_L b_R)^2 - \frac{s_1^2 s_2^2 m_b m_d}{4v_2^2} \left(\frac{1}{m_H^2} + \frac{1}{m_A^2} \right) (\bar{d}_L b_R)(\bar{d}_R b_L) + H.c. \quad (2.32)$$

$$\frac{s_2^2 m_b^2}{8v_2^2} \left(\frac{1}{m_H^2} - \frac{1}{m_A^2} \right) (\bar{s}_L b_R)^2 - \frac{s_2^4 m_b m_s}{4v_2^2} \left(\frac{1}{m_H^2} + \frac{1}{m_A^2} \right) (\bar{s}_L b_R)(\bar{s}_R b_L) + H.c., \quad (2.33)$$

$$\frac{s_1^2 s_2^2 m_s^2}{8v_2^2} \left(\frac{1}{m_H^2} - \frac{1}{m_A^2} \right) (\bar{d}_L s_R)^2 - \frac{s_1^2 s_2^2 m_s m_d}{4v_2^2} \left(\frac{1}{m_H^2} + \frac{1}{m_A^2} \right) (\bar{d}_L s_R)(\bar{d}_R s_L) + H.c. \quad (2.34)$$

The upper bounds on $(1/v_2^2)[(1/m_H^2) - (1/m_A^2)]$ from $\Delta M_B, \Delta M_{B_s}, \Delta M_K$ are then

$$(4.5 \times 10^{-9}, 5.3 \times 10^{-9}, 4.5 \times 10^{-3}) \text{ GeV}^{-4}, \quad (2.35)$$

respectively, whereas those on $(1/v_2^2)[(1/m_H^2) + (1/m_A^2)]$ are

$$(1.4 \times 10^{-4}, 1.7 \times 10^{-5}, 8.0 \times 10^{-5}) \text{ GeV}^{-4}. \quad (2.36)$$

For $v_2 = 10$ GeV, these are easily satisfied with for example $m_H = 500$ GeV and $m_A = 520$ GeV.

2.6 Lepton sector of Model A

With the chosen $U(1)_F$ charges $(0, -2, -4)$ of Table 3, the charged-lepton and Dirac neutrino mass matrices (\mathcal{M}_l and \mathcal{M}_D) are both diagonal. As for the 3×3 Majorana mass matrix \mathcal{M}_R of ν_R , it depends on the choice of scalar singlets which break $U(1)_F$. We have already used $\sigma \sim 1$ [see Eq. (16)] to induce a small v_2 [see Eq. (21)]. Call that σ_1 and add $\sigma_{2,4} \sim 2, 4$, with vacuum expectation values $u_{1,2,4}$ respectively. Then

$$\mathcal{M}_R = \begin{pmatrix} M_0 & M_1 & M_2 \\ M_1 & M_3 & 0 \\ M_2 & 0 & 0 \end{pmatrix}, \quad (2.37)$$

where M_0 is an allowed invariant mass term, M_1 comes from u_2 , and $M_{2,3}$ from u_4 . The seesaw neutrino mass matrix is then

$$\mathcal{M}_\nu = \mathcal{M}_D \mathcal{M}_R^{-1} \mathcal{M}_D^T = \begin{pmatrix} 0 & 0 & a \\ 0 & b & c \\ a & c & d \end{pmatrix}, \quad (2.38)$$

where the two texture zeros appear because of the form of \mathcal{M}_R and \mathcal{M}_D being diagonal [94]. This form is known to be suitable for a best fit [19] to current neutrino-oscillation data with normal ordering of neutrino masses.

2.7 Basic structure of Model B

The quark structure of Model B is basically the same as that of Model A, with the second Higgs doublet now having two units of $U(1)_F$ charge, i.e.

$$\Phi_2 = (\phi_2^+, \phi_2^0) \sim (1, 2, 1/2; 2). \quad (2.39)$$

Hence $\sigma_2 \sim (1, 1, 0; 2)$ is needed for the $\sigma_2 \Phi_2^\dagger \Phi_1$ term in Eq. (17).

In the gauge sector, again $Z_F \rightarrow e^- e^+$ is zero, and the branching fraction $Z_F \rightarrow \mu^- \mu^+$ is now $2/51$. The $c_{u,d}$ coefficients are then

$$c_u = c_d = 2g_F^2(2/51). \quad (2.40)$$

For the same choice of $g_F = 0.13$ for Model A, the present experimental lower bound from LHC data is reduced from 4.0 TeV to 3.7 TeV. For quarks,

$$\mathcal{L}_{Z_F} = g_F Z_F^\mu (\bar{u}' \gamma_\mu u' + \bar{c}' \gamma_\mu c' - \bar{t}' \gamma_\mu t' + \bar{d}' \gamma_\mu d' + \bar{s}' \gamma_\mu s' - \bar{b}' \gamma_\mu b'). \quad (2.41)$$

Using Eqs. (12) and (13) to express the above in terms of mass eigenstates for the d sector, and keeping only the leading flavor-changing terms, we find

$$\mathcal{L}'_{ZF} = 2g_F Z_F^\mu [-s_1(\bar{d}_L \gamma_\mu b_L + \bar{b}_L \gamma_\mu d_L) - s_2(\bar{s}_L \gamma_\mu b_L + \bar{b}_L \gamma_\mu s_L) + s_1 s_2(\bar{d}_L \gamma_\mu s_L + \bar{s}_L \gamma_\mu d_L)]. \quad (2.42)$$

This differs from Eq. (25) only by an overall factor of -2 . As for the scalar sector, Eqs. (30) and (31) remain the same.

2.8 Lepton sector of Model B

With the chosen $U(1)_F$ charges $(0, -1, -2)$ of Table 3, the charged-lepton and Dirac neutrino mass matrices are given by

$$\mathcal{M}_l = \begin{pmatrix} m'_e & 0 & m'_{e\tau} \\ 0 & m'_\mu & 0 \\ 0 & 0 & m'_\tau \end{pmatrix}, \quad \mathcal{M}_D = \begin{pmatrix} m'_1 & 0 & 0 \\ 0 & m'_2 & 0 \\ m'_{31} & 0 & m'_3 \end{pmatrix}. \quad (2.43)$$

Using the scalar singlets $\sigma_1 \sim 1$ as well σ_2 , the ν_R Majorana mass matrix is again given by Eq. (37). Now even though \mathcal{M}_D is not diagonal, Eq. (38) is still obtained, thereby guaranteeing a best fit to current neutrino-oscillation data. The difference from Model A is the presence of $\tau - e$ transitions from the nondiagonal \mathcal{M}_l . However, for $m'_{e\tau}/m'_\tau < 0.1$, the branching fraction of $\tau \rightarrow e\mu^- \mu^+$ is less than 2×10^{-11} , far below the current bound of 4.1×10^{-8} .

2.9 Application to LHC anomalies

Whereas Z_F also mediates $b \rightarrow s\mu^-\mu^+$, its effect is too small in Models A and B to explain the tentative LHC observations of $B \rightarrow K^*\mu^-\mu^+$ and the ratio of $B^+ \rightarrow K^+\mu^-\mu^+$ to $B^+ \rightarrow K^+e^-e^+$ [20]. The reason is the stringent bound on m_{Z_F} from LHC data as a function of g_F through the parameters $c_{u,d}$ of Eqs. (23) and (40). Suppose we take $n_{1,2,3} = (0, 0, 1)$ and $n'_{1,2,3} = (0, -3, 0)$, then Z_F couples to only $\mu^-\mu^+$ and $b'\bar{b}'$, thus allowing for $b - s$ mixing, but $c_{u,d} = 0$. This evades the direct LHC bound, and may be used to explain the B anomalies if they persist. Of course, Eqs. (27) to (29) still hold, and a full analysis of the detailed structure of $B \rightarrow K^*\mu^-\mu^+$ will be required.

2.10 Conclusions

We have generalized the $B - L$ symmetry as a gauge $U(1)_F$ extension of the standard model, where quarks and leptons of each family may transform differently. We have considered two new examples (A and B), each with two Higgs doublets and restricted quark mass matrices consistent with data. The new Z_F gauge boson couples differently to each quark and lepton family, and is constrained by present data to be heavier than about 4 TeV if $g_F = 0.13$. Future data may reveal just such a Z_F belonging to this class of models. Flavor-changing interactions are suitably suppressed by the assignments of quarks and leptons under $U(1)_F$. In the leptonic sector, with the addition of a minimal set of Higgs singlets, a Majorana neutrino mass matrix of two texture zeros may be obtained, leading to a best fit of neutrino-oscillation data with normal ordering of neutrino masses.

Chapter 3

Type II Radiative Seesaw Model of Neutrino Mass with Dark Matter

We consider a model of neutrino mass with a scalar triplet (ξ^{++}, ξ^+, ξ^0) assigned lepton number $L = 0$, so that the tree-level Yukawa coupling $\xi^0 \nu_i \nu_j$ is not allowed. It is generated instead through the interaction of ξ and ν with dark matter and the soft breaking of L to $(-1)^L$. We discuss the phenomenological implications of this model, including ξ^{++} decay and the prognosis of discovering the dark sector at the Large Hadron Collider.

3.1 Introduction

Nonzero neutrino mass is necessary to explain the well-established phenomenon of neutrino oscillations in many experiments. Theoretically, neutrino masses are usually assumed to be Majorana and come from physics at an energy scale higher than that of electroweak symmetry breaking of order 100 GeV. As such, the starting point of any theo-

retical discussion of the underlying theory of neutrino mass is the effective dimension-five operator [21]

$$\mathcal{L}_5 = -\frac{f_{ij}}{2\Lambda}(\nu_i\phi^0 - l_i\phi^+)(\nu_j\phi^0 - l_j\phi^+) + H.c., \quad (3.1)$$

where $(\nu_i, l_i), i = 1, 2, 3$ are the three left-handed lepton doublets of the standard model (SM) and (ϕ^+, ϕ^0) is the one Higgs scalar doublet. As ϕ^0 acquires a nonzero vacuum expectation value $\langle\phi^0\rangle = v$, the neutrino mass matrix is given by

$$\mathcal{M}_{ij}^\nu = \frac{f_{ij}v^2}{\Lambda}. \quad (3.2)$$

Note that \mathcal{L}_5 breaks lepton number L by two units.

It is evident from Eq. (2) that neutrino mass is seesaw in character, because it is inversely proportional to the large effective scale Λ . The three well-known tree-level seesaw realizations [22] of \mathcal{L}_5 may be categorized by the specific heavy particle used to obtain it: (I) neutral fermion singlet N , (II) scalar triplet (ξ^{++}, ξ^+, ξ^0) , (III) fermion triplet $(\Sigma^+, \Sigma^0, \Sigma^-)$. It is also possible to realize \mathcal{L}_5 radiatively in one loop [22] with the particles in the loop belonging to the dark sector, the lightest neutral one being the dark matter of the Universe. The simplest such example [23] is the well-studied ‘‘scotogenic’’ model, from the Greek ‘scotos’ meaning darkness. The one-loop diagram is shown in Fig. 1. The new particles are a second scalar doublet (η^+, η^0) and three neutral singlet fermions N_R . The dark Z_2 is odd for (η^+, η^0) and N_R , whereas all SM particles are even. This is thus a Type I radiative seesaw model. It is of course possible to replace N with Σ^0 , so it becomes a Type III radiative seesaw model [24]. What then about Type II?

Since \mathcal{L}_5 is a dimension-five operator, any loop realization is guaranteed to be finite. On the other hand, if a Higgs triplet (ξ^{++}, ξ^+, ξ^0) is added to the SM, a dimension-

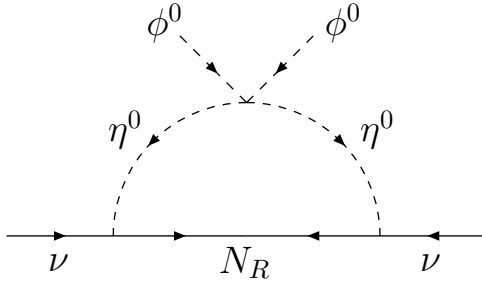


Figure 3.1: One-loop Z_2 scotogenic neutrino mass.

four coupling $\xi^0 \nu_i \nu_j - \xi^+ (\nu_i l_j + l_i \nu_j) / \sqrt{2} + \xi^{++} l_i l_j$ is allowed. As ξ^0 obtains a small vacuum expectation value [7] from its interaction with the SM Higgs doublet, neutrinos acquire small Majorana masses, i.e. Type II tree-level seesaw. If an exact symmetry is used to forbid this dimension-four coupling, it will also forbid any possible loop realization of it. Hence a Type II radiative seesaw is only possible if the symmetry used to forbid the hard dimension-four coupling is softly broken in the loop, as recently proposed [25].

3.2 Type II Radiative Seesaw Neutrino Masses

The symmetry used to forbid the hard $\xi^0 \nu \nu$ coupling is lepton number $U(1)_L$ under which $\xi \sim 0$. The scalar trilinear $\bar{\xi}^0 \phi^0 \phi^0$ term is allowed and induces a small $\langle \xi^0 \rangle$, but ν remains massless. To connect ξ^0 to $\nu \nu$ in one loop, we add a new Dirac fermion doublet (N, E) with $L = 0$, together with three complex neutral scalar singlets s with $L = 1$. The resulting one-loop diagram is shown in Fig. 2. Note that the hard terms $\xi^0 N N$ and $s \bar{\nu}_L N_R$ are allowed by L conservation, whereas the ss terms break L softly by two units to $(-1)^L$. A dark Z_2 parity, i.e. $(-1)^{L+2j}$, exists under which N, E, s are odd and ν, l, ξ are even. Hence

the lightest s is a possible dark-matter candidate. The three s scalars are the analogs of the three right-handed sneutrinos in supersymmetry, and $(N, E)_{L,R}$ are the analogs of the two higgsinos. However, their interactions are simpler here and less constrained.

The usual understanding of the Type II seesaw mechanism is that the scalar trilinear term $\mu\xi^\dagger\Phi\Phi$ induces a small vacuum expectation value $\langle\xi^0\rangle = u$ if either μ is small or m_ξ is large or both. More precisely, consider the scalar potential of Φ and ξ .

$$\begin{aligned}
V &= m^2\Phi^\dagger\Phi + M^2\xi^\dagger\xi + \frac{1}{2}\lambda_1(\Phi^\dagger\Phi)^2 + \frac{1}{2}\lambda_2(\xi^\dagger\xi)^2 + \lambda_3|2\xi^{++}\xi^0 - \xi^+\xi^+|^2 \\
&+ \lambda_4(\Phi^\dagger\Phi)(\xi^\dagger\xi) + \frac{1}{2}\lambda_5[|\sqrt{2}\xi^{++}\phi^- + \xi^+\bar{\phi}^0|^2 + |\xi^+\phi^- + \sqrt{2}\xi^0\bar{\phi}^0|^2] \\
&+ \mu(\xi^0\phi^0\phi^0 + \sqrt{2}\xi^-\phi^0\phi^+ + \xi^{--}\phi^+\phi^+) + H.c.
\end{aligned} \tag{3.3}$$

Let $\langle\phi^0\rangle = v$, then the conditions for the minimum of V are given by [7]

$$m^2 + \lambda_1v^2 + (\lambda_4 + \lambda_5)u^2 + 2\mu u = 0, \tag{3.4}$$

$$u[M^2 + \lambda_2u^2 + (\lambda_4 + \lambda_5)v^2] + \mu v^2 = 0. \tag{3.5}$$

For $\mu \neq 0$ but small, u is also naturally small because it is approximately given by

$$u \simeq \frac{-\mu v^2}{M^2 + (\lambda_4 + \lambda_5)v^2}, \tag{3.6}$$

where $v^2 \simeq -m^2/\lambda_1$. The physical masses of the $L = 0$ Higgs triplet are then given by

$$m^2(\xi^0) \simeq M^2 + (\lambda_4 + \lambda_5)v^2, \tag{3.7}$$

$$m^2(\xi^+) \simeq M^2 + (\lambda_4 + \frac{1}{2}\lambda_5)v^2, \tag{3.8}$$

$$m^2(\xi^{++}) \simeq M^2 + \lambda_4v^2. \tag{3.9}$$

Since the hard term $\xi^0\nu\nu$ is forbidden, u by itself does not generate a neutrino mass. Its value does not have to be extremely small compared to the electroweak breaking scale. For

example $u \sim 0.1$ GeV is acceptable, because its contribution to the precisely measured ρ parameter $\rho_0 = 1.00040 \pm 0.00024$ [26] is only of order 10^{-6} . With the soft breaking of L to $(-1)^L$ shown in Fig. 2, Type II radiative seesaw neutrino masses are obtained. Let the relevant Yukawa interactions be given by

$$\mathcal{L}_Y = f_s s \bar{\nu}_L N_R + \frac{1}{2} f_R \xi^0 N_R N_R + \frac{1}{2} f_L \xi^0 N_L N_L + H.c., \quad (3.10)$$

together with the allowed mass terms $m_E(\bar{N}N + \bar{E}E)$, $m_s^2 s^* s$, and the L breaking soft term $(1/2)(\Delta m_s^2) s^2 + H.c.$, then

$$m_\nu = \frac{f_s^2 u r x}{16\pi^2} [f_R F_R(x) + f_L F_L(x)], \quad (3.11)$$

where $r = \Delta m_s^2 / m_s^2$ and $x = m_s^2 / m_E^2$, with

$$F_R(x) = \frac{1+x}{(1-x)^2} + \frac{2x \ln x}{(1-x)^3}, \quad (3.12)$$

$$F_L(x) = \frac{2}{(1-x)^2} + \frac{(1+x) \ln x}{(1-x)^3}. \quad (3.13)$$

Using for example $x \sim f_R \sim f_L \sim 0.1$, $r \sim f_s \sim 0.01$, we obtain $m_\nu \sim 0.1$ eV for $u \sim 0.1$ GeV. This implies that ξ may be as light as a few hundred GeV and be observable, with $\mu \sim 1$ GeV. For $f_s \sim 0.01$ and m_E a few hundred GeV, the new contributions to the anomalous muon magnetic moment and $\mu \rightarrow e\gamma$ are negligible in this model.

In the case of three neutrinos, there are of course three s scalars. Assuming that the L breaking soft terms $|(\Delta m_s^2)_{ij}| \ll |m_{s_i}^2 - m_{s_j}^2|$ for $i \neq j$, then the 3×3 neutrino mass matrix is diagonal to a very good approximation in the basis where the s mass-squared matrix is diagonal. This means that the dark scalars s_j couples to $U_{ij} l_i$, where U_{ij} is the neutrino mixing matrix linking e, μ, τ to the neutrino mass eigenstates $\nu_{1,2,3}$.

3.3 Doubly Charged Higgs Production and Decay

The salient feature of any Type II seesaw model is the doubly charged Higgs boson ξ^{++} . If there is a tree-level $\xi^{++}l_i^-l_j^-$ coupling, then the dominant decay of ξ^{++} is to $l_i^+l_j^+$. Current experimental limits [46] on the mass of ξ^{++} into $e\mu$, $\mu\mu$, and ee final states are about 490 to 550 GeV, assuming for each a 100% branching fraction. In the present model, since the effective $\xi^{++}l_i^-l_j^-$ coupling is one-loop suppressed, $\xi^{++} \rightarrow W^+W^+$ should be considered [28] instead, for which the present limit on $m(\xi^{++})$ is only about 84 GeV [29]. A dedicated search of the W^+W^+ mode in the future is clearly called for.

If $m(\xi^{++}) > 2m_E$, then the decay channel $\xi^{++} \rightarrow E^+E^+$ opens up and will dominate. In that case, the subsequent decay $E^+ \rightarrow l^+s$, i.e. charged lepton plus missing energy, will be the signature. The present experimental limit [60] on m_E , assuming electroweak pair production, is about 260 GeV if $m_s < 100$ GeV for a 100% branching fraction to e or μ , and no limit if $m_s > 100$ GeV. There is also a lower threshold for ξ^{++} decay, i.e. $m(\xi^{++})$ sufficiently greater than $2m_s$, for which ξ^{++} decays through a virtual E^+E^+ pair to ssl^+l^+ , resulting in same-sign dileptons plus missing energy.

In Fig. 3 we plot the pair production cross section of $\xi^{++}\xi^{--}$ at the Large Hadron Collider (LHC) at a center-of-mass energy of 13 TeV. We assume that ξ^+ and ξ^0 are heavier than ξ^{++} so that we can focus only on the decay products of $\xi^{\pm\pm}$. The $W^\pm W^\pm$ mode is always possible and should be looked for experimentally in any case. However, as already noted, a much more interesting possibility is the case $m(\xi^{++}) > 2m_E$, with the subsequent decay $E^+ \rightarrow l^+s$. This would yield four charged leptons plus missing energy, and depending on the linear combination of charged leptons coupling to s , there could be exotic final

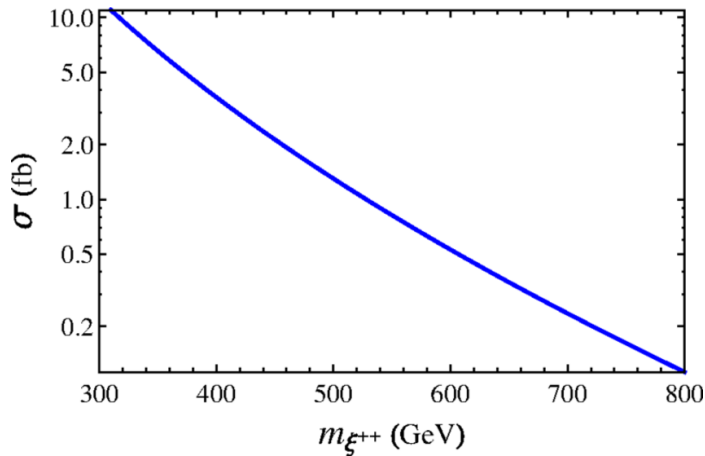


Figure 3.2: LHC Production cross section of $\xi^{++}\xi^{--}$ at 13 TeV.

states which have very little SM background, becoming thus excellent signatures to search for. Suppose s_1 is the lightest scalar, and $s_{2,3}$ are heavier than E^+ , then E^+ decays to $s_1 \sum U_{i1} l_i^+$. Hence the decay of $\xi^{++}\xi^{--}$ could yield for example $e^+e^+\mu^-\mu^-$ plus four s_1 (missing energy) in the final state.

Recent LHC searches for multilepton signatures at 8 TeV by CMS [31] and ATLAS [32] are consistent with SM expectations, and are potential restrictions on our model. In particular, the CMS study includes rare SM events such as $e^+e^+\mu^-\mu^-$ and $e^+e^+\mu^-$. Due to the absence of opposite-sign, same-flavor (OSSF) l^+l^- pairs, both events are classified as OSSF0 where lepton l refers to electron, muon, or hadronically decaying tau. Leptonic tau decays contribute to the electron and muon counts, and this determines the OSSF n category. Details from CMS are shown in Table 1 for ≥ 3 leptons and $N_{\tau\text{had}} = 0$. The CMS study estimates a negligible SM background for SR1-SR3, and in our simulation we use the

Selected CMS results OSSFO $N_{\tau\text{had}} = 0$, $N_b = 0$					
signal regions		$H_T > 200$ GeV		$H_T < 200$ GeV	
≥ 4 leptons	\cancel{E}_T (GeV)	Obs.	Exp.(SM)	Obs.	Exp.(SM)
SR1	(100, ∞)	0	$0.01^{+0.03}_{-0.01}$	0	$0.11^{+0.08}_{-0.08}$
SR2	(50, 100)	0	$0.00^{+0.02}_{-0.00}$	0	$0.01^{+0.03}_{-0.01}$
SR3	(0, 50)	0	$0.00^{+0.02}_{-0.00}$	0	$0.01^{+0.02}_{-0.01}$
3 leptons	\cancel{E}_T (GeV)	Obs.	Exp.(SM)	Obs.	Exp.(SM)
SR4	(100, ∞)	5	3.7 ± 1.6	7	11.0 ± 4.9
SR5	(50, 100)	3	3.5 ± 1.4	35	38 ± 15
SR6	(0, 50)	4	2.1 ± 0.8	53	51 ± 11

Table 3.1: Events observed by CMS at 8 TeV with integrated luminosity 19.5 fb^{-1} .

same selection criteria. We impose the cuts on transverse momentum $p_T > 10$ GeV and pseudorapidity $|\eta| < 2.4$ for each charged lepton, with at least one lepton $p_T > 20$ GeV. In order to be isolated, each lepton with p_T must satisfy $\sum_i p_{Ti} < 0.15p_T$, where the sum is over all objects within a cone of radius $\Delta R = 0.3$ around the lepton direction.

We implement our model with FeynRules 2.0 [33]. Using the CTEQ6L1 parton distribution functions, we generate events using MadGraph5 [34], which includes the Pythia package for hadronization and showering. MadAnalysis [35] is then used with the Delphes card designed for CMS detector simulation. Generated events initially have 4 leptons. About half are detected as 3 lepton events, but the constraints from signal regions SR4-SR6 are less restrictive than SR1-SR3. The number of detected events in the OSSFO ≥ 4 lepton category is almost the same as $e^\pm e^\pm \mu^\mp \mu^\mp 2s_1 2s_1^*$ with very few additional leptons from showering or initial/final state radiation.

To examine the production of $e^\pm e^\pm \mu^\mp \mu^\mp$ we take the mass of s_1 to be 130 GeV, which allows s_1 to be dark matter as discussed in the next section. We use the values $f_R = f_L = 0.1$ and $f_s = 0.01$, although the results are not sensitive to the exact values due

to on-shell production and decay. The effects due to $u \sim 0.1$ GeV may be neglected.

For our model, we scan the mass range of ξ^{++} and E^+ . In Fig. 4 we plot contours showing the expected number of detected events in the OSSFO ≥ 4 lepton category for 13 TeV at luminosity 100 fb^{-1} assuming a negligible background as for the 8 TeV case. Although the branching fractions of E^+ to $\tau^+ s_1$ or $\mu^+ s_1$ are comparable, we find that most of the contributions from τ^\pm decay to e^\pm or μ^\pm in the ≥ 4 lepton final state are not detected. A similar analysis performed for 8 TeV at 19.5 fb^{-1} has a maximum number of detected events of 0.4 in the plot analogous to Fig. 4, which corresponds to a small estimated exclusion at the 15% confidence level.

3.4 Dark Matter Properties

The lightest s , say s_1 , is dark matter. Its interaction with leptons is too weak to provide a large enough annihilation cross section to explain the present dark matter relic density Ω_M of the Universe. However, it also interacts with the SM Higgs boson through the usual quartic coupling $\lambda_s s^* s \Phi^\dagger \Phi$. For a value of λ_s consistent with Ω_M , the direct-detection cross section in underground experiments is determined as a function of m_s . A recent analysis [36] for a real s claims that the resulting allowed parameter space is limited to a small region near $m_s < m_h/2$.

In our model, we can evade this constraint by evoking $s_{2,3}$. The mass-squared matrix spanning $s_i^* s_j$ is given by

$$(\mathcal{M}_s^2)_{ij} = m_{ij}^2 + \lambda_{ij} v^2, \quad (3.14)$$

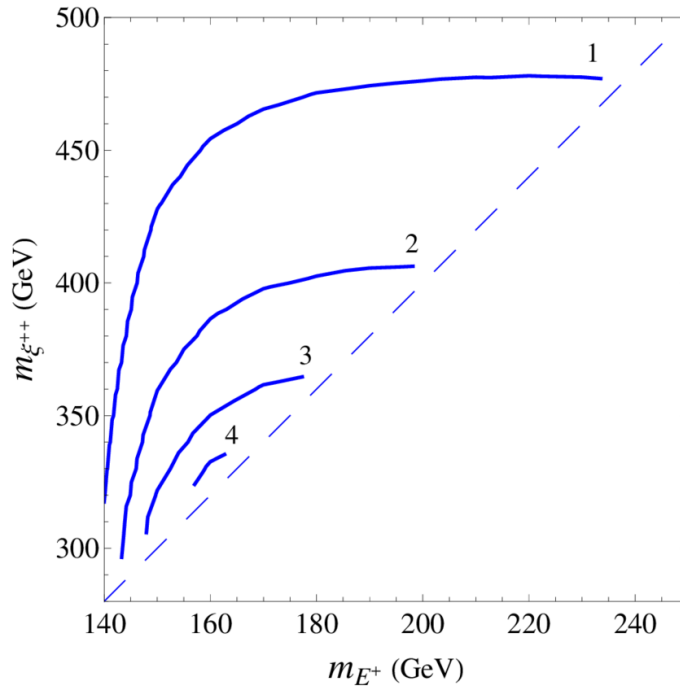


Figure 3.3: Number of $e^\pm e^\pm \mu^\mp \mu^\mp 2s_1 2s_1^*$ events for 13 TeV at luminosity 100 fb^{-1} .

whereas the coupling matrix of the one Higgs h to $s_i^* s_j$ is $\lambda_{ij} v \sqrt{2}$. Upon diagonalizing \mathcal{M}_s^2 , the coupling matrix will not be diagonal in general. In the physical basis, s_1 will interact with s_2 through h . This allows the annihilation of $s_1 s_1^*$ to hh through s_2 exchange, and contributes to Ω_M without affecting the s_1 scattering cross section off nuclei through h . This mechanism restores s_1 as a dark-matter candidate for $m_s > m_h$.

To demonstrate the scale of the values involved, we consider the simplifying case when $m_{s_2} = m_{s_3}$ and $\lambda_{12} = \lambda_{13}$. The additional choice $m_{s_{2,3}}^2 = m_{s_1}^2 + m_h^2$ ensures that

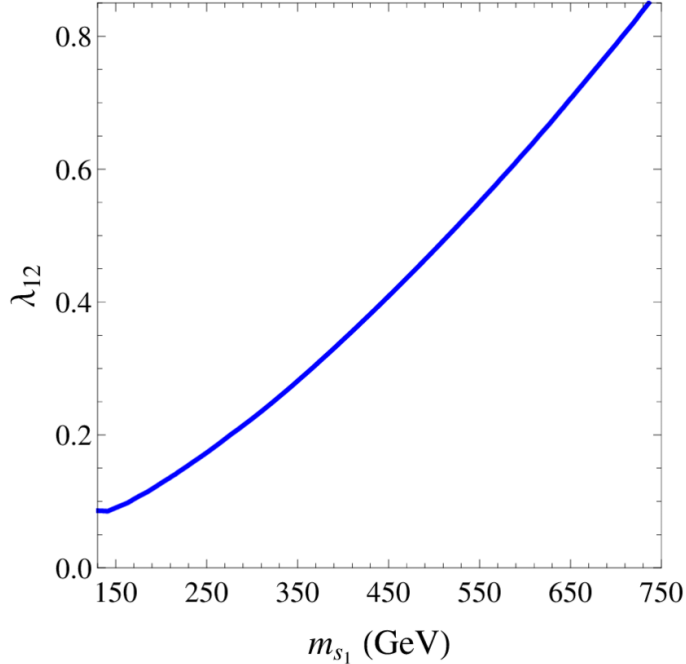


Figure 3.4: Allowed values of λ_{12} plotted against m_{s_1} from relic abundance assuming $\lambda_{11} = 0$.

$s_{2,3}$ are heavier than s_1 , and is convenient because then the relic abundance requirement no longer depends explicitly on $m_{s_{2,3}}^2$. Taking into account that s_1 is a complex scalar, we use $\sigma \times v_{rel} = 4.4 \times 10^{-26} \text{cm}^3 \text{s}^{-1}$ [37] and in Fig. 5 we plot the allowed values for λ_{12} and m_{s_1} taking $\lambda_{11} = 0$ for simplicity to satisfy the LUX data.

Another possible scenario is to add a light scalar χ with $L = 0$, which acts as a mediator for s self-interactions. This has important astrophysical implications [38, 39, 40, 41, 42, 43]. In this case, $s_1 s_1^*$ annihilating to $\chi\chi$ becomes possible.

3.5 Conclusions

We have studied a new radiative Type II seesaw model of neutrino mass with dark matter [25], which predicts a doubly charged Higgs boson ξ^{++} with suppressed decay to l^+l^+ , thereby evading the present LHC bounds of 490 to 550 GeV on its mass. In this model, ξ^{++} may decay to two charged heavy fermions E^+E^+ , each with odd dark parity. The subsequent decay of E^+ is into a charged lepton l^+ and a scalar s which is dark matter. Hence there is the interesting possibility of four charged leptons, such as $\mu^-\mu^-e^+e^+$, plus large missing energy in the final state. We show that the LHC at 13 TeV will be able to probe such a doubly charged Higgs boson with a mass of the order 400 to 500 GeV.

Chapter 4

Gauge $U(1)$ Dark Symmetry and Radiative Light Fermion Masses

A gauge $U(1)$ family symmetry is proposed, spanning the quarks and leptons as well as particles of the dark sector. The breaking of $U(1)$ to Z_2 divides the two sectors and generates one-loop radiative masses for the first two families of quarks and leptons, as well as all three neutrinos. We study the phenomenological implications of this new connection between family symmetry and dark matter. In particular, a scalar or pseudoscalar particle associated with this $U(1)$ breaking may be identified with the 750 GeV diphoton resonance recently observed at the Large Hadron Collider (LHC).

4.1 Introduction

In any extension of the standard model (SM) of particle interactions to include dark matter, a symmetry is usually assumed, which distinguishes quarks and leptons from

dark matter. For example, the simplest choice is Z_2 under which particles of the dark sector are odd and those of the visible sector are even. Suppose Z_2 is promoted to a gauge $U(1)$ symmetry, then the usual assumption is that it will not affect ordinary matter. These models all have a dark vector boson which couples only to particles of the dark sector.

Table 4.1: Particle content of proposed model of gauge $U(1)$ dark symmetry.

particles	$SU(3)_C$	$SU(2)_L$	$U(1)_Y$	$U(1)_D$	Z_2
$Q = (u, d)$	3	2	1/6	0, 0, 0	+
u^c	3^*	1	-2/3	1, -1, 0	+
d^c	3^*	1	1/3	-1, 1, 0	+
$L = (\nu, e)$	1	2	-1/2	0, 0, 0	+
e^c	1	1	1	-1, 1, 0	+
$\Phi = (\phi^+, \phi^0)$	1	2	1/2	0	+
σ_1	1	1	0	1	+
σ_2	1	1	0	2	+
N, N^c	1	1	0	1/2, -1/2	-
S, S^c	1	1	0	-3/2, 3/2	-
(η^0, η^-)	1	2	-1/2	1/2	-
χ^0	1	1	0	1/2	-
χ^-	1	1	-1	-1/2	-
$(\xi^{2/3}, \xi^{-1/3})$	3	2	1/6	1/2	-
$\zeta^{2/3}$	3	1	2/3	-1/2	-
$\zeta^{-1/3}$	3	1	-1/3	-1/2	-

In this paper, it is proposed instead that a gauge $U(1)$ extension of the SM spans both ordinary and dark matter. It is in fact also a horizontal family symmetry. It has a number of interesting consequences, including the radiative mass generation of the first two families of quarks and leptons, and a natural explanation of the 750 GeV diphoton resonance recently observed [44, 16] at the Large Hadron Collider (LHC).

4.2 New Gauge $U(1)_D$ Symmetry

The framework that radiative fermion masses and dark matter are related has been considered previously [45]. Here it is further proposed that families are distinguished by the connecting dark symmetry. In Table 1 we show how they transform under $U(1)_D$ as well as the other particles of the dark sector. The $U(1)_D$ symmetry is broken spontaneously by the vacuum expectation value $\langle \sigma_{1,2} \rangle = u_{1,2}$ to an exactly conserved Z_2 which divides the two sectors.

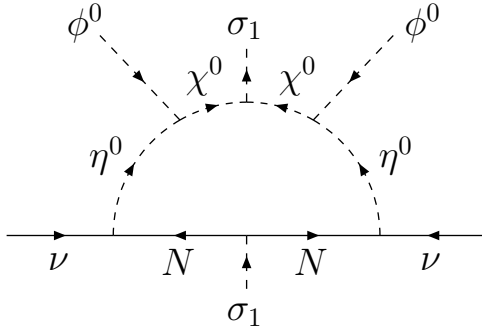


Figure 4.1: One-loop neutrino mass from trilinear couplings.

The gauge $U(1)_D$ symmetry is almost absent of axial-vector anomalies for each family. The $[SU(3)]^2 U(1)_D$ anomaly is zero from the cancellation between u^c and d^c . The $[SU(2)]^2 U(1)_D$ anomaly is zero because Q and L do not transform under $U(1)_D$. The $[U(1)_Y]^2 U(1)_D$ and $U(1)_Y [U(1)_D]^2$ anomalies are cancelled among u^c , d^c , and e^c , i.e.

$$3 \left(-\frac{2}{3} \right)^2 (1) + 3 \left(\frac{1}{3} \right)^2 (-1) + (1)^2 (-1) = 0, \quad (4.1)$$

$$3 \left(-\frac{2}{3} \right) (1)^2 + 3 \left(\frac{1}{3} \right) (-1)^2 + (1)(-1)^2 = 0. \quad (4.2)$$

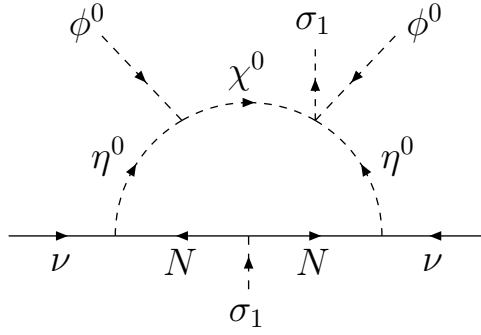


Figure 4.2: One-loop neutrino mass from trilinear and quadrilinear couplings.

The $[U(1)_D]^3$ anomaly is not zero for either the first or second family, but is cancelled between the two. This is thus a generalization of the well-known anomaly-free $L_e - L_\mu$ gauge symmetry [2] to the difference of $B - L - 2Y$ between the first two families.

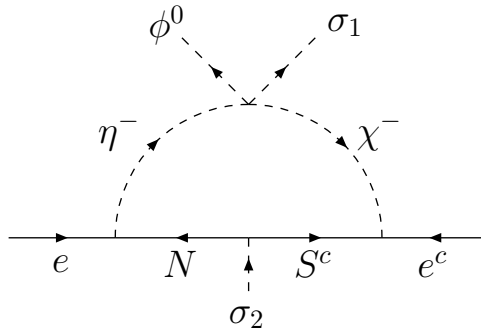


Figure 4.3: One-loop electron mass.

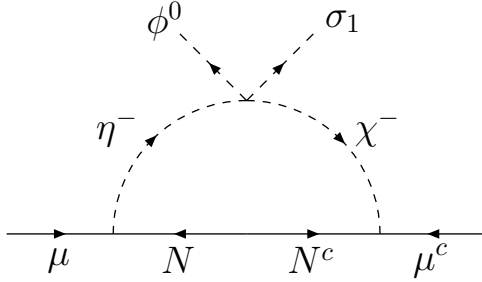


Figure 4.4: One-loop muon mass.

4.3 Radiative Masses for Neutrinos and the First and Second Families

At tree level, only t, b, τ acquire masses from $\langle \phi^0 \rangle = v$ as in the SM. The first two families are massless because of the $U(1)_D$ symmetry. Neutrinos acquire one-loop masses through the scotogenic mechanism [23] as shown in Figs. 1 and 2. With one copy of (N, N^c) , only one neutrino becomes massive. To have three massive scotogenic neutrinos, three copies of (N, N^c) are needed. The one-loop electron and muon masses are shown in Figs. 3 and 4. Note that at least two copies of (N, N^c) are needed for two charged-lepton masses. The mass matrix spanning (N, N^c, S, S^c) is of the form

$$\mathcal{M}_{N,S} = \begin{pmatrix} f_1 u_1 & m_N & f_3 u_1 & f_5 u_2 \\ m_N & f_2 u_1 & f_6 u_2 & f_4 u_1 \\ f_3 u_1 & f_6 u_2 & 0 & m_S \\ f_5 u_2 & f_4 u_1 & m_S & 0 \end{pmatrix}. \quad (4.3)$$

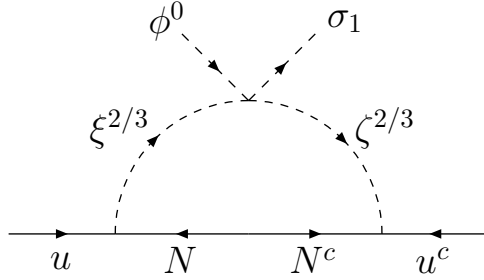


Figure 4.5: One-loop u quark mass.

Note that the $f_{1,2,3,4}u_1$ terms break lepton number by two units, whereas the $f_{5,6}u_2$ terms do not. Lepton number $L = 1$ may be assigned to e, μ, τ, N, S and $L = -1$ to $e^c, \mu^c, \tau^c, N^c, S^c$.

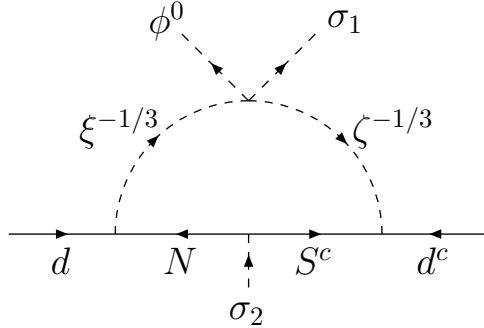


Figure 4.6: One-loop d quark mass.

It is broken down to lepton parity $(-1)^L$ only by neutrino masses. The analogous one-loop u and d quark masses are shown in Figs. 5 and 6. Because the second family has opposite $U(1)_D$ charge assignments relative to the first, the c and s quarks reverse the roles of u and d . Two copies of (S, S^c) are needed to obtain the most general quark mass matrices for both the u and d sectors.

To evaluate the one-loop diagrams of Figs. 1 to 6, we note first that each is a sum of simple diagrams with one internal fermion line and one internal scalar line. Each contribution is infinite, but the sum is finite. There are 10 neutral Majorana fermion fields, spanning 3 copies of N, N^c and 2 copies of S, S^c . We denote their mass eigenstates as ψ_k with mass M_k . There are 4 real scalar fields, spanning $\sqrt{2}Re(\eta^0)$, $\sqrt{2}Im(\eta^0)$, $\sqrt{2}Re(\chi^0)$, $\sqrt{2}Im(\chi^0)$. We denote their mass eigenstates as ρ_l^0 with mass m_l . In Figs. 1 and 2, let the $\nu_i\psi_k\bar{\eta}^0$ coupling be h_{ik}^ν , then the radiative neutrino mass matrix is given by [23]

$$(\mathcal{M}_\nu)_{ij} = \sum_k \frac{h_{ik}^\nu h_{jk}^\nu M_k}{16\pi^2} \sum_l [(y_l^R)^2 F(x_{lk}) - (y_l^I)^2 F(x_{lk})], \quad (4.4)$$

where $\sqrt{2}Re(\eta^0) = \sum_l y_l^R \rho_l^0$, $\sqrt{2}Im(\eta^0) = \sum_l y_l^I \rho_l^0$, with $\sum_l (y_l^R)^2 = \sum_l (y_l^I)^2 = 1$, $x_{lk} = m_l^2/M_k^2$, and the function F is given by

$$F(x) = \frac{x \ln x}{x-1}. \quad (4.5)$$

There are two charged scalar fields, spanning η^\pm, χ^\pm . We denote their mass eigenstates as ρ_r^\pm with mass m_r . In Fig. 3, let the $e_L\psi_k\eta^+$ and the $e_L^c\psi_k\chi^-$ couplings be h_k^e and $h_k^{e^c}$, then

$$m_e = \sum_k \frac{h_k^e h_k^{e^c} M_k}{16\pi^2} \sum_r y_r^\eta y_r^\chi F(x_{rk}), \quad (4.6)$$

where $\eta^+ = \sum_r y_r^\eta \rho_r^+$, $\chi^+ = \sum_r y_r^\chi \rho_r^+$, with $\sum_r (y_r^\eta)^2 = \sum_r (y_r^\chi)^2 = 1$ and $\sum_r y_r^\eta y_r^\chi = 0$. A similar expression is obtained for m_μ , as well as the light quark masses.

4.4 Tree-Level Flavor-Changing Neutral Couplings

Since different $U(1)_D$ charges are assigned to (u^c, c^c, t^c) as well as (d^c, s^c, b^c) , there are unavoidable flavor-changing neutral currents. They can be minimized by the following

assumptions. Let the two 3×3 quark mass matrices linking (u, c, t) to (u^c, c^c, t^c) and (d, s, b) to (d^c, s^c, b^c) be of the form

$$\mathcal{M}_u = U_L^{(u)} \begin{pmatrix} m_u & 0 & 0 \\ 0 & m_c & 0 \\ 0 & 0 & m_t \end{pmatrix}, \quad \mathcal{M}_d = U_L^{(d)} \begin{pmatrix} m_d & 0 & 0 \\ 0 & m_s & 0 \\ 0 & 0 & m_b \end{pmatrix}, \quad (4.7)$$

where $U_{CKM} = (U_L^{(u)})^\dagger U_L^{(d)}$ is the quark charged-current mixing matrix. However, since Z_D does not couple to left-handed quarks, and its couplings to right-handed quarks have been chosen to be diagonal in their mass eigenstates, flavor-changing neutral currents are absent in this sector. Of course, they will appear in the scalar sector, and further phenomenological constraints on its parameters will apply.

4.5 Z_D Gauge Boson

As $\sigma_{1,2}$ acquire vacuum expectation values $u_{1,2}$ respectively, the Z_D gauge boson obtains a mass given by

$$m_{Z_D}^2 = 2g_D^2(u_1^2 + 4u_2^2). \quad (4.8)$$

Since $\sigma_{1,2}$ do not transform under the SM, and Φ does not under $U(1)_D$, there is no mixing between Z_D and Z . Using Table 1 and assuming that all new particles are lighter than Z_D , the branching fraction of Z_D to $e^-e^+ + \mu^-\mu^+$ is estimated to be 0.07. The $c_{u,d}$ coefficients used in the experimental search [46, 60] of Z_D are then

$$c_u = c_d = g_D^2 (0.07). \quad (4.9)$$

For $g_D = 0.3$, a lower bound of about 3.1 TeV on m_{Z_D} is obtained from LHC data based on the 7 and 8 GeV runs. For our subsequent discussion, let $u_1 = 1$ TeV, $u_2 = 4$ TeV, then

$m_{Z_D} = 3.4$ TeV. Note that Z_D does not couple to the third family, so if $\bar{t}t$, $\bar{b}b$, or $\tau^+\tau^-$ final states are observed, this model is ruled out.

4.6 Scalar Sector

There are three scalars with integral charges under $U(1)_D$, i.e. Φ and $\sigma_{1,2}$. Whereas $\langle\phi^0\rangle = v$ breaks the electroweak $SU(2)_L \times U(1)_Y$ gauge symmetry as in the SM, $\langle\sigma_{1,2}\rangle = u_{1,2}$ break $U(1)_D$ to Z_2 , with all those particles with half-integral $U(1)_D$ charges becoming odd under this exactly conserved dark Z_2 parity. The relevant scalar potential is given by

$$\begin{aligned}
V &= \mu_0^2 \Phi^\dagger \Phi + m_1^2 \sigma_1^* \sigma_1 + m_2^2 \sigma_2^* \sigma_2 + m_{12} \sigma_1^2 \sigma_2^* + m_{12} (\sigma_1^*)^2 \sigma_2 \\
&+ \frac{1}{2} \lambda_0 (\Phi^\dagger \Phi)^2 + \frac{1}{2} \lambda_1 (\sigma_1^* \sigma_1)^2 + \frac{1}{2} \lambda_2 (\sigma_2^* \sigma_2)^2 + \lambda_3 (\sigma_1^* \sigma_1) (\sigma_2^* \sigma_2) \\
&+ \lambda_4 (\Phi^\dagger \Phi) (\sigma_1^* \sigma_1) + \lambda_5 (\Phi^\dagger \Phi) (\sigma_2^* \sigma_2),
\end{aligned} \tag{4.10}$$

where m_{12} has been rendered real by absorbing the relative phase between $\sigma_{1,2}$. The conditions for v and $u_{1,2}$ are

$$0 = \mu_0^2 + \lambda_0 v^2 + \lambda_4 u_1^2 + \lambda_5 u_2^2, \tag{4.11}$$

$$0 = m_1^2 + \lambda_1 u_1^2 + \lambda_3 u_2^2 + \lambda_4 v^2 + 2m_{12} u_2, \tag{4.12}$$

$$0 = m_2^2 + \lambda_2 u_2^2 + \lambda_3 u_1^2 + \lambda_5 v^2 + m_{12} u_1^2 / u_2. \tag{4.13}$$

As in the SM, ϕ^\pm and $\sqrt{2}Im(\phi^0)$ become longitudinal components of W^\pm and Z , and $\sqrt{2}Re(\phi^0) = h$ is the one physical Higgs boson associated with electroweak symmetry breaking. Let $\sigma_1 = (\sigma_{1R} + i\sigma_{1I})/\sqrt{2}$ and $\sigma_2 = (\sigma_{2R} + i\sigma_{2I})/\sqrt{2}$, then the mass-squared

matrix spanning $h, \sigma_{1R,2R}$ is

$$\mathcal{M}_R^2 = \begin{pmatrix} 2\lambda_0 v^2 & 2\lambda_4 v u_1 & 2\lambda_5 v u_2 \\ 2\lambda_4 v u_1 & 2\lambda_1 u_1^2 & 2\lambda_3 u_1 u_2 + 2m_{12} u_1 \\ 2\lambda_5 v u_2 & 2\lambda_3 u_1 u_2 + 2m_{12} u_1 & 2\lambda_2 u_2^2 - m_{12} u_1^2 / u_2 \end{pmatrix}, \quad (4.14)$$

and that spanning $\sigma_{1I,2I}$ is

$$\mathcal{M}_I^2 = \begin{pmatrix} -4m_{12} u_2 & 2m_{12} u_1 \\ 2m_{12} u_1 & -m_{12} u_1^2 / u_2 \end{pmatrix}. \quad (4.15)$$

The linear combination $(u_1 \sigma_{1I} + 2u_2 \sigma_{2I}) / \sqrt{u_1^2 + 4u_2^2}$ has zero mass and becomes the longitudinal component of the massive Z_D gauge boson. The orthogonal component is a pseudoscalar, call it A , with a mass given by $m_A^2 = -m_{12}(u_1^2 + 4u_2^2)/u_2$. In Eq. (14), σ_{1R} and σ_{2R} mix in general. For simplicity, let $m_{12} = -\lambda_3 u_2$, then for $v^2 \ll u_{1,2}^2$, we obtain

$$m_{\sigma_{1R}}^2 = 2\lambda_1 u_1^2, \quad m_{\sigma_{2R}}^2 = 2\lambda_2 u_2^2 + \lambda_3 u_1^2, \quad m_A^2 = \lambda_3 (u_1^2 + 4u_2^2), \quad (4.16)$$

$$m_h^2 = 2 \left[\lambda_0 - \frac{\lambda_4^2}{\lambda_1} - \frac{2\lambda_5^2 u_2^2}{2\lambda_2 u_2^2 + \lambda_3 u_1^2} \right] v^2. \quad (4.17)$$

4.7 Relevance to the Diphoton Excess

Any one of the three particles $\sigma_{1R}, \sigma_{2R}, A$ may be identified with the 750 GeV diphoton excess. For illustration, let us consider σ_{1R} . The production cross section through gluon fusion is given by

$$\hat{\sigma}(gg \rightarrow \sigma_{1R}) = \frac{\pi^2}{8m_{\sigma_{1R}}^2} \Gamma(\sigma_{1R} \rightarrow gg) \delta(\hat{s} - m_{\sigma_{1R}}^2). \quad (4.18)$$

For the LHC at 13 TeV, the diphoton cross section is roughly [48]

$$\sigma(gg \rightarrow \sigma_{1R} \rightarrow \gamma\gamma) \simeq (100 \text{ pb}) \times (\lambda_g \text{ TeV})^2 \times B(\sigma_{1R} \rightarrow \gamma\gamma), \quad (4.19)$$

where λ_g is the effective coupling of σ_{1R} to two gluons, normalized by

$$\Gamma(\sigma_{1R} \rightarrow gg) = \frac{\lambda_g^2}{8\pi} m_{\sigma_{1R}}^3, \quad (4.20)$$

and the corresponding λ_γ comes from

$$\Gamma(\sigma_{1R} \rightarrow \gamma\gamma) = \frac{\lambda_\gamma^2}{64\pi} m_{\sigma_{1R}}^3. \quad (4.21)$$

If σ_{1R} decays only to two gluons and two photons, and assuming $\lambda_\gamma^2/8 \ll \lambda_g^2$, then

$$\sigma(gg \rightarrow \sigma_{1R} \rightarrow \gamma\gamma) \simeq (100 \text{ pb}) \times (\lambda_\gamma \text{ TeV})^2/8, \quad (4.22)$$

which is supposed to be about 6.2 fb from the recent data [44, 16]. This means that $\lambda_\gamma \simeq 2.2 \times 10^{-2} (\text{TeV})^{-1}$, and $\Gamma(\sigma_{1R} \rightarrow \gamma\gamma) \simeq 1 \text{ MeV}$.

Now σ_{1R} couples to the new scalars $\xi^{2/3}, \xi^{-1/3}, \zeta^{2/3}, \zeta^{-1/3}, \eta^-, \chi^-$ through $\sqrt{2}u_1$ multiplied by the individual quartic scalar couplings. For simplicity, let all these couplings be the same, say λ_σ , and all the masses be the same, say m_0 , then [49]

$$\lambda_\gamma = \frac{\alpha u_1 \lambda_\sigma}{\sqrt{2}\pi m_{\sigma_{1R}}^2} \left[6 \left(\frac{2}{3} \right)^2 + 6 \left(-\frac{1}{3} \right)^2 + 2(-1)^2 \right] f \left(\frac{m_0^2}{m_{\sigma_{1R}}^2} \right), \quad (4.23)$$

where the function f is given by

$$f(x) = 8x \left[\arctan \left(\frac{1}{\sqrt{4x-1}} \right) \right]^2 - 2. \quad (4.24)$$

Let $m_0 = 700 \text{ GeV}$, then $x = 0.87$ and $f = 1.23$. Hence for $u_1 = 1 \text{ TeV}$ and $\lambda_\sigma = 1.1$, the required $\lambda_\gamma \simeq 0.022 (\text{TeV})^{-1}$ is obtained. For this λ_σ , we find $\lambda_g = 0.128$, hence $\Gamma(\sigma_{1R} \rightarrow gg) \simeq 0.27 \text{ GeV}$, which is below the energy resolution of ATLAS and CMS. This narrow width is not favored by the ATLAS data, but cannot be ruled out at this time.

4.8 Dark Matter

The lightest neutral particle with odd Z_2 is a good dark-matter candidate. In this model, it could be the lightest scalar particle in the sector consisting of $\eta^0 = (\eta_R + i\eta_I)/\sqrt{2}$ and $\chi^0 = (\chi_R + i\chi_I)/\sqrt{2}$. There are two sectors, the mass-squared matrix spanning η_R, χ_R is given by

$$\mathcal{M}_R^2 = \begin{pmatrix} m_\eta^2 & A \\ A & m_\chi^2 + C \end{pmatrix}, \quad (4.25)$$

and that spanning η_I, χ_I is

$$\mathcal{M}_I^2 = \begin{pmatrix} m_\eta^2 & B \\ B & m_\chi^2 - C \end{pmatrix}, \quad (4.26)$$

where A, B come from the $\phi^0\eta^0(\chi^0)^*$ and $\phi^0\eta^0\chi^0(\sigma_1)^*$ couplings and C from the $\chi^0\chi^0(\sigma_1)^*$ coupling. The phenomenology of the lightest particle in this group is similar to that of the so-called inert Higgs doublet model [23, 50, 51]. For details, see for example recent updates [52, 53, 54].

4.9 Conclusions

A new idea linking family symmetry to dark symmetry is proposed using a gauge $U(1)_D$ symmetry, which breaks to exactly conserved Z_2 . The first and second families of quarks and leptons transform under this $U(1)_D$ so that their masses are forbidden at tree level. They interact with the dark sector in such a way that they acquire one-loop finite masses, together with all three neutrinos. The extra Z_D gauge boson may have a mass of order a few TeV, and one particle associated with the breaking of $U(1)_D$ may be identified with the 750 GeV diphoton excess recently observed at the LHC.

Part II

Alternative Left-Right Models Containing Dark Symmetry with Unification

Chapter 5

Dark Gauge U(1) Symmetry for an Alternative Left-Right Model

An alternative left-right model of quarks and leptons, where the $SU(2)_R$ lepton doublet $(\nu, l)_R$ is replaced with $(n, l)_R$ so that n_R is not the Dirac mass partner of ν_L , has been known since 1987. Previous versions assumed a global $U(1)_S$ symmetry to allow n to be identified as a dark-matter fermion. We propose here a gauge extension by the addition of extra fermions to render the model free of gauge anomalies, and just one singlet scalar to break $U(1)_S$. This results in two layers of dark matter, one hidden behind the other.

5.1 Introduction

The alternative left-right model [83] of 1987 was inspired by the E_6 decomposition to the standard $SU(3)_C \times SU(2)_L \times U(1)_Y$ gauge symmetry through an $SU(2)_R$ which does not have the conventional assignments of quarks and leptons. Instead of $(u, d)_R$ and $(\nu, l)_R$

as doublets under $SU(2)_R$, a new quark h and a new lepton n per family are added so that $(u, h)_R$ and $(n, e)_R$ are the $SU(2)_R$ doublets, and h_L, d_R, n_L, ν_R are singlets.

This structure allows for the absence of tree-level flavor-changing neutral currents (unavoidable in the conventional model), as well as the existence of dark matter. The key new ingredient is a $U(1)_S$ symmetry, which breaks together with $SU(2)_R$, such that a residual global S' symmetry remains for the stabilization of dark matter. Previously [55, 56, 57], this $U(1)_S$ was assumed to be global. We show in this paper how it may be promoted to a gauge symmetry. To accomplish this, new fermions are added to render the model free of gauge anomalies. The resulting theory has an automatic discrete Z_2 symmetry which is unbroken, as well as the global S' , which is now broken to Z_3 . Hence dark matter has two components [58]. They are identified as one Dirac fermion (nontrivial under both Z_2 and Z_3) and one complex scalar (nontrivial under Z_3).

5.2 Model

The particle content of our model is given in Table 1, where the scalar $SU(2)_L \times SU(2)_R$ bidoublet is given by

$$\eta = \begin{pmatrix} \eta_1^0 & \eta_2^+ \\ \eta_1^- & \eta_2^0 \end{pmatrix}, \quad (5.1)$$

with $SU(2)_L$ transforming vertically and $SU(2)_R$ horizontally. Without $U(1)_S$ as a gauge symmetry, the model is free of anomalies without the addition of the ψ and χ fermions. In the presence of gauge $U(1)_S$, the additional anomaly-free conditions are all satisfied by the addition of the ψ and χ fermions. The $[SU(3)_C]^2 U(1)_S$ anomaly is canceled between

Table 5.1: Particle content of proposed model of dark gauge $U(1)$ symmetry.

particles	$SU(3)_C$	$SU(2)_L$	$SU(2)_R$	$U(1)_X$	$U(1)_S$
$(u, d)_L$	3	2	1	1/6	0
$(u, h)_R$	3	1	2	1/6	-1/2
d_R	3	1	1	-1/3	0
h_L	3	1	1	-1/3	-1
$(\nu, l)_L$	1	2	1	-1/2	0
$(n, l)_R$	1	1	2	-1/2	1/2
ν_R	1	1	1	0	0
n_L	1	1	1	0	1
(ϕ_L^+, ϕ_L^0)	1	2	1	1/2	0
(ϕ_R^+, ϕ_R^0)	1	1	2	1/2	1/2
η	1	2	2	0	-1/2
ζ	1	1	1	0	1
$(\psi_1^0, \psi_1^-)_R$	1	1	2	-1/2	2
$(\psi_2^+, \psi_2^0)_R$	1	1	2	1/2	1
χ_R^+	1	1	1	1	-3/2
χ_R^-	1	1	1	-1	-3/2
χ_{1R}^0	1	1	1	0	-1/2
χ_{2R}^0	1	1	1	0	-5/2
σ	1	1	1	0	3

$(u, h)_R$ and h_L ; the $[SU(2)_L]^2 U(1)_S$ anomaly is zero because $(u, d)_L$ and $(\nu, l)_L$ do not transform under $U(1)_S$; the $[SU(2)_R]^2 U(1)_S$ and $[SU(2)_R]^2 U(1)_X$ anomalies are both canceled by summing over $(u, h)_R$, $(n, l)_R$, $(\psi_1^0, \psi_1^-)_R$, and $(\psi_2^+, \psi_2^0)_R$; the addition of χ_R^\pm renders the $[U(1)_X]^2 U(1)_S$, $U(1)_X [U(1)_S]^2$, $[U(1)_X]^3$, and $U(1)_X$ anomalies zero; and the further addition of χ_{1R}^0 and χ_{2R}^0 kills both the $[U(1)_S]^3$ and $U(1)_S$ anomalies, i.e.

$$\begin{aligned}
0 &= 3[6(-1/2)^3 - 3(-1)^3 + 2(1/2)^3 - (1)^3] \\
&+ 2(2)^3 + 2(1)^3 + 2(-3/2)^3 + (-1/2)^3 + (-5/2)^3,
\end{aligned} \tag{5.2}$$

$$\begin{aligned}
0 &= 3[6(-1/2) - 3(-1) + 2(1/2) - (1)] \\
&+ 2(2) + 2(1) + 2(-3/2) + (-1/2) + (-5/2).
\end{aligned} \tag{5.3}$$

Under $T_{3R} + S$, the neutral scalars ϕ_R^0 and η_2^0 are zero, so that their vacuum expectation values do not break $T_{3R} + S$ which remains as a global symmetry. However, $\langle \sigma \rangle \neq 0$ does break $T_{3R} + S$ and gives masses to $\psi_{1R}^0 \psi_{2R}^0 - \psi_{1R}^- \psi_{2R}^+$, $\chi_R^+ \chi_R^-$, and $\chi_{1R}^0 \chi_{2R}^0$. These exotic fermions all have half-integral charges [59] under $T_{3R} + S$ and only communicate with the others with integral charges through W_R^\pm , $\sqrt{2}Re(\phi_R^0)$, ζ , and the two extra neutral gauge bosons beyond the Z . Some explicit Yukawa terms are

$$(\psi_{1R}^0 \phi_R^- + \psi_{1R}^- \bar{\phi}_R^0) \chi_R^+, \quad (\psi_{2R}^+ \phi_R^0 - \psi_{2R}^0 \phi_R^+) \chi_R^-, \quad (5.4)$$

$$(\psi_{1R}^0 \phi_R^0 - \psi_{1R}^- \phi_R^+) \chi_{2R}^0, \quad (\psi_{2R}^+ \phi_R^- + \psi_{2R}^0 \bar{\phi}_R^0) \chi_{1R}^0. \quad (5.5)$$

This dichotomy of particle content results in an additional unbroken symmetry of the Lagrangian, i.e. discrete Z_2 under which the exotic fermions are odd. Hence dark matter has two layers: those with nonzero $T_{3R} + S$ and even Z_2 , i.e. $n, h, W_R^\pm, \phi_R^\pm, \eta_1^\pm, \eta_1^0, \bar{\eta}_1^0, \zeta$, and the underlying exotic fermions with odd Z_2 . Without ζ , a global S' symmetry remains. With ζ , because of the $\zeta^3 \sigma^*$ and $\chi_{1R}^0 \chi_{1R}^0 \zeta$ terms, the S' symmetry breaks to Z_3 .

Table 5.2: Particle content of proposed model under $(T_{3R} + S) \times Z_2$.

particles	gauge $T_{3R} + S$	global S'	Z_3	Z_2
u, d, ν, l	0	0	1	+
$(\phi_L^+, \phi_L^0), (\eta_2^+, \eta_2^0), \phi_R^0$	0	0	1	+
n, ϕ_R^+, ζ	1	1	ω	+
$h, (\eta_1^0, \eta_1^-)$	-1	-1	ω^2	+
ψ_{2R}^+, χ_R^+	3/2, -3/2	0	1	-
ψ_{1R}^-, χ_R^-	3/2, -3/2	0	1	-
ψ_{1R}^0, ψ_{2R}^0	5/2, 1/2	1, -1	ω, ω^2	-
χ_{1R}^0, χ_{2R}^0	-1/2, -5/2	1, -1	ω, ω^2	-
σ	3	0	1	+

Let

$$\langle \phi_L^0 \rangle = v_1, \quad \langle \eta_2^0 \rangle = v_2, \quad \langle \phi_R^0 \rangle = v_R, \quad \langle \sigma \rangle = v_S, \quad (5.6)$$

then the $SU(3)_C \times SU(2)_L \times SU(2)_R \times U(1)_X \times U(1)_S$ gauge symmetry is broken to $SU(3)_C \times U(1)_Q$ with S' , which becomes Z_3 , as shown in Table 2 with $\omega^3 = 1$. The discrete Z_2 symmetry is unbroken. Note that the global S' assignments for the exotic fermions are not $T_{3R} + S$ because of v_S which breaks the gauge $U(1)_S$ by 3 units.

5.3 Gauge sector

Consider now the masses of the gauge bosons. The charged ones, W_L^\pm and W_R^\pm , do not mix because of $S'(Z_3)$, as in the original alternative left-right models. Their masses are given by

$$M_{W_L}^2 = \frac{1}{2}g_L^2(v_1^2 + v_2^2), \quad M_{W_R}^2 = \frac{1}{2}g_R^2(v_R^2 + v_2^2). \quad (5.7)$$

Since $Q = I_{3L} + I_{3R} + X$, the photon is given by

$$A = \frac{e}{g_L}W_{3L} + \frac{e}{g_R}W_{3R} + \frac{e}{g_X}X, \quad (5.8)$$

where $e^{-2} = g_L^{-2} + g_R^{-2} + g_X^{-2}$. Let

$$Z = (g_L^2 + g_Y^2)^{-1/2} \left(g_L W_{3L} - \frac{g_Y^2}{g_R} W_{3R} - \frac{g_Y^2}{g_X} X \right), \quad (5.9)$$

$$Z' = (g_R^2 + g_X^2)^{-1/2} (g_R W_{3R} - g_X X), \quad (5.10)$$

where $g_Y^{-2} = g_R^{-2} + g_X^{-2}$, then the 3×3 mass-squared matrix spanning (Z, Z', S) has the entries:

$$M_{ZZ}^2 = \frac{1}{2}(g_L^2 + g_Y^2)(v_1^2 + v_2^2), \quad (5.11)$$

$$M_{Z'Z'}^2 = \frac{1}{2}(g_R^2 + g_X^2)v_R^2 + \frac{g_X^4 v_1^2 + g_R^4 v_2^2}{2(g_R^2 + g_X^2)}, \quad (5.12)$$

$$M_{SS}^2 = 18g_S^2 v_S^2 + \frac{1}{2}g_S^2(v_R^2 + v_2^2), \quad (5.13)$$

$$M_{ZZ'}^2 = \frac{\sqrt{g_L^2 + g_Y^2}}{2\sqrt{g_R^2 + g_X^2}}(g_X^2 v_1^2 - g_R^2 v_2^2), \quad (5.14)$$

$$M_{ZS}^2 = \frac{1}{2}g_S \sqrt{g_L^2 + g_Y^2} v_2^2, \quad (5.15)$$

$$M_{Z'S}^2 = -\frac{1}{2}g_S \sqrt{g_R^2 - g_X^2} v_R^2 - \frac{g_S g_R v_2^2}{2\sqrt{g_R^2 + g_X^2}}. \quad (5.16)$$

Their neutral-current interactions are given by

$$\begin{aligned} \mathcal{L}_{NC} &= eA_\mu j_Q^\mu + g_Z Z_\mu (j_{3L}^\mu - \sin^2 \theta_W j_Q^\mu) \\ &+ (g_R^2 + g_X^2)^{-1/2} Z'_\mu (g_R^2 j_{3R}^\mu - g_X^2 j_X^\mu) + g_S S_\mu j_S^\mu, \end{aligned} \quad (5.17)$$

where $g_Z^2 = g_L^2 + g_Y^2$ and $\sin^2 \theta_W = g_Y^2/g_Z^2$.

In the limit $v_{1,2}^2 \ll v_R^2, v_S^2$, the mass-squared matrix spanning (Z', S) may be simplified if we assume

$$\frac{v_S^2}{v_R^2} = \frac{(g_R^2 + g_X^2 + g_S^2)^2}{36g_S^2(g_R^2 + g_X^2 - g_S^2)}, \quad (5.18)$$

and let

$$\tan \theta_D = \frac{\sqrt{g_R^2 + g_X^2} - g_S}{\sqrt{g_R^2 + g_X^2} + g_S}, \quad (5.19)$$

then

$$\begin{pmatrix} D_1 \\ D_2 \end{pmatrix} = \begin{pmatrix} \cos \theta_D & \sin \theta_D \\ -\sin \theta_D & \cos \theta_D \end{pmatrix} \begin{pmatrix} Z' \\ S \end{pmatrix}, \quad (5.20)$$

with mass eigenvalues given by

$$M_{D_1}^2 = \sqrt{g_R^2 + g_X^2} \sqrt{g_R^2 + g_X^2 + g_S^2} \frac{v_R^2}{2\sqrt{2} \cos \theta_D}, \quad (5.21)$$

$$M_{D_2}^2 = \sqrt{g_R^2 + g_X^2} \sqrt{g_R^2 + g_X^2 + g_S^2} \frac{v_R^2}{2\sqrt{2} \sin \theta_D}. \quad (5.22)$$

In addition to the assumption of Eq. (18), let us take for example

$$2g_S = \sqrt{g_R^2 + g_X^2}, \quad (5.23)$$

then $\sin \theta_D = 1/\sqrt{10}$ and $\cos \theta_D = 3/\sqrt{10}$. Assuming also that $g_R = g_L$, we obtain

$$\frac{g_X^2}{g_Z^2} = \frac{\sin^2 \theta_W \cos^2 \theta_W}{\cos 2\theta_W}, \quad \frac{g_S}{g_Z} = \frac{\cos^2 \theta_W}{2\sqrt{\cos 2\theta_W}}, \quad (5.24)$$

$$\frac{v_S^2}{v_R^2} = \frac{25}{108}, \quad M_{D_2}^2 = 3M_{D_1}^2 = \frac{5 \cos^4 \theta_W}{4 \cos 2\theta_W} g_Z^2 v_R^2. \quad (5.25)$$

The resulting gauge interactions of $D_{1,2}$ are given by

$$\begin{aligned} \mathcal{L}_D = & \frac{g_Z}{\sqrt{10}\sqrt{\cos 2\theta_W}} \{ [3 \cos 2\theta_W j_{3R}^\mu - 3 \sin^2 \theta_W j_X^\mu + (1/2) \cos^2 \theta_W j_S^\mu] D_{1\mu} \\ & + [-\cos 2\theta_W j_{3R}^\mu + \sin^2 \theta_W j_X^\mu + (3/2) \cos^2 \theta_W j_S^\mu] D_{2\mu} \}. \end{aligned} \quad (5.26)$$

Since D_2 is $\sqrt{3}$ times heavier than D_1 in this example, the latter would be produced first in pp collisions at the Large Hadron Collider (LHC).

5.4 Fermion sector

All fermions obtain masses through the four vacuum expectation values of Eq. (6) except ν_R which is allowed to have an invariant Majorana mass. This means that neutrino masses may be small from the usual canonical seesaw mechanism. The various Yukawa

terms for the quark and lepton masses are

$$\begin{aligned}
-\mathcal{L}_Y &= \frac{m_u}{v_2} [\bar{u}_R(u_L\eta_2^0 - d_L\eta_2^+) + \bar{h}_R(-u_L\eta_2^- + d_L\eta_1^0)] \\
&+ \frac{m_d}{v_1} (\bar{u}_L\phi_L^+ + \bar{d}_L\phi_L^0)d_R + \frac{m_h}{v_R} (\bar{u}_R\phi_R^+ + \bar{h}_R\phi_R^0)h_L \\
&+ \frac{m_l}{v_2} [(\bar{\nu}_L\eta_1^0 + \bar{l}_L\eta_1^-)n_R + (\bar{\nu}_L\eta_2^+ + \bar{l}_L\eta_2^0)l_R] \\
&+ \frac{m_D}{v_1} \bar{\nu}_R(\nu_L\phi_L^0 - l_L\phi_L^+) + \frac{m_n}{v_R} \bar{n}_L(n_R\phi_R^0 - l_R\phi_R^-) + H.c. \quad (5.27)
\end{aligned}$$

These terms show explicitly that the assignments of Tables 1 and 2 are satisfied.

As for the exotic ψ and χ fermions, they have masses from the Yukawa terms of Eqs. (4) and (5), as well as

$$(\phi_{1R}^0\psi_{2R}^0 - \psi_{1R}^-\psi_{2R}^+)\sigma^*, \quad \chi_R^-\chi_R^+\sigma, \quad \chi_{1R}^0\chi_{2R}^0\sigma. \quad (5.28)$$

As a result, two neutral Dirac fermions are formed from the matrix linking χ_{1R}^0 and ψ_{1R}^0 to χ_{2R}^0 and ψ_{2R}^0 . Let us call the lighter of these two Dirac fermions χ_0 , then it is one component of dark matter of our model. The other will be the scalar ζ , to be discussed later. Note that χ_0 communicates with ζ through the allowed $\chi_{1R}^0\chi_{1R}^0\zeta$ interaction. Note also that the allowed Yukawa terms

$$\bar{d}_R h_L \zeta, \quad \bar{n}_L \nu_R \zeta \quad (5.29)$$

enable the dark fermions h and n to decay into ζ .

5.5 Scalar sector

Consider the most general scalar potential consisting of $\Phi_{L,R}$, η , and σ . Let

$$\eta = \begin{pmatrix} \eta_1^0 & \eta_2^+ \\ \eta_1^- & \eta_2^0 \end{pmatrix}, \quad \tilde{\eta} = \sigma_2 \eta^* \sigma_2 = \begin{pmatrix} \bar{\eta}_2^0 & -\eta_1^+ \\ -\eta_2^- & \bar{\eta}_1^0 \end{pmatrix}, \quad (5.30)$$

then

$$\begin{aligned}
V &= -\mu_L^2 \Phi_L^\dagger \Phi_L - \mu_R^2 \Phi_R^\dagger \Phi_R - \mu_\sigma^2 \sigma^* \sigma - \mu_\eta^2 \text{Tr}(\eta^\dagger \eta) + [\mu_3 \Phi_L^\dagger \eta \Phi_R + H.c.] \\
&+ \frac{1}{2} \lambda_L (\Phi_L^\dagger \Phi_L)^2 + \frac{1}{2} \lambda_R (\Phi_R^\dagger \Phi_R)^2 + \frac{1}{2} \lambda_\sigma (\sigma^* \sigma)^2 + \frac{1}{2} \lambda_\eta [\text{Tr}(\eta^\dagger \eta)]^2 + \frac{1}{2} \lambda'_\eta \text{Tr}(\eta^\dagger \eta \eta^\dagger \eta) \\
&+ \lambda_{LR} (\Phi_L^\dagger \Phi_L) (\Phi_R^\dagger \Phi_R) + \lambda_{L\sigma} (\Phi_L^\dagger \Phi_L) (\sigma^* \sigma) + \lambda_{R\sigma} (\Phi_R^\dagger \Phi_R) (\sigma^* \sigma) + \lambda_{\sigma\eta} (\sigma^* \sigma) \text{Tr}(\eta^\dagger \eta) \\
&+ \lambda_{L\eta} \Phi_L^\dagger \eta \eta^\dagger \Phi_L + \lambda'_{L\eta} \Phi_L^\dagger \tilde{\eta} \tilde{\eta}^\dagger \Phi_L + \lambda_{R\eta} \Phi_R^\dagger \eta^\dagger \eta \Phi_R + \lambda'_{R\eta} \Phi_R^\dagger \tilde{\eta}^\dagger \tilde{\eta} \Phi_R.
\end{aligned} \tag{5.31}$$

Note that

$$2|\det(\eta)|^2 = [\text{Tr}(\eta^\dagger \eta)]^2 - \text{Tr}(\eta^\dagger \eta \eta^\dagger \eta), \tag{5.32}$$

$$(\Phi_L^\dagger \Phi_L) \text{Tr}(\eta^\dagger \eta) = \Phi_L^\dagger \eta \eta^\dagger \Phi_L + \Phi_L^\dagger \tilde{\eta} \tilde{\eta}^\dagger \Phi_L, \tag{5.33}$$

$$(\Phi_R^\dagger \Phi_R) \text{Tr}(\eta^\dagger \eta) = \Phi_R^\dagger \eta^\dagger \eta \Phi_R + \Phi_R^\dagger \tilde{\eta}^\dagger \tilde{\eta} \Phi_R. \tag{5.34}$$

The minimum of V satisfies the conditions

$$\mu_L^2 = \lambda_L v_1^2 + \lambda_{L\eta} v_2^2 + \lambda_{LR} v_R^2 + \lambda_{L\sigma} v_S^2 + \mu_3 v_2 v_R / v_1, \tag{5.35}$$

$$\mu_\eta^2 = (\lambda_\eta + \lambda'_\eta) v_2^2 + \lambda_{L\eta} v_1^2 + \lambda_{R\eta} v_R^2 + \lambda_{\sigma\eta} v_S^2 + \mu_3 v_1 v_R / v_2, \tag{5.36}$$

$$\mu_R^2 = \lambda_R v_R^2 + \lambda_{LR} v_1^2 + \lambda_{R\eta} v_2^2 + \lambda_{R\sigma} v_S^2 + \mu_3 v_1 v_2 / v_R, \tag{5.37}$$

$$\mu_\sigma^2 = \lambda_\sigma v_S^2 + \lambda_{L\sigma} v_1^2 + \lambda_{\sigma\eta} v_2^2 + \lambda_{R\sigma} v_R^2. \tag{5.38}$$

The 4×4 mass-squared matrix spanning $\sqrt{2} \text{Im}(\phi_L^0, \eta_2^0, \phi_R^0, \sigma)$ is then given by

$$\mathcal{M}_I^2 = \mu_3 \begin{pmatrix} -v_2 v_R / v_1 & v_R & v_2 & 0 \\ v_R & -v_1 v_R / v_2 & v_1 & 0 \\ v_2 & v_1 & -v_1 v_2 / v_R & 0 \\ 0 & 0 & 0 & 0 \end{pmatrix}. \tag{5.39}$$

and that spanning $\sqrt{2}Re(\phi_L^0, \eta_2^0, \phi_R^0, \sigma)$ is

$$\mathcal{M}_R^2 = \mathcal{M}_I^2 + 2 \begin{pmatrix} \lambda_L v_1^2 & \lambda_{L\eta} v_1 v_2 & \lambda_{LR} v_1 v_R & \lambda_{L\sigma} v_1 v_S \\ \lambda_{L\eta} v_1 v_2 & (\lambda_\eta + \lambda'_\eta) v_2^2 & \lambda_{R\eta} v_2 v_R & \lambda_{\sigma\eta} v_2 v_S \\ \lambda_{LR} v_1 v_R & \lambda_{R\eta} v_2 v_R & \lambda_R v_R^2 & \lambda_{R\sigma} v_R v_S \\ \lambda_{L\sigma} v_1 v_S & \lambda_{\sigma\eta} v_2 v_S & \lambda_{R\sigma} v_R v_S & \lambda_\sigma v_S^2 \end{pmatrix}. \quad (5.40)$$

Hence there are three zero eigenvalues in \mathcal{M}_I^2 with one nonzero eigenvalue $-\mu_3[v_1 v_2/v_R + v_R(v_1^2 + v_2^2)/v_1 v_2]$ corresponding to the eigenstate $(-v_1^{-1}, v_2^{-1}, v_R^{-1}, 0)/\sqrt{v_1^{-2} + v_2^{-2} + v_R^{-2}}$.

In \mathcal{M}_R^2 , the linear combination $H = (v_1, v_2, 0, 0)/\sqrt{v_1^2 + v_2^2}$, is the standard-model Higgs boson, with

$$m_H^2 = 2[\lambda_L v_1^4 + (\lambda_\eta + \lambda'_\eta) v_2^4 + 2\lambda_{L\eta} v_1^2 v_2^2]/(v_1^2 + v_2^2). \quad (5.41)$$

The other three scalar bosons are much heavier, with suppressed mixing to H , which may all be assumed to be small enough to avoid the constraints from dark-matter direct-search experiments. The addition of the scalar ζ introduces two important new terms:

$$\zeta^3 \sigma^*, \quad (\eta_1^0 \eta_2^0 - \eta_1^- \eta_2^+) \zeta. \quad (5.42)$$

The first term breaks global S' to Z_3 , and the second term mixes ζ with η_1^0 through v_2 . We assume the latter to be negligible, so that the physical dark scalar is mostly ζ .

5.6 Present phenomenological constraints

Many of the new particles of this model interact with those of the standard model. The most important ones are the neutral $D_{1,2}$ gauge bosons, which may be produced at the LHC through their couplings to u and d quarks, and decay to charged leptons ($e^- e^+$ and

$\mu^- \mu^+$). As noted previously, in our chosen example, D_1 is the lighter of the two. Hence current search limits for a Z' boson are applicable [46, 60]. The $c_{u,d}$ coefficients used in the data analysis are

$$c_u = (g_{uL}^2 + g_{uR}^2)B = 0.0273 B, \quad c_d = (g_{dL}^2 + g_{dR}^2)B = 0.0068 B, \quad (5.43)$$

where B is the branching fraction of Z' to $e^- e^+$ and $\mu^- \mu^+$. Assuming that D_1 decays to all the particles listed in Table 2, except for the scalars which become the longitudinal components of the various gauge bosons, we find $B = 1.2 \times 10^{-2}$. Based on the 2016 LHC 13 TeV data set, this translates to a bound of about 4 TeV on the D_1 mass.

The would-be dark-matter candidate n is a Dirac fermion which couples to $D_{1,2}$ which also couples to quarks. Hence severe limits exist on the masses of $D_{1,2}$ from underground direct-search experiments as well. The annihilation cross section of n through $D_{1,2}$ would then be too small, so that its relic abundance would be too big for it to be a dark-matter candidate. Its annihilation at rest through s -channel scalar exchange is p -wave suppressed and does not help. As for the t -channel diagrams, they also turn out to be too small. Previous studies where n is chosen as dark matter are now ruled out.

5.7 Dark sector

Dark matter is envisioned to have two components. One is a Dirac fermion χ_0 which is a mixture of the four neutral fermions of odd Z_2 , and the other is a complex scalar boson which is mostly ζ . The annihilation $\chi_0 \bar{\chi}_0 \rightarrow \zeta \zeta^*$ determines the relic abundance of χ_0 , and the annihilation $\zeta \zeta^* \rightarrow HH$, where H is the standard-model Higgs boson, determines that of ζ . The direct $\zeta \zeta^* H$ coupling is assumed small to avoid the severe constraint in

direct-search experiments.

Let the interaction of ζ with χ_0 be $f_0\zeta\chi_0R\chi_0R + H.c.$, then the annihilation cross section of $\chi_0\bar{\chi}_0$ to $\zeta\zeta^*$ times relative velocity is given by

$$\langle\sigma\times v_{rel}\rangle_{\chi}=\frac{f_0^4}{4\pi m_{\chi_0}}\frac{(m_{\chi_0}^2-m_{\zeta}^2)^{3/2}}{(2m_{\chi_0}^2-m_{\zeta}^2)^2}. \quad (5.44)$$

Let the effective interaction strength of $\zeta\zeta^*$ with HH be λ_0 , then the annihilation cross section of $\zeta\zeta^*$ to HH times relative velocity is given by

$$\langle\sigma_{\zeta}\times v_{rel}\rangle_{\zeta}=\frac{\lambda_0^2}{16\pi}\frac{(m_{\zeta}^2-m_H^2)^{1/2}}{m_{\zeta}^3}. \quad (5.45)$$

Note that λ_0 is the sum over several interactions. The quartic coupling $\lambda_{\zeta H}$ is assumed negligible, to suppress the trilinear $\zeta\zeta^*H$ coupling which contributes to the elastic ζ scattering cross section off nuclei. However, the trilinear couplings $\zeta\zeta^*Re(\phi_R^0)$ and $Re(\phi_R^0)HH$ are proportional to v_R , and the trilinear couplings $\zeta\zeta^*Re(\sigma)$ and $Re(\sigma)HH$ are proportional to v_S . Hence their effective contributions to λ_0 are proportional to $v_R^2/m^2[\sqrt{2}Re(\phi_R^0)]$ and $v_S^2/m^2[\sqrt{2}Re(\sigma)]$, which are not suppressed.

As a rough estimate, we will assume that

$$\langle\sigma\times v_{rel}\rangle_{\chi}^{-1}+\langle\sigma_{\zeta}\times v_{rel}\rangle_{\zeta}^{-1}=(4.4\times 10^{-26}\text{ cm}^3/s)^{-1} \quad (5.46)$$

to satisfy the condition of dark-matter relic abundance [61] of the Universe. For given values of m_{ζ} and m_{χ_0} , the parameters λ_0 and f_0 are thus constrained. We show in Fig. 1 the plots of λ_0 versus f_0 for $m_{\zeta}=150$ GeV and various values of m_{χ_0} . Since m_{ζ} is fixed at 150 GeV, λ_0 is also fixed for a given fraction of $\Omega_{\zeta}/\Omega_{DM}$. To adjust for the rest of dark matter, f_0 must then vary as a function of m_{χ_0} according to Eq. (44).

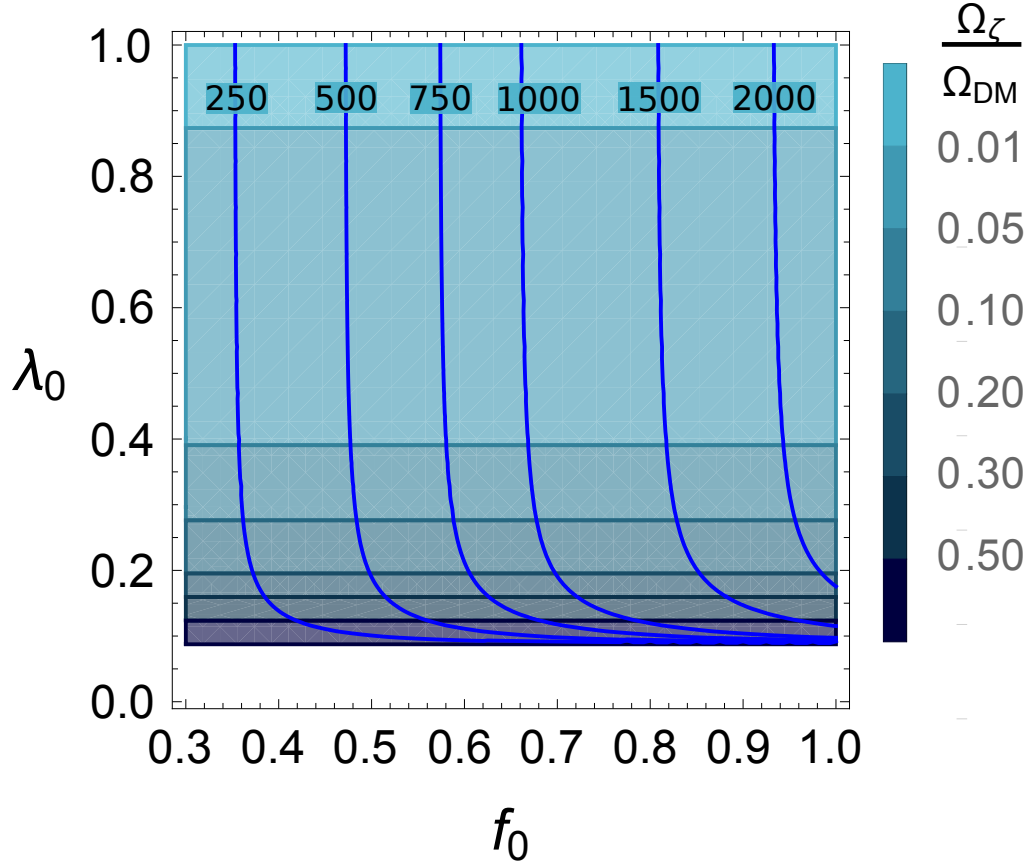


Figure 5.1: Relic-abundance constraints on λ_0 and f_0 for $m_\zeta = 150$ GeV and various values of m_{χ_0} .

As for direct detection, both χ_0 and ζ have possible interactions with quarks through the gauge bosons $D_{1,2}$ and the standard-model Higgs boson H . They are suppressed by making the $D_{1,2}$ masses heavy, and the H couplings to χ_0 and ζ small. In our example with $m_\zeta = 150$ GeV, let us choose $m_{\chi_0} = 500$ GeV and the relic abundances of both to be equal. From Fig. 1, these choices translate to $\lambda_0 = 0.12$ and $f_0 = 0.56$.

Consider first the $D_{1,2}$ interactions. Using Eq. (26), we obtain

$$g_u^V(D_1) = 0.0621, \quad g_d^V(D_1) = 0.0184, \quad g_\zeta(D_1) = 0.1234, \quad (5.47)$$

$$g_u^V(D_2) = -0.1235, \quad g_d^V(D_2) = -0.0062, \quad g_\zeta(D_2) = 0.3701. \quad (5.48)$$

The effective ζ elastic scattering cross section through $D_{1,2}$ is then completely determined as a function of the D_1 mass (because $M_{D_2} = \sqrt{3}M_{D_1}$ in our example), i.e.

$$\mathcal{L}_{\zeta q}^V = \frac{(\zeta^* \partial_\mu - \zeta \partial_\mu \zeta^*)}{M_{D_1}^2} [(-7.57 \times 10^{-3}) \bar{u} \gamma^\mu u + (1.51 \times 10^{-3}) \bar{d} \gamma^\mu d]. \quad (5.49)$$

Using the latest LUX result [62] and Eq. (25), we obtain $v_R > 35$ TeV which translates to $M_{D_1} > 18$ TeV, and $M_{W_R} > 16$ TeV.

The $\bar{\chi}_0 \gamma_\mu \chi_0$ couplings to $D_{1,2}$ depend on the 2×2 mass matrix linking (χ_1, ψ_1) to (χ_2, ψ_2) which has two mixing angles and two mass eigenvalues, the lighter one being m_{χ_0} . By adjusting these parameters, it is possible to make the effective χ_0 interaction with xenon negligibly small. Hence there is no useful limit on the D_1 mass in this case.

Direct search also constrains the coupling of the Higgs boson to ζ (through a possible trilinear $\lambda_{\zeta H} \sqrt{2} v_H \zeta^* \zeta$ interaction) or χ_0 (through an effective Yukawa coupling ϵ from H mixing with σ_R and ϕ_R^0). Let their effective interactions with quarks through H exchange be given by

$$\mathcal{L}_{\zeta q}^S = \frac{\lambda_{\zeta H} m_q}{m_H^2} \zeta^* \zeta \bar{q} q + \frac{\epsilon f_q}{m_H^2} \bar{\chi}_0 \chi_0 \bar{q} q, \quad (5.50)$$

where $f_q = m_q / \sqrt{2} v_H = m_q / (246 \text{ GeV})$. The spin-independent direct-detection cross section per nucleon in the former is given by

$$\sigma^{SI} = \frac{\mu_\zeta^2}{\pi A^2} [\lambda_p Z + (A - Z) \lambda_n]^2, \quad (5.51)$$

where $\mu_\zeta = m_\zeta M_A / (m_\zeta + M_A)$ is the reduced mass of the dark matter, and [63]

$$\lambda_N = \left[\sum_{u,d,s} f_q^N + \frac{2}{27} \left(1 - \sum_{u,d,s} f_q^N \right) \right] \frac{\lambda_{\zeta H} m_N}{2m_\zeta m_H^2}, \quad (5.52)$$

with [64]

$$f_u^p = 0.023, \quad f_d^p = 0.032, \quad f_s^p = 0.020, \quad (5.53)$$

$$f_u^n = 0.017, \quad f_d^n = 0.041, \quad f_s^n = 0.020. \quad (5.54)$$

For $m_\zeta = 150$ GeV, we have

$$\lambda_p = 2.87 \times 10^{-8} \lambda_{\zeta H} \text{ GeV}^{-2}, \quad \lambda_n = 2.93 \times 10^{-8} \lambda_{\zeta H} \text{ GeV}^{-2}. \quad (5.55)$$

Using $A = 131$, $Z = 54$, and $M_A = 130.9$ atomic mass units for the LUX experiment [62], and twice the most recent bound of $2 \times 10^{-46} \text{ cm}^2$ (because ζ is assumed to account for only half of the dark matter) at this mass, we find

$$\lambda_{\zeta H} < 9.1 \times 10^{-4}. \quad (5.56)$$

As noted earlier, this is negligible for considering the annihilation cross section of ζ to H .

For the H contribution to the χ_0 elastic cross section off nuclei, we replace m_ζ with $m_{\chi_0} = 500$ GeV in Eq. (51) and $\lambda_{\zeta H} / 2m_\zeta$ with $\epsilon / \sqrt{2} v_H$ in Eq. (52). Using the experimental data at 500 GeV, we obtain the bound.

$$\epsilon < 9.6 \times 10^{-4}. \quad (5.57)$$

From the above discussion, it is clear that our model allows for the discovery of dark matter in direct-search experiments in the future if these bounds are only a little above the actual values of $\lambda_{\zeta H}$ and ϵ .

5.8 Conclusions

In the context of the alternative left-right model, a new gauge $U(1)_S$ symmetry has been proposed to stabilize dark matter. This is accomplished by the addition of a few new fermions to cancel all the gauge anomalies, as shown in Table 1. As a result of this particle content, an automatic unbroken Z_2 symmetry exists on top of $U(1)_S$ which is broken to a conserved residual Z_3 symmetry. Thus dark matter has two components. One is the Dirac fermion $\chi_0 \sim (\omega, -)$ and the other the complex scalar $\zeta \sim (\omega, +)$ under $Z_3 \times Z_2$. We have shown how they may account for the relic abundance of dark matter in the Universe, and satisfy present experimental search bounds.

Whereas we have no specific prediction for discovery in direct-search experiments, our model will be able to accommodate any positive result in the future, just like many other existing proposals. To single out our model, many additional details must also be confirmed. Foremost are the new gauge bosons $D_{1,2}$. Whereas the LHC bound is about 4 TeV, the direct-search bound is much higher provided that ζ is a significant fraction of dark matter. If χ_0 dominates instead, the adjustment of free parameters of our model can lower this bound to below 4 TeV. In that case, future $D_{1,2}$ observations are still possible at the LHC as more data become available.

Another is the exotic h quark which is easily produced if kinematically allowed. It would decay to d and ζ through the direct $\bar{d}_R h_L \zeta$ coupling of Eq. (29). Assuming that this branching fraction is 100%, the search at the LHC for 2 jets plus missing energy puts a limit on m_h of about 1.0 TeV, as reported by the CMS Collaboration [65] based on the $\sqrt{s} = 13$ TeV data at the LHC with an integrated luminosity of 35.9 fb^{-1} for a single scalar

quark.

If the $\bar{d}_R h_L \zeta$ coupling is very small, then h may also decay significantly to u and a virtual W_R^- , with W_R^- becoming $\bar{n}l^-$, and \bar{n} becoming $\bar{\nu}\zeta^*$. This has no analog in the usual searches for supersymmetry or the fourth family because W_R is heavy (> 16 TeV). To be specific, the final states of 2 jets plus $l_1^- l_2^+$ plus missing energy should be searched for. As more data are accumulated at the LHC, such events may become observable.

Chapter 6

Quartified Leptonic Color, Bound States, and Future Electron-Positron Collider

The $[SU(3)]^4$ quartification model of Babu, Ma, and Willenbrock (BMW), proposed in 2003, predicts a confining leptonic color $SU(2)$ gauge symmetry, which becomes strong at the keV scale. It also predicts the existence of three families of half-charged leptons (hemions) below the TeV scale. These hemions are confined to form bound states which are not so easy to discover at the Large Hadron Collider (LHC). However, just as J/ψ and Υ appeared as sharp resonances in e^-e^+ colliders of the 20th century, the corresponding 'hemionium' states are expected at a future e^-e^+ collider of the 21st century.

6.1 Introduction

Fundamental matter consists of quarks and leptons, but why are they so different? Both interact through the $SU(2)_L \times U(1)_Y$ electroweak gauge bosons W^\pm, Z^0 and the photon A , but only quarks interact through the strong force as mediated by the gluons of the unbroken (and confining) color $SU(3)$ gauge symmetry, called quantum chromodynamics (QCD). Suppose this is only true of the effective low-energy theory. At high energy, there may in fact be three 'colors' of leptons transforming as a triplet under a leptonic color $SU(3)$ gauge symmetry. Unlike QCD, only its $SU(2)_l$ subgroup remains exact, thus confining only two of the three 'colored' leptons, called 'hemions' in Ref. [66] because they have $\pm 1/2$ electric charges, leaving the third ones free as the known leptons.

The notion of leptonic color was already discussed many years ago [67, 68], and its incorporation into $[SU(3)]^4$ appeared in Ref. [69], but without full unification. Its relevance today is threefold. (1) The $[SU(3)]^4$ quartification model [66] of Babu, Ma, and Willenbrock (BMW) is non-supersymmetric, and yet achieves gauge-coupling unification at 4×10^{11} GeV without endangering proton decay. This unification of gauge couplings is only possible if the three families of hemions have masses below the TeV scale. Given the absence of experimental evidence for supersymmetry at the Large Hadron Collider (LHC) to date, this alternative scenario deserves a closer look. (2) The quartification scale determines the common gauge coupling for the $SU(2)_l$ symmetry. Its extrapolation to low energy predicts that it becomes strong at the keV scale, in analogy to that of QCD becoming strong at somewhat below the GeV scale. This may alter the thermal history of the Universe and allows the formation of gauge-boson bound states, the lightest of which is a potential

warm dark-matter candidate [70]. (3) The hemions (called 'liptons' previously [68]) have $\pm 1/2$ electric charges and are confined to form bound states by the $SU(2)_l$ 'stickons' in analogy to quarks forming hadrons through the $SU(3)_C$ gluons. They have been considered previously [71] as technifermions responsible for electroweak symmetry breaking. Their electroweak production at the LHC is possible [72] but the background is large. However, in a future e^-e^+ collider (ILC, CEPC, FCC-ee), neutral vector resonances of their bound states (hemionia) would easily appear, in analogy to the observations of quarkonia (J/ψ , Υ) at past e^-e^+ colliders.

6.2 The BMW model

Under the $[SU(3)]^4$ quartification gauge symmetry, quarks and leptons transform as $(3, \bar{3})$ in a moose chain linking $SU(3)_q$ to $SU(3)_L$ to $SU(3)_l$ to $SU(3)_R$ back to $SU(3)_q$ as depicted in Fig. 1.

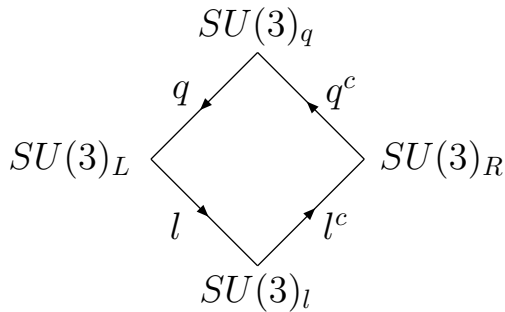


Figure 6.1: Moose diagram of $[SU(3)]^4$ quartification.

Specifically,

$$q \sim (3, \bar{3}, 1, 1) \sim \begin{pmatrix} d & u & h \\ d & u & h \\ d & u & h \end{pmatrix}, \quad l \sim (1, 3, \bar{3}, 1) \sim \begin{pmatrix} x_1 & x_2 & \nu \\ y_1 & y_2 & e \\ z_1 & z_2 & N \end{pmatrix}, \quad (6.1)$$

$$l^c \sim (1, 1, 3, \bar{3}) \sim \begin{pmatrix} x_1^c & y_1^c & z_1^c \\ x_2^c & y_2^c & z_2^c \\ \nu^c & e^c & N^c \end{pmatrix}, \quad q^c \sim (\bar{3}, 1, 1, 3) \sim \begin{pmatrix} d^c & d^c & d^c \\ u^c & u^c & u^c \\ h^c & h^c & h^c \end{pmatrix}. \quad (6.2)$$

Below the TeV energy scale, the gauge symmetry is reduced [66] to $SU(3)_C \times SU(2)_l \times SU(2)_L \times U(1)_Y$ with the particle content given in Table 1. The electric charge Q is given

Table 6.1: Particle content of proposed model.

particles	$SU(3)_C$	$SU(2)_l$	$SU(2)_L$	$U(1)_Y$
$(u, d)_L$	3	1	2	1/6
u_R	3	1	1	2/3
d_R	3	1	1	-1/3
$(x, y)_L$	1	2	2	0
x_R	1	2	1	1/2
y_R	1	2	1	-1/2
$(\nu, l)_L$	1	1	2	-1/2
ν_R	1	1	1	0
l_R	1	1	1	-1
(ϕ^+, ϕ^0)	1	1	2	1/2

by $Q = I_{3L} + Y$ as usual. The exotic $SU(2)_l$ doublets x, y have $\pm 1/2$ charges, hence the name hemions. Whereas the quarks and charged leptons must obtain masses through electroweak symmetry breaking, the hemions have invariant mass terms, i.e. $x_{1L}y_{2L} - x_{2L}y_{1L}$ and $x_{1R}y_{2R} - x_{2R}y_{1R}$. This is important because they are then allowed to be heavy without disturbing the electroweak oblique parameters S, T, U which are highly constrained

experimentally. In the following, the mass terms from electroweak symmetry breaking, i.e. $\bar{x}_L x_R \bar{\phi}^0$ and $\bar{y}_L y_R \phi^0$, will be assumed negligible.

6.3 Gauge coupling unification and the leptonic color confinement scale

The renormalization-group evolution of the gauge couplings is dictated at leading order by

$$\frac{1}{\alpha_i(\mu)} - \frac{1}{\alpha_i(\mu')} = \frac{b_i}{2\pi} \ln\left(\frac{\mu'}{\mu}\right), \quad (6.3)$$

where b_i are the one-loop beta-function coefficients,

$$b_C = -11 + \frac{4}{3}N_F, \quad (6.4)$$

$$b_l = -\frac{22}{3} + \frac{4}{3}N_F, \quad (6.5)$$

$$b_L = -\frac{22}{3} + 2N_F + \frac{1}{6}N_\Phi, \quad (6.6)$$

$$b_Y = \frac{13}{9}N_F + \frac{1}{12}N_\Phi. \quad (6.7)$$

The number of families N_F is set to three, and the number of Higgs doublets N_Φ is set to two, as in the original BMW model. Here we make a small adjustment by separating the three hemion families into two light ones at the electroweak scale M_Z and one at a somewhat higher scale M_X . We then input the values [14]

$$\alpha_C(M_Z) = 0.1185, \quad (6.8)$$

$$\alpha_L(M_Z) = (\sqrt{2}/\pi)G_F M_W^2 = 0.0339, \quad (6.9)$$

$$\alpha_Y(M_Z) = 2\alpha_L(M_Z) \tan^2 \theta_W = 0.0204, \quad (6.10)$$

where α_Y has been normalized by a factor of 2 (and b_Y by a factor of 1/2) to conform to $[SU(3)]^4$ quartification. We find

$$M_U = 4 \times 10^{11} \text{ GeV}, \quad \alpha_U = 0.0301, \quad M_X = 486 \text{ GeV}. \quad (6.11)$$

We then use b_l to extrapolate back to M_Z and obtain $\alpha_l(M_Z) = 0.0469$. Below the electroweak scale, the evolution of α_l comes only from the stickons and it becomes strong at about 1 keV. Hence 'stickballs' are expected at this confinement mass scale. Unlike QCD where glueballs are heavier than the π mesons so that they decay quickly, the stickballs are so light that they could decay only to lighter stickballs or to photon pairs through their interactions with hemions.

6.4 Thermal history of stickons

At temperatures above the electroweak symmetry scale, the hemions are active and the stickons (ζ) are in thermal equilibrium with the standard-model particles. Below the hemion mass scale, the stickon interacts with photons through $\zeta\zeta \rightarrow \gamma\gamma$ scattering with a cross section

$$\sigma \sim \frac{9\alpha^2\alpha_l^2 T^6}{16M_{eff}^8}. \quad (6.12)$$

The decoupling temperature of ζ is then obtained by matching the Hubble expansion rate

$$H = \sqrt{(8\pi/3)G_N(\pi^2/30)g_*T^4} \quad (6.13)$$

to $[6\zeta(3)/\pi^2]T^3\langle\sigma v\rangle$. Hence

$$T^{14} \sim \frac{2^8}{3^8} \left(\frac{\pi^7}{5[\zeta(3)]^2} \right) \frac{G_N g_* M_{eff}^{16}}{\alpha^4 \alpha_l^4}, \quad (6.14)$$

where $6M_{eff}^{-4} = \sum(M_{xy}^i)^{-4}$. For $M_{eff} = 110$ GeV and $g_* = 92.25$ which includes all particles with masses up to a few GeV, $T \sim 6.66$ GeV. Hence the contribution of stickons to the effective number of neutrinos at the time of big bang nucleosynthesis (BBN) is given by [73]

$$\Delta N_\nu = \frac{8}{7}(3) \left(\frac{10.75}{92.25} \right)^{4/3} = 0.195, \quad (6.15)$$

compared to the value 0.50 ± 0.23 from a recent analysis [74]. The most recent PLANCK measurement [75] coming from the cosmic microwave background (CMB) is

$$N_{eff} = 3.15 \pm 0.23. \quad (6.16)$$

However, at the time of photon decoupling, the stickons have disappeared, hence $N_{eff} = 3.046$ as in the SM. This is discussed in more detail below.

6.5 Formation and decay of stickballs

As the Universe further cools below a few keV, leptonic color goes through a phase transition and stickballs are formed. If the lightest stickball ω is stable, it may be a candidate for warm dark matter. It has strong self-interactions and the $3 \rightarrow 2$ process determines its relic abundance. Following Ref. [76] and using Ref. [70], we estimate that it is overproduced by a factor of about 3. However, ω is not absolutely stable. It is allowed to mix with a scalar bound state of two hemions which would decay to two photons. We assume this mixing to be $f_\omega m_\omega / M_{xy}$, so that its decay rate is given by

$$\Gamma(\omega \rightarrow \gamma\gamma) = \frac{9\alpha^2 f_\omega^2 m_\omega^5}{64\pi^3 M_{eff}^4}, \quad (6.17)$$

where M_{eff} is now defined by $6M_{eff}^{-2} = \sum(M_{xy}^i)^{-2}$. Setting $m_\omega = 5$ keV to be above the astrophysical bound of 4 keV from Lyman α forest observations [77] and $M_{eff} = 150$ GeV, its lifetime is estimated to be $4.4 \times 10^{17}s$ for $f_\omega = 1$. This is exactly the age of the Universe, and it appears that ω may be a candidate for dark matter after all. However, CMB measurements constrain [78] a would-be dark-matter lifetime to be greater than about $10^{25}s$, and x -ray line measurements in this mass range constrain [79] it to be greater than $10^{27}s$, so this scenario is ruled out. On the other hand, if $m_\omega = 10$ keV, then the ω lifetime is $1.4 \times 10^{16}s$, which translates to a fraction of 2×10^{-14} of the initial abundance of ω to remain at the present Universe. Compared to the upper bound of 10^{-10} for a lifetime of $10^{16}s$ given in Ref. [78], this is easily satisfied, even though ω is overproduced at the leptonic color phase transition by a factor of 3.

At the time of photon decoupling, the $SU(2)_l$ sector contributes no additional relativistic degrees of freedom, hence N_{eff} remains the same as in the SM, i.e. 3.046, coming only from neutrinos. In this scenario, ω is not dark matter. However, there are many neutral scalars and fermions in the BMW model which are not being considered here. They are naturally very heavy, but some may be light enough and stable, and be suitable as dark matter.

6.6 Revelation of leptonic color at future e^-e^+ colliders

Unlike quarks, all fermions are heavy. Hence the lightest bound state is likely to be at least 200 GeV. Its cross section through electroweak production at the LHC is probably too small for it to be discovered. On the other hand, in analogy to the observations of J/ψ

and Υ at e^-e^+ colliders of the last century, the resonance production of the corresponding neutral vector bound states (hemionia) of these hemions is expected at a future e^-e^+ collider (ILC, CEPC, FCC-ee) with sufficient reach in total center-of-mass energy. Their decays will be distinguishable from heavy quarkonia (such as toponia) experimentally.

The formation of hemion bound states is analogous to that of QCD. Instead of one-gluon exchange, the Coulomb potential binding a hemion-antihemion pair comes from one-stickon exchange. The difference is just the change in an SU(3) color factor of 4/3 to an SU(2) color factor of 3/4. The Bohr radius is then $a_0 = [(3/8)\bar{\alpha}_l m]^{-1}$, and the effective $\bar{\alpha}_l$ is defined by

$$\bar{\alpha}_l = \alpha_l(a_0^{-1}). \quad (6.18)$$

Using Eqs. (3) and (5), and $\alpha_l(M_Z) = 0.047$ with $m = 100$ GeV, we obtain $\bar{\alpha}_l = 0.059$ and $a_0^{-1} = 2.2$ GeV. Consider the lowest-energy vector bound state Ω of the lightest hemion of mass $m = 100$ GeV. In analogy to the hydrogen atom, its binding energy is given by

$$E_b = \frac{1}{4} \left(\frac{3}{4} \right)^2 \bar{\alpha}_l^2 m = 0.049 \text{ GeV}, \quad (6.19)$$

and its wavefunction at the origin is

$$|\psi(0)|^2 = \frac{1}{\pi a_0^3} = 3.4 \text{ GeV}^3. \quad (6.20)$$

Since Ω will appear as a narrow resonance at a future e^-e^+ collider, its observation depends on the integrated cross section over the energy range \sqrt{s} around m_Ω :

$$\int d\sqrt{s} \sigma(e^-e^+ \rightarrow \Omega \rightarrow X) = \frac{6\pi^2 \Gamma_{ee}\Gamma_X}{m_\Omega^2 \Gamma_{tot}}, \quad (6.21)$$

where Γ_{tot} is the total decay width of Ω , and Γ_{ee}, Γ_X are the respective partial widths.

Since Ω is a vector meson, it couples to both the photon and Z boson through its constituent hemions. Hence it will decay to W^-W^+ , $q\bar{q}$, l^-l^+ , and $\nu\bar{\nu}$. Using

$$\langle 0|\bar{x}\gamma^\mu x|\Omega\rangle = \epsilon_\Omega^\mu\sqrt{8m_\Omega}|\psi(0)|, \quad (6.22)$$

the $\Omega \rightarrow e^-e^+$ decay rate is given by

$$\Gamma(\Omega \rightarrow \gamma, Z \rightarrow e^-e^+) = \frac{2m_\Omega^2}{3\pi}(|C_V|^2 + |C_A|^2)|\psi(0)|^2, \quad (6.23)$$

where

$$C_V = \frac{e^2(1/2)(-1)}{m_\Omega^2} + \frac{g_Z^2(-\sin^2\theta_W/4)[(-1 + 4\sin^2\theta_W)/4]}{m_\Omega^2 - M_Z^2}, \quad (6.24)$$

$$C_A = \frac{g_Z^2(-\sin^2\theta_W/4)(1/4)}{m_\Omega^2 - M_Z^2}. \quad (6.25)$$

In the above, Ω is assumed to be composed of the singlet hemions x_R and y_R with invariant mass term $x_{1R}y_{2R} - x_{2R}y_{1R}$ (case A). Hence $\Gamma_{ee} = 43$ eV. If Ω comes instead from x_L and y_L with invariant mass term $x_{1L}y_{2L} - x_{2L}y_{1L}$ (case B), then the factor $(-\sin^2\theta_W/4)$ in C_V and C_A is replaced with $(\cos^2\theta_W/4)$ and $\Gamma_{ee} = 69$ eV. Similar expressions hold for the other fermions of the Standard Model (SM).

For $\Omega \rightarrow W^-W^+$, the triple γW^-W^+ and ZW^-W^+ vertices have the same structure. The decay rate is calculated to be

$$\Gamma(\Omega \rightarrow \gamma, Z \rightarrow W^-W^+) = \frac{m_\Omega^2(1-r)^{3/2}}{6\pi r^2} (4 + 20r + 3r^2) C_W^2 |\psi(0)|^2, \quad (6.26)$$

where $r = 4M_W^2/m_\Omega^2$ and

$$C_W = \frac{e^2(1/2)}{m_\Omega^2} + \frac{g_Z^2(-\sin^2\theta_W/4)}{m_\Omega^2 - M_Z^2} \quad (6.27)$$

in case A. Because of the accidental cancellation of the two terms in the above, C_W turns out to be very small. Hence $\Gamma_{WW} = 3.2$ eV. In addition to the s -channel decay of Ω to

W^-W^+ through γ and Z , there is also a t -channel electroweak contribution in case B because x_L and y_L form an electroweak doublet. Replacing $(-\sin^2\theta_W/4)$ with $(\cos^2\theta_W/4)$ in C_W , and adding this contribution, we obtain

$$\begin{aligned}\Gamma(\Omega \rightarrow W^-W^+) &= \frac{m_\Omega^2(1-r)^{3/2}}{6\pi r^2}[(4+20r+3r^2)C_W^2 \\ &+ 2r(10+3r)C_W D_W + r(8-r)D_W^2]|\psi(0)|^2,\end{aligned}\quad (6.28)$$

where

$$D_W = \frac{-g^2}{4(m_\Omega^2 - 2M_W^2)}.\quad (6.29)$$

Thus a much larger $\Gamma_{WW} = 190$ eV is obtained. For $\Omega \rightarrow ZZ$, there is only the t -channel contribution, i.e.

$$\Gamma(\Omega \rightarrow ZZ) = \frac{m_\Omega^2(1-r_Z)^{5/2}}{3\pi r_Z} D_Z^2 |\psi(0)|^2,\quad (6.30)$$

where $r_Z = 4M_Z^2/m_\Omega^2$ and $D_Z = g_Z^2 \sin^4\theta_W/4(m_\Omega^2 - 2m_Z^2)$ in case A, with $\sin^4\theta_W$ replaced by $\cos^4\theta_W$ in case B. Hence Γ_{ZZ} is negligible in case A and only 2.5 eV in case B.

The Ω decay to two stickons is forbidden by charge conjugation. Its decay to three stickons is analogous to that of quarkonium to three gluons. Whereas the latter forms a singlet which is symmetric in $SU(3)_C$, the former forms a singlet which is antisymmetric in $SU(2)_l$. However, the two amplitudes are identical because the latter is symmetrized with respect to the exchange of the three gluons and the former is antisymmetrized with respect to the exchange of the three stickons. Taking into account the different color factors of $SU(2)_l$ versus $SU(3)_C$, the decay rate of Ω to three stickons and to two stickons plus a

photon are given by

$$\Gamma(\Omega \rightarrow \zeta\zeta\zeta) = \frac{16}{27}(\pi^2 - 9)\frac{\alpha_l^3}{m_\Omega^2}|\psi(0)|^2, \quad (6.31)$$

$$\Gamma(\Omega \rightarrow \gamma\zeta\zeta) = \frac{8}{9}(\pi^2 - 9)\frac{\alpha\alpha_l^2}{m_\Omega^2}|\psi(0)|^2. \quad (6.32)$$

Hence $\Gamma_{\zeta\zeta\zeta} = 4.5$ eV and $\Gamma_{\gamma\zeta\zeta} = 1.1$ eV. The integrated cross section of Eq. (21) for $X = \mu^-\mu^+$ is then 3.8×10^{-33} cm²-keV in case A and 2.1×10^{-33} cm²-keV in case B. For comparison, this number is 7.9×10^{-30} cm²-keV for the $\Upsilon(1S)$. At a high-luminosity e^-e^+ collider, it should be feasible to make this observation. Table 2 summarizes all the partial decay widths.

Table 6.2: Partial decay widths of the hemionium Ω .

Channel	Width (A)	Width (B)
$\nu\bar{\nu}$	11 eV	123 eV
e^-e^+	43 eV	69 eV
$\mu^-\mu^+$	43 eV	69 eV
$\tau^-\tau^+$	43 eV	69 eV
$u\bar{u}$	50 eV	175 eV
$c\bar{c}$	50 eV	175 eV
$d\bar{d}$	10 eV	147 eV
$s\bar{s}$	10 eV	147 eV
$b\bar{b}$	10 eV	147 eV
W^-W^+	3.2 eV	190 eV
ZZ	0.02 eV	2.5 eV
$\zeta\zeta\zeta$	4.5 eV	4.5 eV
$\zeta\zeta\gamma$	1.1 eV	1.1 eV
sum	279 eV	1319 eV

6.7 Conclusions

There are important differences between QCD and QHD (quantum hemiodynamics). In the former, because of the existence of light u and d quarks, it is easy to pop up $u\bar{u}$ and $d\bar{d}$ pairs from the QCD vacuum. Hence the production of open charm in an e^-e^+ collider is described well by the fundamental process $e^-e^+ \rightarrow c\bar{c}$. In the latter, there are no light hemions. Instead it is easy to pop up the light stickballs from the QHD vacuum. As a result, just above the threshold of making the Ω resonance, the many-body production of $\Omega +$ stickballs becomes possible. This cross section is presumably also well described by the fundamental process $e^-e^+ \rightarrow x\bar{x}$. In case A, the cross section is given by

$$\begin{aligned} \sigma(e^-e^+ \rightarrow x\bar{x}) &= \frac{2\pi\alpha^2}{3} \sqrt{1 - \frac{4m^2}{s}} \left[\frac{(s + 2m^2)}{s^2} + \frac{x_W^2}{2(1 - x_W)^2} \frac{(s - m^2)}{(s - m_Z^2)^2} \right. \\ &\quad \left. + \frac{x_W}{(1 - x_W)} \frac{(s - m^2)}{s(s - m_Z^2)} - \frac{(1 - 4x_W)}{4(1 - x_W)} \frac{m^2}{s(s - m_Z^2)} \right], \end{aligned} \quad (6.33)$$

where $x_W = \sin^2 \theta_W$ and $s = 4E^2$ is the square of the center-of-mass energy. In case B, it is

$$\begin{aligned} \sigma(e^-e^+ \rightarrow x\bar{x}) &= \frac{2\pi\alpha^2}{3} \sqrt{1 - \frac{4m^2}{s}} \left[\frac{(s + 2m^2)}{s^2} + \frac{(s - m^2)}{2(s - m_Z^2)^2} \right. \\ &\quad \left. - \frac{(s - m^2)}{s(s - m_Z^2)} + \frac{(1 - 4x_W)}{4x_W} \frac{m^2}{s(s - m_Z^2)} \right]. \end{aligned} \quad (6.34)$$

Using $m = 100$ GeV and $s = (250 \text{ GeV})^2$ as an example, we find these cross sections to be 0.79 and 0.44 pb respectively.

In QCD, there are $q\bar{q}$ bound states which are bosons, and qqq bound states which are fermions. In QHD, there are only bound-state bosons, because the confining symmetry is $SU(2)_I$. Also, unlike baryon (or quark) number in QCD, there is no such thing as hemion

number in QHD, because y is effectively \bar{x} . This explains why there are no stable analog fermion in QHD such as the proton in QCD.

The SM Higgs boson h couples to the hemions, but these Yukawa couplings could be small, because hemions have invariant masses themselves as already explained. So far we have assumed these couplings to be negligible. If not, then h may decay to two photons and two stickons through a loop of hemions. This may show up in precision Higgs studies as a deviation of $h \rightarrow \gamma\gamma$ from the SM prediction. It will also imply a partial invisible width of h proportional to this deviation. Neither would be large effects and that is perfectly consistent with present data.

The absence of observations of new physics at the LHC is a possible indication that fundamental new physics may not be accessible using the strong interaction, i.e. quarks and gluons. It is then natural to think about future e^-e^+ colliders. But is there some fundamental issue of theoretical physics which may only reveal itself there? and not at hadron colliders? The BMW model is one possible answer. It assumes a quartification symmetry based on $[SU(3)]^4$. It has gauge-coupling unification without supersymmetry, but requires the existence of new half-charged fermions (hemions) under a confining $SU(2)_l$ leptonic color symmetry, with masses below the TeV scale. It also predicts the $SU(2)_l$ confining scale to be keV, so that stickball bound states of the vector gauge stickons are formed. These new particles have no QCD interactions, but hemions have electroweak couplings, so they are accessible in a future e^-e^+ collider, as described in this paper.

Chapter 7

Dark Revelations of the $[SU(3)]^3$ and $[SU(3)]^4$

Two theoretically well-motivated gauge extensions of the standard model are $SU(3)_C \times SU(3)_L \times SU(3)_R$ and $SU(3)_q \times SU(3)_L \times SU(3)_l \times SU(3)_R$, where $SU(3)_q$ is the same as $SU(3)_C$ and $SU(3)_l$ is its color leptonic counterpart. Each has three variations, according to how $SU(3)_R$ is broken. It is shown here for the first time that a built-in dark $U(1)_D$ gauge symmetry exists in all six versions, and may be broken to discrete Z_2 dark parity. The available dark matter candidates in each case include fermions, scalars, as well as *vector gauge bosons*. This work points to the unity of matter with dark matter, the origin of which is not *ad hoc*.

7.1 Introduction

To extend the $SU(3)_C \times SU(2)_L \times U(1)_Y$ gauge symmetry of the standard model (SM) of quarks and leptons, there are many possibilities. We focus in this paper on two such theoretically well-motivated ideas. The first [80, 81] is $SU(3)_C \times SU(3)_L \times SU(3)_R$, and the second [69, 66, 82] is $SU(3)_q \times SU(3)_L \times SU(3)_l \times SU(3)_R$, where $SU(3)_q$ is the same as $SU(3)_C$ and $SU(3)_l$ is its color leptonic counterpart. It has been known for a long time that $[SU(3)]^3$ has three distinct variations, according to how $SU(3)_R$ is broken to $SU(2)_R$.

- (A) $(u, d)_R$ is a doublet, which corresponds to the conventional left-right model.
- (B) $(u, h)_R$ is a doublet [83, 84, 55, 56, 57, 85], where h is an exotic quark with the same charge as d , which corresponds to the alternative left-right model.
- (C) $(h, d)_R$ is a doublet [86, 87, 88, 89], which implies that the vector gauge bosons of this $SU(2)_R$ are all neutral.

Note that in the early days of flavor $SU(3)$ for the u, d, s quarks, these $SU(2)$ subgroups are called T, V, U spins. The same three versions are obviously also possible for $[SU(3)]^4$.

Whereas these structures have been known for a long time, an important property of these models has been overlooked, i.e. the existence of a built-in dark $U(1)_D$ gauge symmetry already present in $[SU(3)]^3$ and $[SU(3)]^4$ under which the SM particles are distinguished from those of the dark sector. We will identify this symmetry in all six cases and discuss how it may fit into a viable extension of the SM.

7.2 Dark Symmetries in $[SU(3)]^3$

The fermion assignments under $SU(3)_C \times SU(3)_L \times SU(3)_R$ are

$$q \sim (3, 3^*, 1) \sim \begin{pmatrix} d & u & h \\ d & u & h \\ d & u & h \end{pmatrix}, \quad (7.1)$$

where the I_{3L} values from left to right are $(-1/2, 1/2, 0)$ and the Y_L values from left to right are $(-1/3, -1/3, 2/3)$;

$$\lambda \sim (1, 3, 3^*) \sim \begin{pmatrix} N & E^c & \nu \\ E & N^c & e \\ \nu^c & e^c & S \end{pmatrix}, \quad (7.2)$$

where the I_{3L} values from top to bottom are now $(1/2, -1/2, 0)$ and the Y_L values from top to bottom are $(1/3, 1/3, -2/3)$, the I_{3R} values from left to right are $(-1/2, 1/2, 0)$ and the Y_R values from left to right are $(-1/3, -1/3, 2/3)$;

$$q^c \sim (3^*, 1, 3) \sim \begin{pmatrix} d^c & d^c & d^c \\ u^c & u^c & u^c \\ h^c & h^c & h^c \end{pmatrix}, \quad (7.3)$$

where the I_{3R} values from top to bottom are $(1/2, -1/2, 0)$ and the Y_R values from top to bottom are $(1/3, 1/3, -2/3)$. The electric charge operator is given by

$$Q = I_{3L} - \frac{Y_L}{2} + I_{3R} - \frac{Y_R}{2}. \quad (7.4)$$

Since (d^c, u^c) and (e^c, ν^c) are $SU(2)_R$ doublets, this reduces to the conventional left-right model. Consider now

$$D_A = 3(Y_L - Y_R). \quad (7.5)$$

The $[Q, D_A]$ assignments of q , λ , and q^c are then given by

$$Q_q = \begin{pmatrix} -1/3 & 2/3 & -1/3 \\ -1/3 & 2/3 & -1/3 \\ -1/3 & 2/3 & -1/3 \end{pmatrix}, \quad D_q = \begin{pmatrix} -1 & -1 & 2 \\ -1 & -1 & 2 \\ -1 & -1 & 2 \end{pmatrix}, \quad (7.6)$$

$$Q_\lambda = \begin{pmatrix} 0 & 1 & 0 \\ -1 & 0 & -1 \\ 0 & 1 & 0 \end{pmatrix}, \quad D_\lambda = \begin{pmatrix} 2 & 2 & -1 \\ 2 & 2 & -1 \\ -1 & -1 & -4 \end{pmatrix}, \quad (7.7)$$

$$Q_{q^c} = \begin{pmatrix} 1/3 & 1/3 & 1/3 \\ -2/3 & -2/3 & -2/3 \\ 1/3 & 1/3 & 1/3 \end{pmatrix}, \quad D_{q^c} = \begin{pmatrix} -1 & -1 & -1 \\ -1 & -1 & -1 \\ 2 & 2 & 2 \end{pmatrix}. \quad (7.8)$$

This shows that $u, u^c, d, d^c, \nu, \nu^c, e, e^c$ have $D_A = -1$ (odd), whereas $h, h^c, N, N^c, E, E^c, S$ have even D_A charges, i.e. 2 and -4 . Let us define a parity [25] using the particle's spin j :

$$R_A = (-1)^{D_A + 2j}. \quad (7.9)$$

Since $j = 1/2$, R_A is even for $u, u^c, d, d^c, \nu, \nu^c, e, e^c$ and odd for $h, h^c, N, N^c, E, E^c, S$, thereby allowing the latter to be considered as belonging to the dark sector, as long as $U(1)_D$ is broken only by two units, in analogy to the breaking of $B - L$ in models of neutrino mass, where lepton parity $(-1)^L$ remains conserved.

To break $[SU(3)]^3$, a scalar bitriplet $\phi \sim (1, 3, 3^*)$ is used. It transforms exactly as λ and has the same $[Q, D]$ assignments. Now $\langle \phi_{33} \rangle$ breaks $SU(3)_L \times SU(3)_R$ to $SU(2)_L \times SU(2)_R \times U(1)_{Y_L + Y_R}$. The $U(1)_D$ symmetry is broken by 4 units at the same time. This gives masses to the exotic fermions h, N, E . Two other neutral scalars ϕ_{11}, ϕ_{22} have $D_A = 2$. Their vacuum expectation values would break $SU(2)_L \times SU(2)_R$ to $U(1)_{I_{3L} + I_{3R}}$, and $U(1)_D$

by 2 units, allowing mass terms for uu^c , dd^c , ee^c , $\nu\nu^c$, NS , and N^cS . At this point, it looks like a dark residual Z_2 symmetry is still possible. However this is not a viable scenario, because the $SU(2)_L$ and $SU(2)_R$ breaking are now at the same scale, contrary to what is observed. Furthermore, both $I_{3L} + I_{3R}$ and $Y_L + Y_R$ are still unbroken. Whereas Q is a linear combination of the two, there remains another unbroken $U(1)$ gauge symmetry. To solve these problems, the usual procedure is to allow ϕ_{31} and ϕ_{13} to acquire nonzero vacuum expectation values as well, thus breaking $SU(2)_R$ and $SU(2)_L$ separately. However, since they have $D_A = -1$ (odd R_A), the dark symmetry is lost.

To save the dark symmetry, we insert another bitriplet $\eta \sim (1, 3, 3^*)$ with an extra Z_2 symmetry under which it is odd and all other fields are even. This extra symmetry prevents η from coupling to the quarks and leptons, so that the absolute R_A values of the η components are not fixed by them as in ϕ . However their relative R_A values are still fixed by the gauge bosons. Using Eqs. (5) and (9), we see that of the eight $SU(3)_L$ and eight $SU(3)_R$ gauge bosons, the four gauge bosons which take u and d to h , and the corresponding ones which take u^c and d^c to h^c are odd under R_A , and the others are even. We can now choose $\langle\eta_{31}\rangle \neq 0$ and $\langle\eta_{13}\rangle \neq 0$ to break $SU(3)_L \times SU(3)_R$ to just $U(1)_Q$ and preserve R_A , because $\eta_{31}, \eta_{32}, \eta_{13}, \eta_{23}$ may be defined to be even and the other components odd without breaking R_A .

Of the 27 fermion fields for each family, 16 are in the visible sector (R_A even), i.e. $u, u^c, d, d^c, \nu, \nu^c, e, e^c$, and 11 are in the dark sector (R_A odd), i.e. $h, h^c, N, N^c, E, E^c, S$. Of the 24 gauge bosons, 16 are visible, i.e. the 8 gluons, W_L^\pm, W_R^\pm , the photon, Z , and two other heavier neutral ones, a linear combination of which couples to the dark charge

D_A , and 8 are dark, i.e. those with odd R_A . The scalars are also divided into sectors with even and odd R_A . This is thus a model with possible fermion, scalar, and *vector* dark-matter candidates. Their existence is not an *ad hoc* invention, but a possible outcome of the postulated theoretical framework beyond the standard model.

Consider next the alternative left-right model, i.e. variation (B), where d^c is switched with h^c and (ν, e, S) are switched with (N, E, ν^c) , i.e.

$$q^c \sim \begin{pmatrix} h^c & h^c & h^c \\ u^c & u^c & u^c \\ d^c & d^c & d^c \end{pmatrix}, \quad \lambda \sim \begin{pmatrix} \nu & E^c & N \\ e & N^c & E \\ S & e^c & \nu^c \end{pmatrix}. \quad (7.10)$$

The electric charge is given as before by Eq. (4), but the dark charge is now

$$D_B = 3(Y_L + I_{3R} + \frac{Y_R}{2}). \quad (7.11)$$

Hence D_q remains the same as in Eq. (6), but D_λ and D_{q^c} are now given by

$$D_\lambda = \begin{pmatrix} -1 & 2 & 2 \\ -1 & 2 & 2 \\ -4 & -1 & -1 \end{pmatrix}, \quad D_{q^c} = \begin{pmatrix} 2 & 2 & 2 \\ -1 & -1 & -1 \\ -1 & -1 & -1 \end{pmatrix}. \quad (7.12)$$

Again using $R_B = (-1)^{D_B+2j}$, we find it to be even for $u, u^c, d, d^c, \nu, \nu^c, e, e^c$ and odd for $h, h^c, N, N^c, E, E^c, S$. Choosing $\phi_{13}, \phi_{22}, \phi_{31}$ to have nonzero vacuum expectation values, the symmetry breaking pattern is as in (A), only that the $SU(2)$ subgroup of $SU(3)_R$ is now different. It suffers from the same problems as in (A), which may be solved again by adding η , with $\langle \eta_{33} \rangle \neq 0$ and $\langle \eta_{11} \rangle \neq 0$.

In the third variation (C), u^c is switched with h^c , and (ν, e, S) are switched with

(E^c, N^c, e^c) , i.e.

$$q^c \sim \begin{pmatrix} d^c & d^c & d^c \\ h^c & h^c & h^c \\ u^c & u^c & u^c \end{pmatrix}, \quad \lambda \sim \begin{pmatrix} N & \nu & E^c \\ E & e & N^c \\ \nu^c & S & e^c \end{pmatrix}. \quad (7.13)$$

The electric charge and dark charge are now given by

$$Q = I_{3L} - \frac{Y_L}{2} + Y_R, \quad D_C = 3(Y_L - I_{3R} + \frac{Y_R}{2}). \quad (7.14)$$

Hence

$$Q_\lambda = \begin{pmatrix} 0 & 0 & 1 \\ -1 & -1 & 0 \\ 0 & 0 & 1 \end{pmatrix}, \quad D_\lambda = \begin{pmatrix} 2 & -1 & 2 \\ 2 & -1 & 2 \\ -1 & -4 & -1 \end{pmatrix}, \quad (7.15)$$

$$Q_{q^c} = \begin{pmatrix} 1/3 & 1/3 & 1/3 \\ 1/3 & 1/3 & 1/3 \\ -2/3 & -2/3 & -2/3 \end{pmatrix}, \quad D_{q^c} = \begin{pmatrix} -1 & -1 & -1 \\ 2 & 2 & 2 \\ -1 & -1 & -1 \end{pmatrix}. \quad (7.16)$$

Again using $R_C = (-1)^{D_C+2j}$, we find it to be even for $u, u^c, d, d^c, \nu, \nu^c, e, e^c$ and odd for $h, h^c, N, N^c, E, E^c, S$. Choosing $\phi_{11}, \phi_{23}, \phi_{32}$ to have nonzero vacuum expectation values, the pattern of symmetry breaking is the same as in (A) and (B), but the $SU(2)_R$ subgroup is different from either. It suffers from the same problems as the two previous cases, and they are again solved by adding η , with $\langle \eta_{31} \rangle \neq 0$ and $\langle \eta_{12} \rangle \neq 0$. However, in contrast to the variations (A) and (B), the ϕ_{33} and η_{33} entries are not neutral, so it is not possible to preserve $SU(2)_L \times SU(2)_R$ as a low-energy subgroup.

7.3 Gauge Boson Masses in (B)

Consider the breaking of $SU(3)_L \times SU(3)_R$ by a very large $\langle \eta_{33} \rangle = v_{33}$. Of the 8 vector gauge bosons W_i^L of $SU(3)_L$ and the 8 vector gauge bosons W_i^R of $SU(3)_R$, 9 become very heavy. The remaining 7 are the 3 of $SU(2)_L$, the 3 of $SU(2)_R$, and the one linear combination $W_8^V = (W_8^L + W_8^R)/\sqrt{2}$. We assume that they survive to just above the electroweak scale with equal couplings (g) for $SU(2)_L$ and $SU(2)_R$ and a different one (g') for $Y_L + Y_R$. Let $\langle \eta_{11} \rangle = v_{11}$, $\langle \phi_{22} \rangle = v_{22}$, $\langle \phi_{13} \rangle = v_{13}$, $\langle \phi_{31} \rangle = v_{31}$, then

$$M^2(W_{1,2}^R) = \frac{g^2}{2}[v_{11}^2 + v_{22}^2 + v_{31}^2], \quad (7.17)$$

where $(W_1^R \mp iW_2^R)/\sqrt{2} = W_R^\pm$ are the charged $SU(2)_R$ gauge bosons with odd R_B . The other gauge bosons have even R_B with

$$M^2(W_{1,2}^L) = \frac{g^2}{2}[v_{11}^2 + v_{22}^2 + v_{13}^2], \quad (7.18)$$

and the massless photon given by

$$A = \frac{e}{g}(W_3^L + W_3^R) - \frac{e}{g'}\sqrt{\frac{2}{3}}W_8^V. \quad (7.19)$$

This implies

$$\frac{e^2}{g'^2} = \frac{3}{2}(1 - 2\sin^2\theta_W). \quad (7.20)$$

If $g' = g$ (which is valid at the unification scale), then $\sin^2\theta_W = 3/8$ as expected. Now v_{31} breaks $SU(2)_R$ without breaking $SU(2)_L$, so its value may be greater than the electroweak scale. Its associated gauge boson Z' is given by

$$Z' = \frac{\sqrt{2}gW_3^R + \sqrt{3}g'W_8^V}{\sqrt{2g^2 + 3g'^2}} = \frac{1}{\cos\theta_W}[\sqrt{1 - 2\sin^2\theta_W}W_3^R + \sin\theta_W W_8^V]. \quad (7.21)$$

Hence the SM Z boson is now

$$Z = \cos \theta_W W_3^L - \tan \theta_W [\sin \theta_W W_3^R - \sqrt{1 - 2 \sin^2 \theta_W} W_8^V]. \quad (7.22)$$

The (Z, Z') mass-squared matrix is given by

$$M_{ZZ}^2 = \frac{g^2}{2 \cos^2 \theta_W} [v_{11}^2 + v_{22}^2 + v_{13}^2], \quad (7.23)$$

$$M_{Z'Z'}^2 = \frac{g^2}{2} \left[\frac{\cos^2 \theta_W}{1 - 2 \sin^2 \theta_W} v_{31}^2 + \frac{1 - 2 \sin^2 \theta_W}{\cos^2 \theta_W} (v_{11}^2 + v_{22}^2) + 2 \tan^2 \theta_W v_{13}^2 \right], \quad (7.24)$$

$$M_{ZZ'}^2 = \frac{g^2 \tan^2 \theta_W}{2 \sqrt{1 - 2 \sin^2 \theta_W}} [\sin^2 \theta_W v_{13}^2 - (1 - 2 \sin^2 \theta_W) (v_{11}^2 + v_{22}^2)]. \quad (7.25)$$

To avoid $Z - Z'$ mixing so as not to upset precision electroweak measurements, $M_{ZZ'}^2$ may be chosen to be negligible in the above.

In this alternative left-right model, $(u, h)_R$ and $(S, e)_R$ are $SU(2)_R$ doublets with h and S odd under R_B . The mass terms for u and ν come from v_{22} , those for d and e from v_{13} , those for h, E from v_{31} , and the 3×3 matrix spanning (N, N^c, S) from all three. As such, it contains the necessary ingredients for a consistent model of built-in dark matter. In variation (C), it has already been noted that $SU(2)_L \times SU(2)_R$ cannot be maintained as a low-energy subgroup. Hence the associated dark sector must be very heavy and does not lead to a realistic model. In variation (A), whereas $SU(2)_L \times SU(2)_R$ may emerge as a low-energy subgroup, the dark sector consists of singlets under this symmetry and must also be very heavy.

7.4 Dark Symmetries in $[SU(3)]^4$

The notion of leptonic color [67, 68] is based on quark-lepton interchange symmetry. Postulating $SU(3)_l$ to go with $SU(3)_q$, leptons have three color components to begin

with, but $SU(3)_l$ is broken to $SU(2)_l$ which remains exact, so that two of these leptonic color fields are confined in analogy to the three color quarks being confined. The third unconfined component is the observed lepton of the SM. The new particles of this model are not easily produced and observed at the Large Hadron Collider, but will have unique signatures in a future lepton collider, as recently discussed [82]. Under $SU(3)_q \times SU(3)_L \times SU(3)_l \times SU(3)_R$, $q \sim (3, 3^*, 1, 1)$ as in Eq. (1) and $q^c \sim (3^*, 1, 1, 3)$ as in Eqs. (3), (10), and (13) for the three variations (A,B,C) in parallel to what has been discussed for $[SU(3)]^3$. As for the leptonic sector,

$$l \sim (1, 3, 3^*, 1) \sim \begin{pmatrix} x_1 & x_2 & \nu \\ y_1 & y_2 & e \\ z_1 & z_2 & n \end{pmatrix} \quad (7.26)$$

is the same in all three variations, in analogy to q , whereas l^c has three variations to match q^c , i.e.

$$l^c \sim (1, 1, 3, 3^*) \sim \begin{pmatrix} x_1^c & y_1^c & z_1^c \\ x_2^c & y_2^c & z_2^c \\ \nu^c & e^c & n^c \end{pmatrix}, \quad \begin{pmatrix} z_1^c & y_1^c & x_1^c \\ z_2^c & y_2^c & x_2^c \\ n^c & e^c & \nu^c \end{pmatrix}, \quad \begin{pmatrix} x_1^c & z_1^c & y_1^c \\ x_2^c & z_2^c & y_2^c \\ \nu^c & n^c & e^c \end{pmatrix}. \quad (7.27)$$

The electric charge and dark charge in (A) are given by

$$Q = I_{3L} - \frac{Y_L}{2} + I_{3R} - \frac{Y_R}{2} - \frac{Y_l}{2}, \quad D_A = 3(Y_L - Y_R). \quad (7.28)$$

Hence

$$Q_l = \begin{pmatrix} 1/2 & 1/2 & 0 \\ -1/2 & -1/2 & -1 \\ 1/2 & 1/2 & 0 \end{pmatrix}, \quad Q_{l^c} = \begin{pmatrix} -1/2 & 1/2 & -1/2 \\ -1/2 & 1/2 & -1/2 \\ 0 & 1 & 0 \end{pmatrix}, \quad (7.29)$$

and $D_l = -D_{q^c}$ of Eq. (8), $D_{l^c} = -D_q$ of Eq. (6), i.e. $u, u^c, d, d^c, \nu, \nu^c, e, e^c, x, x^c, y, y^c$ have $D_A = 1$ (odd), whereas h, h^c, n, n^c, z, z^c have $D_A = -2$ (even). Again let $R_A = (-1)^{D_A+2j}$, then the former group of fermions is even and the latter odd, i.e. belonging to the dark sector if $U(1)_D$ is broken only by two units.

The breaking of $SU(3)_L \times SU(3)_R$ by a scalar bitriplet $\phi \sim (1, 3, 1, 3^*)$, which couples also to the fermions, proceeds as before. It has the same problems as discussed in the $[SU(3)]^3$ case. However, there are now two additional scalar bitriplets [66] in $[SU(3)]^4$ with nonzero vacuum expectation values, i.e.

$$\phi^L \sim (1, 3, 3^*, 1) \sim l, \quad \phi^R \sim (1, 1, 3, 3^*) \sim l^c. \quad (7.30)$$

They have thus the same would-be $[Q, D]$ assignments. They are not responsible for fermion masses, but are required to break leptonic color $SU(3)_l$ to $SU(2)_l$. Now ϕ_{33}^L has $D_A = 2$ which may be used to break $SU(3)_l \times SU(2)_L$ to $SU(2)_l \times SU(2)_L \times U(1)_{Y_l+Y_L}$. To break $SU(2)_R$ as well without breaking R_A , we use the same trick as before by assigning ϕ^R an odd parity under Z_2 as in $[SU(3)]^3$ for η . To preserve the R_A parity for the gauge bosons, we may again define ϕ_{i1}^R, ϕ_{i2}^R to be even, and ϕ_{i3}^R to be odd. Now $\langle \phi_{31}^R \rangle$ breaks $SU(3)_l$ to $SU(2)_l$, but it also breaks $SU(2)_R$ without breaking $SU(2)_L$. It allows thus the separation of the $SU(2)_R$ scale without breaking the dark parity R_A .

In the second variation (B), the electric charge is again the same as in (A) and the dark charge is the same as in (B) of $[SU(3)]^3$, i.e. Eq. (11). Using the same changes in the pattern of symmetry breaking as discussed before, a model with dark Z_2 symmetry is again achieved. Here $\langle \phi_{33}^R \rangle$ breaks $SU(3)_l \times SU(3)_R$ to $SU(2)_l \times SU(2)_R \times U(1)_{Y_l+Y_R}$ and separates the $SU(2)_l$ scale from the breaking of $SU(2)_R$ by $\langle \phi_{31} \rangle$. This is the analog of the

alternative left-right model in the $[SU(3)]^3$ case. Applying $\langle \phi_{33}^L \rangle$ as well, the residual $U(1)$ symmetry is now $Y_L + Y_R + Y_l$, exactly as needed for the electric charge of Eq. (28). In the third variation (C), the electric charge is

$$Q = I_{3L} - \frac{Y_L}{2} + Y_R - \frac{Y_l}{2}, \quad (7.31)$$

and the dark charge is the same as D_C of Eq. (14). It also results in a model with dark Z_2 symmetry. However, as with its $[SU(3)]^3$ analog, it is not possible to preserve $SU(2)_L \times SU(2)_R$ as a low-energy subgroup. Note that $\sin^2 \theta_W = 1/3$ at the unification scale for $[SU(3)]^4$ which is of order 10^{11} GeV for a nonsupersymmetric model [66, 82].

7.5 Conclusions

The existence of a dark sector is easily implemented by adding a new symmetry and new particles to the standard model. There are indeed numerous such proposals. As a guiding principle, supersymmetry is a well-known and perhaps the only example, where superpartners of all SM particles belong to the dark sector. In this paper, we suggest another, i.e. that such a dark symmetry may have a gauge origin buried inside a complete extended theoretical framework for the understanding of quarks and leptons. The inevitable consequence of this hypothesis is to divide all fermions, scalars, as well as *vector gauge bosons* into two categories. One includes all known particles of the SM and some new ones; the other is the dark sector. They are however intrinsically linked to each other as essential components of the unifying framework.

We consider as first examples $[SU(3)]^3$ and $[SU(3)]^4$, and identified the exact nature of this dark symmetry in three variations of the above two unified symmetries. We

have shown how this dark gauge symmetry is broken to the discrete Z_2 dark parity which stabilizes dark matter. Whereas all these models contain dark matter, only variation (B) in either $[SU(3)]^3$ or $[SU(3)]^4$ allows it to be such that it exists at or near the electroweak scale. They may serve as the prototypes for a deeper understanding of the origin of dark matter as a built-in symmetry of a theoretically motivated extension of the Standard Model. Our study points to the unity of matter with dark matter, the origin of which is not *ad hoc*. Other possible candidates are $SU(6)$ [90, 91] and $SU(7)$ [91]. Future more detailed explorations are called for.

Chapter 8

Alternative $[SU(3)]^4$ Model of Leptonic Color and Dark Matter

The alternative $[SU(3)]^4$ model of leptonic color and dark matter is discussed. It unifies at $M_U \sim 10^{14}$ GeV and has the low-energy subgroup $SU(3)_q \times SU(2)_l \times SU(2)_L \times SU(2)_R \times U(1)_X$ with $(u, h)_R$ instead of $(u, d)_R$ as doublets under $SU(2)_R$. It has the built-in global $U(1)$ dark symmetry which is generalized $B - L$. In analogy to $SU(3)_q$ quark triplets, it has $SU(2)_l$ hemion doublets which have half-integral charges and are confined by $SU(2)_l$ gauge bosons (stickons). In analogy to quarkonia, their vector bound states (hemionia) are uniquely suited for exploration at a future e^-e^+ collider.

8.1 Introduction

To venture beyond the Standard Model (SM) of quarks and leptons, there have been many trailblazing ideas. One is the notion of grand unification, i.e. the embedding

of the SM gauge symmetry $SU(3)_C \times SU(2)_L \times U(1)_Y$ in a single larger symmetry such as $SU(5) \sim E_4$, $SO(10) \sim E_5$, or E_6 . There are indeed very many papers devoted to this topic. Less visited are the symmetries $[SU(3)]^N$, where $N = 3, 4, 6$ have been considered [80, 81, 92, 66, 82, 93, 94, 95]. Another idea is that the $SU(2)_R$ quark doublet may not be $(u, d)_R$ but rather $(u, h)_R$ where h is an exotic quark of charge $-1/3$. This was originally motivated by superstring-inspired E_6 models [83, 84] and later generalized to nonsupersymmetric models [55, 56, 57, 85], but is easily implemented in $[SU(3)]^N$ models. A third idea is quark-lepton interchange symmetry [67, 68] which assumes $SU(3)_l$ for leptons in parallel to $SU(3)_q$ for quarks, but with $SU(3)_l$ broken to $SU(2)_l \times U(1)_{Y_l}$. This is naturally embedded in $[SU(3)]^4$ [66] and implies that only one component of the color lepton triplet is free, i.e. the observed lepton, whereas the other two color components (with half-integral charges) are confined in analogy to the three color components of a quark triplet. Finally a fourth idea has been put forward recently [93, 96] that a dark symmetry may exist within $[SU(3)]^N$ itself or perhaps $[SU(3)]^N \times U(1)$. This new insight points to the possible intrinsic unity of matter with dark matter [90, 91, 97].

In this paper, all four of the above ideas are incorporated into a single consistent framework based on the symmetry $SU(3)_q \times SU(3)_L \times SU(3)_l \times SU(3)_R$. The three families of quarks and leptons are contained in the bifundamental chain $(3, 3^*, 1, 1) + (1, 3, 3^*, 1) + (1, 1, 3, 3^*) + (3^*, 1, 1, 3)$ which also include other fermions beyond the SM. This unifying symmetry is broken by two bifundamental scalars at M_U to $SU(3)_q \times SU(2)_l \times SU(2)_L \times SU(2)_R \times U(1)_X$ in such a way that a residual global $U(1)_D$ symmetry remains. This important property guarantees that a dark sector exists for a set of fermions, scalars, and

vector gauge bosons. Because of the necessary particle content of $[SU(3)]^4$, this $U(1)_D$ may be identified as generalized $B - L$ [25], under which quarks have charge $1/3$ and leptons have charge -1 , but the other particles have different values.

At M_R of order a TeV, $SU(2)_R \times U(1)_X$ is broken to $U(1)_Y$ of the SM, with particle content of the SM plus possible light particles transforming under the leptonic color $SU(2)_l$ symmetry. We will discuss their impact on cosmology as well as their possible revelation at a future e^-e^+ collider, following closely our previous work [82] on the subject. We will also consider the phenomenology associated with the $SU(2)_R$ gauge symmetry and the possible dark-matter candidates of this model.

8.2 Fermion Content and Dark Symmetry

All fermions belong to bitriplet representations $(3, 3^*)$ under $SU(3)_A \times SU(3)_B$, where $SU(3)_A$ acts vertically from up to down with $I_{3A} = (1/2, -1/2, 0)$ and $Y_A = (1, 1, -2)/(2\sqrt{3})$, and $SU(3)_B$ horizontally from left to right with $I_{3B} = (-1/2, 1/2, 0)$ and $Y_B = (-1, -1, 2)/(2\sqrt{3})$. The dark symmetry we will consider is

$$D = \sqrt{3}(-2Y_L + \sqrt{3}I_{3R} + Y_R - 2Y_l). \quad (8.1)$$

Under $SU(3)_q \times SU(3)_L \times SU(3)_l \times SU(3)_R$, the fermion content of our model is then given by

$$q \sim (3, 3^*, 1, 1) \sim \begin{pmatrix} d & u & h \\ d & u & h \\ d & u & h \end{pmatrix}, \quad D_q \sim \begin{pmatrix} 1 & 1 & -2 \\ 1 & 1 & -2 \\ 1 & 1 & -2 \end{pmatrix}, \quad (8.2)$$

$$l \sim (1, 3, 3^*, 1) \sim \begin{pmatrix} x_1 & x_2 & \nu \\ y_1 & y_2 & e \\ z_1 & z_2 & n \end{pmatrix}, \quad D_l \sim \begin{pmatrix} 0 & 0 & -3 \\ 0 & 0 & -3 \\ 3 & 3 & 0 \end{pmatrix}, \quad (8.3)$$

$$l^c \sim (1, 1, 3, 3^*) \sim \begin{pmatrix} z_1^c & y_1^c & x_1^c \\ z_2^c & y_2^c & x_2^c \\ n^c & e^c & \nu^c \end{pmatrix}, \quad D_{l^c} \sim \begin{pmatrix} -3 & 0 & 0 \\ -3 & 0 & 0 \\ 0 & 3 & 3 \end{pmatrix}, \quad (8.4)$$

$$q^c \sim (3^*, 1, 1, 3) \sim \begin{pmatrix} h^c & h^c & h^c \\ u^c & u^c & u^c \\ d^c & d^c & d^c \end{pmatrix}, \quad D_{q^c} \sim \begin{pmatrix} 2 & 2 & 2 \\ -1 & -1 & -1 \\ -1 & -1 & -1 \end{pmatrix}, \quad (8.5)$$

where u has charge $2/3$, d, h have charge $-1/3$, x, z have charge $1/2$, y has charge $-1/2$, ν, n have charge 0 , and e has charge -1 . Using

$$R_D = (-1)^{D+2j}, \quad (8.6)$$

we see that $u, u^c, d, d^c, \nu, \nu^c, e, e^c, z, z^c$ are even, and $h, h^c, x, x^c, y, y^c, n, n^c$ are odd. Further, the gauge bosons which take h to u, d in $SU(3)_L$ and h^c to u^c, d^c in $SU(3)_R$ are odd, as well as the corresponding ones in $SU(3)_l$, and the others even, including all those of the SM. Hence R_D would remain a good symmetry for dark matter provided that the scalar sector responsible for the symmetry breaking obeys it as well.

The scalar bitriplets responsible for the masses of the fermions in Eqs. (2) to (5) come from three chains, each of the form $(3, 1, 3^*, 1) + (1, 3, 1, 3^*) + (3^*, 1, 3, 1) + (1, 3^*, 1, 3)$. Specifically,

$$\phi^{(1,3,5)} \sim (1, 3, 1, 3^*) \sim \begin{pmatrix} \eta^0 & \phi_2^+ & \phi_1^0 \\ \eta^- & \phi_2^0 & \phi_1^- \\ \chi^0 & \chi^+ & \lambda^0 \end{pmatrix}, \quad D_\phi \sim \begin{pmatrix} -3 & 0 & 0 \\ -3 & 0 & 0 \\ 0 & 3 & 3 \end{pmatrix}, \quad (8.7)$$

$$\bar{\phi}^{(2,4,6)} \sim (1, 3^*, 1, 3) \sim \begin{pmatrix} \bar{\eta}^0 & \eta^+ & \bar{\chi}^0 \\ \phi_2^- & \bar{\phi}_2^0 & \chi^- \\ \bar{\phi}_1^0 & \phi_1^+ & \bar{\lambda}^0 \end{pmatrix}, \quad D_{\bar{\phi}} \sim \begin{pmatrix} 3 & 3 & 0 \\ 0 & 0 & -3 \\ 0 & 0 & -3 \end{pmatrix}. \quad (8.8)$$

From the $q^c q \phi$ terms, we obtain masses of hh^c from $\langle \chi^0 \rangle^{(1)}$, dd^c from $\langle \phi_1^0 \rangle^{(3)}$, uu^c from $\langle \phi_2^0 \rangle^{(5)}$. From the $l^c \bar{\phi}$ terms, we obtain masses of nn^c, zz^c from $\langle \bar{\chi}^0 \rangle^{(2)}$, $\nu\nu^c, xx^c$ from $\langle \bar{\phi}_1^0 \rangle^{(4)}$, ee^c, yy^c from $\langle \bar{\phi}_2^0 \rangle^{(6)}$. It is clear that D and thus R_D remain unbroken by the above vacuum expectation values.

8.3 Symmetry Breaking Pattern

We consider the breaking of $[SU(3)]^4$ at M_U by two scalar bitriplets, one transforming as $\phi^{L+} \sim (1, 3, 3^*, 1) \sim l$, belonging to a chain in parallel to the fermions, the other transforming as $\phi^{R-} \sim (1, 1, 3, 3^*) \sim l^c$, belonging to a chain with an additional overall imposed assignment of odd R_D , i.e. an additional Z_2 factor [93]. This preserves the relative R_D among its components, but prevents it from coupling to the fermions. Using $\langle \phi_{33}^{L+} \rangle$ with even R_D to break $SU(3)_L \times SU(3)_l$ to $SU(2)_L \times SU(2)_l \times U(1)_{(Y_L+Y_l)/\sqrt{2}}$ and $\langle \phi_{33}^{R-} \rangle$ which also has even R_D to break $SU(3)_l \times SU(3)_R$ to $SU(2)_l \times SU(2)_R \times U(1)_{(Y_l+Y_R)/\sqrt{2}}$,

the resulting theory preserves R_D . Assuming also that all the particles of the chain associated with ϕ^{R-} are superheavy, the low-energy theory with the residual gauge symmetry $SU(3)_q \times SU(2)_l \times SU(2)_L \times SU(2)_R \times U(1)_X$, where $X = (Y_L + Y_R + Y_l)/\sqrt{3}$, also preserves D .

Since there are three fermion chains, and five scalar chains, the b coefficients for the renormalization-group running of each $SU(3)$ gauge coupling are all given by

$$b = -11 + \frac{2}{3} \left(\frac{1}{2}\right) (2)(3)(3) + \frac{1}{3} \left(\frac{1}{2}\right) (2)(3)(5) = 0. \quad (8.9)$$

This shows that we have a possible finite field theory [92] above M_U .

At M_R , the $SU(2)_R \times U(1)_X$ gauge symmetry is broken to $U(1)_Y$ of the SM, where $Y = I_{3R} - X$, by an $SU(2)_R$ doublet whose neutral component is a linear combination of χ^0 from $\phi^{(1)}$, the conjugate of $\bar{\chi}^0$ from $\bar{\phi}^{(2)}$, and ϕ_{31}^{R+} from the $(1, 1, 3, 3^*)$ component of the chain containing ϕ^{L+} discussed previously. From the allowed antisymmetric trilinear term $l^c l^c \phi^{R+}$, the mass term $x_1^c y_2^c - x_2^c y_1^c$ is then obtained. Note that the corresponding mass term $x_1 y_2 - x_2 y_1$ is superheavy because it comes from $\langle \phi_{33}^{L+} \rangle$. Note also that the corresponding term $l^c l^c \phi^{R-}$ is forbidden because of the overall assignment of odd R_D for ϕ^{R-} . Finally the symmetry $SU(2)_L \times U(1)_Y$ is broken by two $SU(2)_L$ doublets to $U(1)_{em}$ with $Q = I_{3L} + Y$.

8.4 Renormalization-Group Running of Gauge Couplings

The renormalization-group evolution of the gauge couplings is dictated at leading order by

$$\frac{1}{\alpha_i(\mu)} = \frac{1}{\alpha_i(\mu')} + \frac{b_i}{2\pi} \ln \left(\frac{\mu'}{\mu} \right), \quad (8.10)$$

where b_i are the one-loop beta-function coefficients. From M_U to M_R , we assume that all fermions are light except the three families of (x, y) hemions. As for the scalars, we assume that only the following multiplets are light under $SU(2)_L \times SU(2)_R \times U(1)_X$: 1 copy of $(1, 2, -1/2)$, 6 copies of $(2, 2, 0)$, 3 copies of $(2, 1, -1/2)$, and 4 copies of $(2, 1, 1/2)$. This choice requires fine tuning in the scalar sector as in other models of grand unification such as $SU(5)$ and $SO(10)$. As a result, the five b coefficients are given by

$$b_q = -11 + \frac{2}{3} \left(\frac{1}{2} \right) (6)(3) = -5, \quad (8.11)$$

$$b_l = -\frac{22}{3} + \frac{2}{3} \left(\frac{1}{2} \right) (4)(3) = -\frac{10}{3}, \quad (8.12)$$

$$b_L = -\frac{22}{3} + \frac{2}{3} \left(\frac{1}{2} \right) (3+1)(3) + \frac{1}{3} \left(\frac{1}{2} \right) [7+6(2)] = -\frac{1}{6}, \quad (8.13)$$

$$b_R = -\frac{22}{3} + \frac{2}{3} \left(\frac{1}{2} \right) (3+2+1)(3) + \frac{1}{3} \left(\frac{1}{2} \right) [1+6(2)] = \frac{5}{6}, \quad (8.14)$$

$$b_X = \frac{2}{3} \left[\frac{1}{6}(3) + \frac{1}{6}(3) + \frac{1}{4}(4) + \frac{1}{4}(4) \right] (3) + \frac{1}{3} \left(\frac{1}{4} \right) [2+7(2)] = \frac{22}{3}. \quad (8.15)$$

From M_R to M_Z , we assume the SM quark and lepton content together with 1 copy of (x^c, y^c) hemions and two $SU(2)_L$ Higgs scalar doublets. The massless $SU(2)_l$ stickons are of course included but they affect only α_l . The four b coefficients are then

$$b_q = -11 + \frac{2}{3} \left(\frac{1}{2} \right) (4)(3) = -7, \quad (8.16)$$

$$b_l = -\frac{22}{3} + \frac{2}{3} \left(\frac{1}{2} \right) (2) = -\frac{20}{3}, \quad (8.17)$$

$$b_L = -\frac{22}{3} + \frac{2}{3} \left(\frac{1}{2} \right) (3+1)(3) + \frac{1}{3} \left(\frac{1}{2} \right) (2) = -3, \quad (8.18)$$

$$b_Y = \frac{1}{2} \left[\frac{2}{3} \left\{ \frac{10}{3}(3) + \frac{1}{4}(4) \right\} + \frac{1}{3} \left(\frac{1}{4} \right) (4) \right] = \frac{23}{6}, \quad (8.19)$$

where a factor of 1/2 has been inserted to normalize b_Y . The boundary condition at M_R

for $SU(2)_R \times U(1)_X$ to become $U(1)_Y$ is

$$\frac{2}{\alpha_Y(M_R)} = \frac{1}{\alpha_R(M_R)} + \frac{1}{\alpha_X(M_R)}. \quad (8.20)$$

We then obtain

$$\frac{1}{\alpha_q(M_Z)} = \frac{1}{\alpha_U} - \frac{7}{2\pi} \ln \frac{M_R}{M_Z} - \frac{5}{2\pi} \ln \frac{M_U}{M_R}, \quad (8.21)$$

$$\frac{1}{\alpha_L(M_Z)} = \frac{1}{\alpha_U} - \frac{3}{2\pi} \ln \frac{M_R}{M_Z} - \frac{1}{6(2\pi)} \ln \frac{M_U}{M_R}, \quad (8.22)$$

$$\frac{1}{\alpha_Y(M_Z)} = \frac{1}{\alpha_U} + \frac{23}{6(2\pi)} \ln \frac{M_R}{M_Z} + \frac{49}{12(2\pi)} \ln \frac{M_U}{M_R}. \quad (8.23)$$

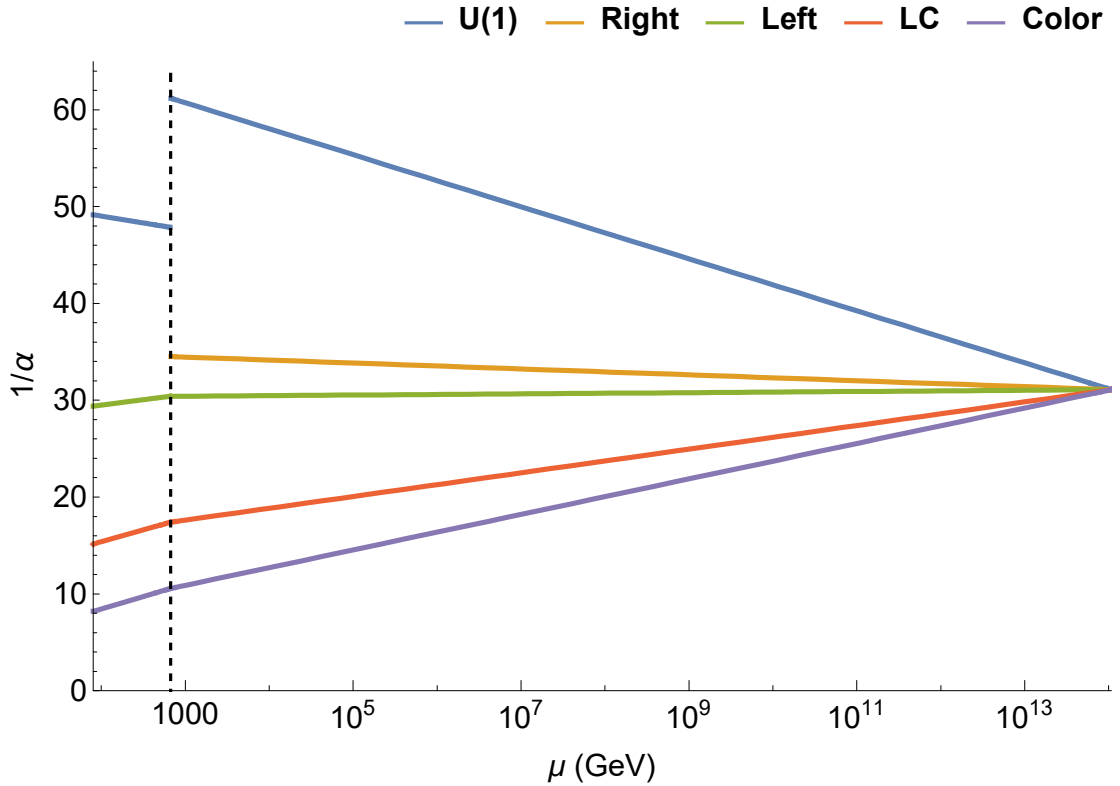


Figure 8.1: Evolution of α_i^{-1} as a function of energy scale.

Using the experimental inputs

$$\alpha_q(M_Z) = 0.1185, \quad (8.24)$$

$$\alpha_L(M_Z) = (\sqrt{2}/\pi)G_F M_W^2 = 0.0339, \quad (8.25)$$

$$\alpha_Y(M_Z) = 2\alpha_L(M_Z) \tan^2 \theta_W = 0.0204, \quad (8.26)$$

where a factor of 2 has been used to normalize α_Y , we find

$$\frac{1}{0.0339} - \frac{1}{0.1185} = 21.06 = \frac{4}{2\pi} \ln \frac{M_R}{M_Z} + \frac{29}{6(2\pi)} \ln \frac{M_U}{M_R}, \quad (8.27)$$

$$\frac{1}{0.0204} - \frac{1}{0.0339} = 19.52 = \frac{41}{6(2\pi)} \ln \frac{M_R}{M_Z} + \frac{17}{4(2\pi)} \ln \frac{M_U}{M_R}. \quad (8.28)$$

This implies $M_R \simeq 600$ GeV and $M_U \simeq 10^{14}$ GeV, as shown in Fig. 1. The 5 lines emanating from a common point at 10^{14} GeV represent $U(1)_X$, $SU(2)_R$, $SU(2)_L$, $SU(2)_l$, and $SU(3)_q$ from top to bottom. The line between M_R and M_Z represents normalized $U(1)_Y$. Since there are uncertainties (both theoretical and experimental) in the above estimate, the value of M_R should not be taken too literally, but rather an indication that particles transforming under $SU(2)_R$ have masses of an order of magnitude greater than those of the SM. As a result, $\alpha_U = 0.0322$. Using

$$\frac{1}{\alpha_R(M_R)} = \frac{1}{\alpha_U} + \frac{5}{6(2\pi)} \ln \frac{M_U}{M_R}, \quad (8.29)$$

we obtain $\alpha_R(M_R) = 0.0290$. Using

$$\frac{1}{\alpha_l(M_Z)} - \frac{1}{\alpha_q(M_Z)} = \frac{1}{3(2\pi)} \ln \frac{M_R}{M_Z} + \frac{5}{3(2\pi)} \ln \frac{M_U}{M_R}, \quad (8.30)$$

we obtain $\alpha_l = 0.0650$, implying a confining scale of about 0.4 MeV from leptonic color.

This is significantly different from the result of the $[SU(3)]^4$ model with $M_R = M_U$, where it is a few keV [66, 82].

8.5 Low-Energy Particle Content

The particles of this model at or below a few TeV are listed in Table 1 under $SU(3)_q \times SU(2)_l \times SU(2)_L \times SU(2)_R \times U(1)_X \times D$, where $X = (Y_L + Y_R + Y_l)/\sqrt{3}$ (each Y normalized according to $\sum Y^2 = 1/2$), $D = \sqrt{3}(-2Y_L + \sqrt{3}I_{3R} + Y_R - 2Y_l)$, and $Q = I_{3L} + I_{3R} - X$. The $SU(2)_L \times SU(2)_R$ scalar bidoublet contains the $SU(2)_L$ doublets

Table 8.1: Particle content of proposed model.

particles	$SU(3)_q$	$SU(2)_l$	$SU(2)_L$	$SU(2)_R$	$U(1)_X$	D	S	$I_{3R} + S$
$(u, d)_L$	3	1	2	1	-1/6	(1,1)	1/3	1/3
$(u, h)_R$	3	1	1	2	-1/6	(1, -2)	-1/6	(1/3, -2/3)
d_R	3	1	1	1	1/3	1	1/3	1/3
h_L	3	1	1	1	1/3	-2	-2/3	-2/3
$(\nu, l)_L$	1	1	2	1	1/2	(-3, -3)	-1	-1
$(n, l)_R$	1	1	1	2	1/2	(0, -3)	-1/2	(0, -1)
ν_R	1	1	1	1	0	-3	-1	-1
n_L	1	1	1	1	0	0	0	0
$(z, y)_R$	1	2	1	2	0	(3, 0)	1/2	(1, 0)
x_R	1	2	1	1	-1/2	0	0	0
z_L	1	2	1	1	-1/2	3	1	1
(ϕ_1^0, ϕ_1^-)	1	1	2	1	1/2	0	0	0
(χ^+, χ^0)	1	1	1	2	-1/2	(3, 0)	1/2	(1, 0)
(η, Φ_2)	1	1	2	2	0	(-3, 0)	-1/2	(-1, 0)
λ^0	1	1	1	1	0	3	1	1

$\eta = (\eta^0, \eta^-)$ and $\Phi_2 = (\phi_2^+, \phi_2^0)$, with η heavy at the M_R scale. Because of the assumed symmetry breaking pattern, our model actually possesses a conserved global symmetry

$$S = \frac{1}{\sqrt{3}}(Y_R - 2Y_L - 2Y_l) \quad (8.31)$$

before $SU(2)_R$ breaking, even though the corresponding gauge symmetry has been broken.

Whereas both S and I_{3R} are broken by $\langle \chi^0 \rangle$, the combination

$$I_{3R} + S = \frac{D}{3} \quad (8.32)$$

is unbroken. Although this idea was used previously [55, 56], the important observation here is that $I_{3R} + S$ coincides with the usual definition of $B - L$ for the known quarks and leptons, but takes on different values for the other particles. Hence $D/3$ may be defined as generalized $B - L$ and functions as a global dark $U(1)$ symmetry. Now

$$R_D = (-1)^{3B-3L+2j} \quad (8.33)$$

so that it is identical to the usual definition of R parity in supersymmetry for the SM particles. Here the odd R_D particles are the h, n, x, y fermions, $(\eta^0, \eta^-), \lambda^0$ scalars, and W_R^\pm vector bosons. Note that leptonic color $SU(2)_l$ confines the x, y hemions to bosons which must then have even R_D .

To verify that generalized $B - L$ is indeed a global dark $U(1)$ symmetry of our model, consider the $SU(2)_R$ gauge bosons (W_R^+, W_R^0, W_R^-) which has $S = 0$. Hence they have $I_{3R} + S$ values $(1, 0, -1)$. This is expected because W_R^+ takes h_R to u_R and l_R to n_R . Consider next the Yukawa terms allowed by the gauge symmetry and S , i.e.

$$\bar{d}_R(u_L\phi_1^- - d_L\phi_1^0), \quad \bar{u}_R(u_L\phi_2^0 - d_L\phi_2^+) + \bar{h}_R(-u_L\eta^- + d_L\eta^0), \quad (\chi^+\bar{u}_R - \chi^0\bar{h}_R)h \quad (8.34)$$

$$(\phi_1^0\bar{\nu}_L + \phi_1^-\bar{l}_L)\nu_R, \quad \bar{\nu}_L(n_R\eta^0 + l_R\phi_2^+) + \bar{l}_L(n_R\eta^- + l_R\phi_2^0), \quad \bar{n}_L(n_R\chi^0 - l_R\chi^+), \quad (8.35)$$

$$\bar{z}_L(z_R\chi^0 - y_R\chi^+), \quad \bar{x}_R(\bar{z}_R\chi^+ + \bar{y}_R\chi^0), \quad \bar{d}_Rh_L\lambda^0, \quad \bar{n}_L\nu_R\lambda^0, \quad \bar{z}_Lx_R\lambda^0, \quad z_Ry_R\bar{\lambda}^0 \quad (8.36)$$

and the scalar trilinear terms

$$\phi_1^-(\eta^0\chi^+ + \phi_2^+\chi^0) - \phi_1^0(\eta^-\chi^+ + \phi_2^0\chi^0), \quad \lambda^0(\eta^0\phi_2^0 - \eta^-\phi_2^+). \quad (8.37)$$

It is easily confirmed from the above that $I_{3R} + S$ is not broken by $\langle \phi_{1,2}^0 \rangle$ and $\langle \chi^0 \rangle$. Note that in the familiar case of $SU(5)$ grand unification, neither B nor L is part of $SU(5)$ but both exist as low-energy conserved quantities. Here, B and L are again not part of $[SU(3)]^4$ separately, but a generalized $B-L$ emerges, and remains unbroken to be naturally interpreted as a global dark symmetry.

8.6 Gauge Sector

Let

$$\langle \phi_1^0 \rangle = v_1, \quad \langle \phi_2^0 \rangle = v_2, \quad \langle \chi^0 \rangle = v_R, \quad (8.38)$$

then the $SU(3)_q \times SU(2)_l \times SU(2)_L \times SU(2)_R \times U(1)_X$ gauge symmetry is broken to $SU(3)_q \times SU(2)_l \times U(1)_{em}$ with a residual global $I_{3R} + S$ as the dark symmetry, as explained previously.

Consider now the masses of the gauge bosons. The charged ones, W_L^\pm and W_R^\pm , do not mix because the latter have dark charge ± 1 . Their masses are given by

$$M_{W_L}^2 = \frac{1}{2}g_L^2(v_1^2 + v_2^2), \quad M_{W_R}^2 = \frac{1}{2}g_R^2(v_R^2 + v_2^2). \quad (8.39)$$

Since $Q = I_{3L} + I_{3R} - X$, the photon is given by

$$A = \frac{e}{g_L}W_{3L} + \frac{e}{g_R}W_{3R} + \frac{e}{g_X}Z_X, \quad (8.40)$$

where $e^{-2} = g_L^{-2} + g_R^{-2} + g_X^{-2}$. Let

$$Z = (g_L^2 + g_Y^2)^{-1/2} \left(g_L W_{3L} - \frac{g_Y^2}{g_R} W_{3R} - \frac{g_Y^2}{g_X} Z_X \right), \quad (8.41)$$

$$Z' = (g_R^2 + g_X^2)^{-1/2} (g_R W_{3R} - g_X Z_X), \quad (8.42)$$

where $g_Y^{-2} = g_R^{-2} + g_X^{-2}$, then the 2×2 mass-squared matrix spanning (Z, Z') is given by

$$\frac{1}{2} \begin{pmatrix} (g_L^2 + g_Y^2)(v_1^2 + v_2^2) & (\sqrt{g_L^2 + g_Y^2}/\sqrt{g_R^2 + g_X^2})(g_X^2 v_1^2 - g_R^2 v_2^2) \\ (\sqrt{g_L^2 + g_Y^2}/\sqrt{g_R^2 + g_X^2})(g_X^2 v_1^2 - g_R^2 v_2^2) & (g_R^2 + g_X^2)v_R^2 + (g_X^4 v_1^2 + g_R^4 v_2^2)/(g_R^2 + g_X^2) \end{pmatrix} \quad (8.43)$$

Their neutral-current interactions are given by

$$\mathcal{L}_{NC} = eA_\mu j_Q^\mu + g_Z Z_\mu (j_{3L}^\mu - \sin^2 \theta_W j_{em}^\mu) + (g_R^2 + g_X^2)^{-1/2} Z'_\mu (g_R^2 j_{3R}^\mu + g_X^2 j_X^\mu), \quad (8.44)$$

where $g_Z^2 = g_L^2 + g_Y^2$ and $\sin^2 \theta_W = g_Y^2/g_Z^2$. Since $Z - Z'$ mixing is constrained by experiment to be less than 10^{-4} or so, we assume $(g_X^2 v_1^2 - g_R^2 v_2^2)/v_R^2$ to be negligible.

The new gauge boson Z' may be produced at the Large Hadron Collider (LHC) through their couplings to u and d quarks, and decay to charged leptons ($e^- e^+$ and $\mu^- \mu^+$). Hence current search limits for a Z' boson are applicable. Using $\alpha_R(M_R) = 0.0290$ and $\alpha_X(M_R) = 0.0163$, the $c_{u,d}$ coefficients [46, 16] used in the data analysis for our model are

$$c_u = (g_{uL}^2 + g_{uR}^2)B = 0.04 B, \quad c_d = (g_{dL}^2 + g_{dR}^2)B = 0.01 B, \quad (8.45)$$

where B is the branching fraction of Z' to $e^- e^+$ and $\mu^- \mu^+$. Assuming that Z' decays to all the particles listed in Table 1, except for the scalars which become the longitudinal components of the various gauge bosons, we find $B = 0.044$. Based on the 2016 LHC 13 TeV data set [98], this translates to a bound of about 3 to 4 TeV on the Z' mass.

8.7 Scalar Sector

Consider the most general scalar potential consisting of $\Phi_L = (\phi_1^0, \phi_1^-)$, $\chi_R = (\chi^+, \chi^0)$, λ^0 , and

$$\eta = \begin{pmatrix} \eta^0 & \phi_2^+ \\ \eta^- & \phi_2^0 \end{pmatrix}, \quad \tilde{\eta} = \sigma_2 \eta^* \sigma_2 = \begin{pmatrix} \bar{\phi}_2^0 & -\eta^+ \\ -\phi_2^- & \bar{\eta}^0 \end{pmatrix}, \quad (8.46)$$

then

$$\begin{aligned} V &= -\mu_L^2 \Phi_L^\dagger \Phi_L - \mu_R^2 \chi_R^\dagger \chi_R - \mu_\eta^2 \text{Tr}(\eta^\dagger \eta) - \mu_\lambda^2 \bar{\lambda} \lambda + [\mu_1 \Phi_L^\dagger \eta \chi_R + \mu_2 \lambda \det(\eta) + H.c.] \\ &+ \frac{1}{2} f_L (\Phi_L^\dagger \Phi_L)^2 + \frac{1}{2} f_R (\chi_R^\dagger \chi_R)^2 + \frac{1}{2} f_\lambda (\bar{\lambda} \lambda)^2 + \frac{1}{2} f_\eta [\text{Tr}(\eta^\dagger \eta)]^2 + \frac{1}{2} f'_\eta \text{Tr}(\eta^\dagger \eta \eta^\dagger \eta) \\ &+ f_{LR} (\Phi_L^\dagger \Phi_L) (\chi_R^\dagger \chi_R) + f_{L\lambda} (\Phi_L^\dagger \Phi_L) (\bar{\lambda} \lambda) + f_{R\lambda} (\chi_R^\dagger \chi_R) (\bar{\lambda} \lambda) + f_{\lambda\eta} (\bar{\lambda} \lambda) \text{Tr}(\eta^\dagger \eta) \\ &+ f_{L\eta} \Phi_L^\dagger \eta \eta^\dagger \Phi_L + f'_{L\eta} \Phi_L^\dagger \tilde{\eta} \tilde{\eta}^\dagger \Phi_L + f_{R\eta} \chi_R^\dagger \eta^\dagger \eta \chi_R + f'_{R\eta} \chi_R^\dagger \tilde{\eta}^\dagger \tilde{\eta} \chi_R. \end{aligned} \quad (8.47)$$

Note that

$$2|\det(\eta)|^2 = [\text{Tr}(\eta^\dagger \eta)]^2 - \text{Tr}(\eta^\dagger \eta \eta^\dagger \eta), \quad (8.48)$$

$$(\Phi_L^\dagger \Phi_L) \text{Tr}(\eta^\dagger \eta) = \Phi_L^\dagger \eta \eta^\dagger \Phi_L + \Phi_L^\dagger \tilde{\eta} \tilde{\eta}^\dagger \Phi_L, \quad (8.49)$$

$$(\chi_R^\dagger \chi_R) \text{Tr}(\eta^\dagger \eta) = \chi_R^\dagger \eta^\dagger \eta \chi_R + \chi_R^\dagger \tilde{\eta}^\dagger \tilde{\eta} \chi_R. \quad (8.50)$$

The minimum of V satisfies the conditions

$$\mu_L^2 = f_L v_1^2 + f_{L\eta} v_2^2 + f_{LR} v_R^2 + \mu_1 v_2 v_R / v_1, \quad (8.51)$$

$$\mu_\eta^2 = (f_\eta + f'_\eta) v_2^2 + f_{L\eta} v_1^2 + f_{R\eta} v_R^2 + \mu_1 v_1 v_R / v_2, \quad (8.52)$$

$$\mu_R^2 = f_R v_R^2 + f_{LR} v_1^2 + f_{R\eta} v_2^2 + \mu_1 v_1 v_2 / v_R. \quad (8.53)$$

The 3×3 mass-squared matrix spanning $\sqrt{2}Im(\phi_1^0, \phi_2^0, \chi^0)$ is then given by

$$\mathcal{M}_I^2 = \mu_1 \begin{pmatrix} -v_2 v_R / v_1 & v_R & v_2 \\ v_R & -v_1 v_R / v_2 & v_1 \\ v_2 & v_1 & -v_1 v_2 / v_R \end{pmatrix}. \quad (8.54)$$

and that spanning $\sqrt{2}Re(\phi_1^0, \phi_2^0, \chi^0)$ is

$$\mathcal{M}_R^2 = \mathcal{M}_I^2 + 2 \begin{pmatrix} f_L v_1^2 & f_{L\eta} v_1 v_2 & f_{LR} v_1 v_R \\ f_{L\eta} v_1 v_2 & (f_\eta + f'_\eta) v_2^2 & f_{R\eta} v_2 v_R \\ f_{LR} v_1 v_R & f_{R\eta} v_2 v_R & f_R v_R^2 \end{pmatrix}. \quad (8.55)$$

Hence there are two zero eigenvalues in \mathcal{M}_I^2 with one nonzero eigenvalue $-\mu_1[v_1 v_2 / v_R + v_R(v_1^2 + v_2^2) / v_1 v_2]$ corresponding to the eigenstate $(-v_1^{-1}, v_2^{-1}, v_R^{-1}) / \sqrt{v_1^{-2} + v_2^{-2} + v_R^{-2}}$. In \mathcal{M}_R^2 , the linear combination $H = (v_1, v_2, 0) / \sqrt{v_1^2 + v_2^2}$, is the standard-model Higgs boson, with

$$m_H^2 = 2[f_L v_1^4 + (f_\eta + f'_\eta) v_2^4 + 2f_{L\eta} v_1^2 v_2^2] / (v_1^2 + v_2^2). \quad (8.56)$$

The other two scalar bosons are much heavier, with suppressed mixing to H , which may all be assumed to be small enough to avoid the constraints from dark-matter direct-search experiments.

The dark scalars are λ^0 , χ^\pm , and (η^0, η^-) . Whereas χ^\pm become the longitudinal components of W_R^\pm , the other scalars have the interaction

$$\mu_2 \lambda^0 (\eta^0 \phi_2^0 - \eta^- \phi_2^+) + H.c. \quad (8.57)$$

The 2×2 mass-squared matrix linking $(\lambda, \bar{\eta})$ to $(\bar{\lambda}, \eta)$ is given by

$$\mathcal{M}_{\lambda-\eta}^2 = \begin{pmatrix} -\mu_\lambda^2 + f_{L\lambda} v_1^2 + f_{R\lambda} v_R^2 + f_{\lambda\eta} v_2^2 & \mu_2 v_2 \\ \mu_2 v_2 & -\mu_\eta^2 + f_\eta v_2^2 + f'_{L\eta} v_1^2 + f'_{R\eta} v_R^2 \end{pmatrix}. \quad (8.58)$$

We assume μ_2 to be very small so that there is negligible mixing, with λ^0 as the lighter particle which is our dark-matter candidate. Note of course that η^0 is not a suitable candidate because it has Z^0 interactions.

8.8 Dark Matter Interactions

Consider the scalar singlet λ^0 as our dark-matter candidate. Let its coupling with the SM Higgs boson be $f_{\lambda H}\sqrt{2}v_H$, then it has been shown [85] that for $m_\lambda = 150$ GeV, $f_{\lambda H} < 4.4 \times 10^{-4}$ from the most recent direct-search result [99]. With such a small coupling, the λ^0 annihilation cross section in the early Universe through the SM Higgs boson is much too small for λ^0 to have the correct observed relic abundance. Hence a different process is required.

Consider then the Yukawa sector. As noted in Eq. (36), the interactions $f_x\lambda^0\bar{z}_Lx_R$ and $f_y\bar{\lambda}^0z_Ry_R$ exist. Now x_R/y_R forms a Dirac hemion and has been assumed to be light in the previous analysis on the renormalization-group running of gauge couplings. For convenience, the outgoing y_R may be redefined as incoming x_L . Let $m_\lambda > m_x$, then $\lambda^0\bar{\lambda}^0 \rightarrow x\bar{x}$ through z exchange is possible as shown in Fig. 2. Let $f_y = f_x^*$ so that the $\lambda^0\bar{z}x$ interaction is purely scalar. The cross section \times relative velocity is then given by

$$\sigma v_{rel} = \frac{f_x^4}{4\pi} \left(1 - \frac{m_x^2}{m_\lambda^2}\right)^{3/2} \frac{(m_z + m_x)^2}{(m_z^2 + m_\lambda^2 - m_x^2)^2}. \quad (8.59)$$

As an example, let $m_\lambda = 150$ GeV, $m_x = 100$ GeV, and $m_z = 600$ GeV, then $\sigma v_{rel} = 1$ pb is obtained for $f_x = 0.385$. The $x\bar{x}$ final states remain in thermal equilibrium through the photon, with their confined bound states (which are bosons with even R_D) decaying to SM

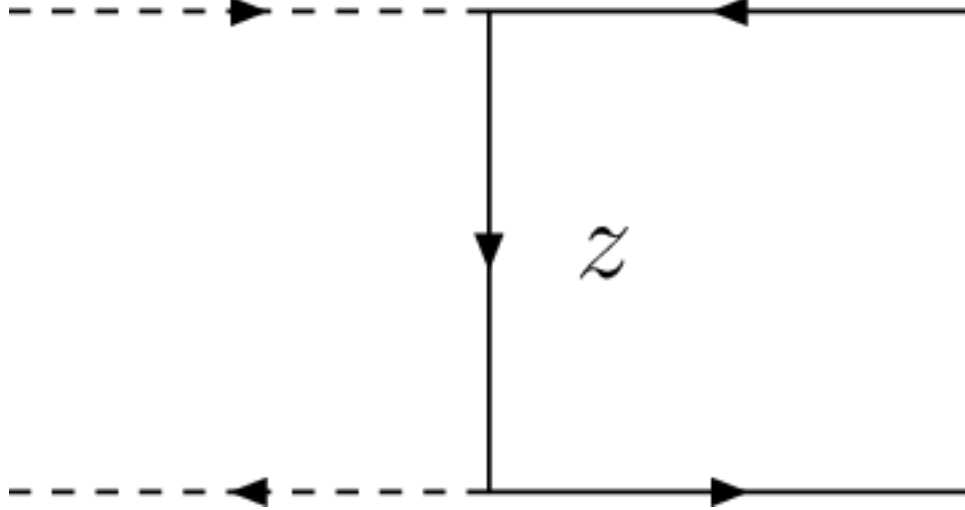


Figure 8.2: Dark scalar annihilation to hemions.

particles as described in a following section.

8.9 Leptonic Color in the Early Universe

As discussed in our earlier paper [82], the $SU(2)_l$ massless stickons (ζ) play a role in the early Universe. The important difference is that $\alpha_l(M_Z)$ is bigger here than in the Babu-Ma-Willenbrock (BMW) model [66], i.e. 0.065 versus 0.047. Hence the leptonic color confinement scale is about 0.4 MeV instead of 4 keV. At temperatures above the electroweak symmetry scale, the hemions are active and the stickons are in thermal equilibrium with the standard-model particles. Below the hemion mass scale, the stickon interacts with photons through $\zeta\zeta \rightarrow \gamma\gamma$ scattering with a cross section

$$\sigma \sim \frac{\alpha^2 \alpha_l^2 T^6}{64m^8}, \quad (8.60)$$

where m is the mass of the one light $x_R y_R$ hemion of this model. The decoupling temperature of ζ is then obtained by matching the Hubble expansion rate

$$H = \sqrt{(8\pi/3)G_N(\pi^2/30)g_*T^4} \quad (8.61)$$

to $[6\zeta(3)/\pi^2]T^3\langle\sigma v\rangle$. Hence

$$T^{14} \sim \frac{2^{12}}{3^4} \left(\frac{\pi^7}{5[\zeta(3)]^2} \right) \frac{G_N g_* m^{16}}{\alpha^4 \alpha_t^4}. \quad (8.62)$$

For $m = 100$ GeV and $g_* = 92.25$ which includes all particles with masses up to a few GeV, $T \sim 9$ GeV. Hence the contribution of stickons to the effective number of neutrinos at the time of big bang nucleosynthesis (BBN) is given by [73]

$$\Delta N_\nu = \frac{8}{7}(3) \left(\frac{10.75}{92.25} \right)^{4/3} = 0.195, \quad (8.63)$$

compared to the value 0.50 ± 0.23 from a recent analysis [74].

As the Universe further cools below a few MeV, leptonic color goes through a phase transition and stickballs are formed. However, they are not stable because they are allowed to mix with a scalar bound state of two hemions which would decay to two photons. For a stickball ω of mass m_ω , we assume this mixing to be $f_\omega m_\omega/m$, so that its decay rate is given by

$$\Gamma(\omega \rightarrow \gamma\gamma) = \frac{\alpha^2 f_\omega^2 m_\omega^5}{256\pi^3 m^4}. \quad (8.64)$$

Using $m_\omega = 1$ MeV as an example with $m = 100$ GeV as before, its lifetime is estimated to be $1.0 \times 10^7 s$ for $f_\omega = 1$. This means that it disappears long before the time of photon decoupling, so the $SU(2)_l$ sector contributes no additional relativistic degrees of freedom. Hence N_{eff} remains the same as in the SM, i.e. 3.046, coming only from neutrinos. This

agrees with the PLANCK measurement [75] of the cosmic microwave background (CMB),
i.e.

$$N_{eff} = 3.15 \pm 0.23. \quad (8.65)$$

8.10 Leptonic Color at Future e^-e^+ Colliders

Unlike quarks, all hemions are heavy. Hence the lightest bound state is likely to be at least 200 GeV. Its cross section through electroweak production at the LHC is probably too small for it to be discovered. On the other hand, in analogy to the observations of J/ψ and Υ at e^-e^+ colliders of the last century, the resonance production of the corresponding neutral vector bound states (hemionia) of these hemions is expected at a future e^-e^+ collider (ILC, CEPC, FCC-ee) with sufficient reach in total center-of-mass energy. Their decays will be distinguishable from heavy quarkonia (such as toponia) experimentally.

As discussed in Ref. [82], the formation of hemion bound states is analogous to that of QCD. Instead of one-gluon exchange, the Coulomb potential binding a hemion-antihemion pair comes from one-stickon exchange. The difference is just the change in an SU(3) color factor of 4/3 to an SU(2) color factor of 3/4. The Bohr radius is then $a_0 = [(3/8)\bar{\alpha}_l m]^{-1}$, and the effective $\bar{\alpha}_l$ is defined by

$$\bar{\alpha}_l = \alpha_l(a_0^{-1}). \quad (8.66)$$

Using $\alpha_l(M_Z) = 0.065$ with $m = 100$ GeV, we obtain $\bar{\alpha}_l = 0.087$ and $a_0^{-1} = 3.26$ GeV. Consider the lowest-energy vector bound state Ω of the lightest hemion of mass $m = 100$

GeV. In analogy to the hydrogen atom, its binding energy is given by

$$E_b = \frac{1}{4} \left(\frac{3}{4} \right)^2 \bar{\alpha}_l^2 m = 106 \text{ MeV}, \quad (8.67)$$

and its wavefunction at the origin is

$$|\psi(0)|^2 = \frac{1}{\pi a_0^3} = 11.03 \text{ GeV}^3. \quad (8.68)$$

Since Ω will appear as a narrow resonance at a future e^-e^+ collider, its observation depends on the integrated cross section over the energy range \sqrt{s} around m_Ω :

$$\int d\sqrt{s} \sigma(e^-e^+ \rightarrow \Omega \rightarrow X) = \frac{6\pi^2 \Gamma_{ee} \Gamma_X}{m_\Omega^2 \Gamma_{tot}}, \quad (8.69)$$

where Γ_{tot} is the total decay width of Ω , and Γ_{ee}, Γ_X are the respective partial widths.

Since Ω is a vector meson, it couples to both the photon and Z boson through its constituent hemions. Hence it will decay to $W^-W^+, q\bar{q}, l^-l^+$, and $\nu\bar{\nu}$. Using

$$\langle 0 | \bar{x} \gamma^\mu x | \Omega \rangle = \epsilon_\Omega^\mu \sqrt{8m_\Omega} |\psi(0)|, \quad (8.70)$$

the $\Omega \rightarrow e^-e^+$ decay rate is given by

$$\Gamma(\Omega \rightarrow \gamma, Z \rightarrow e^-e^+) = \frac{2m_\Omega^2}{3\pi} (|C_V|^2 + |C_A|^2) |\psi(0)|^2, \quad (8.71)$$

where

$$C_V = \frac{e^2(1/2)(-1)}{m_\Omega^2} + \frac{g_Z^2(-\sin^2 \theta_W/4)[(-1 + 4\sin^2 \theta_W)/4]}{m_\Omega^2 - M_Z^2}, \quad (8.72)$$

$$C_A = \frac{g_Z^2(-\sin^2 \theta_W/4)(1/4)}{m_\Omega^2 - M_Z^2}. \quad (8.73)$$

In the above, Ω is composed of the singlet hemions x_R and y_R with invariant mass term $x_{1R}y_{2R} - x_{2R}y_{1R}$. The (x_L, y_L) option, considered in the BMW model, is not available here

because they are superheavy from the breaking of $SU(3)_L$ at M_U . Here $\Gamma_{ee} = 139$ eV. Similar expressions hold for the other fermions of the SM.

For $\Omega \rightarrow W^-W^+$, the triple γW^-W^+ and ZW^-W^+ vertices have the same structure. The decay rate is calculated to be

$$\Gamma(\Omega \rightarrow \gamma, Z \rightarrow W^-W^+) = \frac{m_\Omega^2(1-r)^{3/2}}{6\pi r^2} (4 + 20r + 3r^2) C_W^2 |\psi(0)|^2, \quad (8.74)$$

where $r = 4M_W^2/m_\Omega^2$ and

$$C_W = \frac{e^2(1/2)}{m_\Omega^2} + \frac{g_Z^2(-\sin^2\theta_W/4)}{m_\Omega^2 - M_Z^2}. \quad (8.75)$$

Because of the accidental cancellation of the two terms in the above, C_W turns out to be very small. Hence $\Gamma_{WW} = 10$ eV. For $\Omega \rightarrow ZZ$, there is only the t -channel contribution, i.e.

$$\Gamma(\Omega \rightarrow ZZ) = \frac{m_\Omega^2(1-r_Z)^{5/2}}{3\pi r_Z} D_Z^2 |\psi(0)|^2, \quad (8.76)$$

where $r_Z = 4M_Z^2/m_\Omega^2$ and $D_Z = g_Z^2 \sin^4\theta_W/4(m_\Omega^2 - 2m_Z^2)$. Hence Γ_{ZZ} is negligible. The Ω decay to two stickons is forbidden by charge conjugation. Its decay to three stickons is analogous to that of quarkonium to three gluons. Whereas the latter forms a singlet which is symmetric in $SU(3)_C$, the former forms a singlet which is antisymmetric in $SU(2)_I$. However, the two amplitudes are identical because the latter is symmetrized with respect to the exchange of the three gluons and the former is antisymmetrized with respect to the exchange of the three stickons. Taking into account the different color factors of $SU(2)_I$ versus $SU(3)_C$, the decay rate of Ω to three stickons and to two stickons plus a photon are

$$\Gamma(\Omega \rightarrow \zeta\zeta\zeta) = \frac{16}{27}(\pi^2 - 9) \frac{\alpha_I^3}{m_\Omega^2} |\psi(0)|^2, \quad (8.77)$$

$$\Gamma(\Omega \rightarrow \gamma\zeta\zeta) = \frac{8}{9}(\pi^2 - 9) \frac{\alpha\alpha_I^2}{m_\Omega^2} |\psi(0)|^2. \quad (8.78)$$

Hence $\Gamma_{\zeta\zeta\zeta} = 39$ eV and $\Gamma_{\gamma\zeta\zeta} = 7$ eV. The integrated cross section for $X = \mu^-\mu^+$ is then 1.2×10^{-32} cm²-keV. For comparison, this number is 7.9×10^{-30} cm²-keV for the $\Upsilon(1S)$. At a high-luminosity e^-e^+ collider, it should be feasible to make this observation. Table 2 summarizes all the partial decay widths.

Table 8.2: Partial decay widths of the hemionium Ω .

Channel	Width
$\sum \nu\bar{\nu}$	36 eV
$e^-e^+, \mu^-\mu^+, \tau^-\tau^+$	0.4 keV
$u\bar{u}, c\bar{c}$	0.3 keV
$d\bar{d}, s\bar{s}, b\bar{b}$	0.1 keV
W^-W^+	10 eV
ZZ	< 0.1 eV
$\zeta\zeta\zeta$	39 eV
$\zeta\zeta\gamma$	7 eV
sum	0.9 keV

There are important differences between QCD and QHD (quantum hemiodynamics). In the former, because of the existence of light u and d quarks, it is easy to pop up $u\bar{u}$ and $d\bar{d}$ pairs from the QCD vacuum. Hence the production of open charm in an e^-e^+ collider is described well by the fundamental process $e^-e^+ \rightarrow c\bar{c}$. In the latter, there are no light hemions. Instead it is easy to pop up the light stickballs from the QHD vacuum. As a result, just above the threshold of making the Ω resonance, the many-body production of $\Omega +$ stickballs becomes possible. This cross section is presumably also well described by the fundamental process $e^-e^+ \rightarrow x\bar{x}$, i.e.

$$\begin{aligned} \sigma(e^-e^+ \rightarrow x\bar{x}) &= \frac{2\pi\alpha^2}{3} \sqrt{1 - \frac{4m^2}{s}} \left[\frac{(s + 2m^2)}{s^2} + \frac{x_W^2}{2(1 - x_W)^2} \frac{(s - m^2)}{(s - m_Z^2)^2} \right. \\ &\quad \left. + \frac{x_W}{(1 - x_W)} \frac{(s - m^2)}{s(s - m_Z^2)} - \frac{(1 - 4x_W)}{4(1 - x_W)} \frac{m^2}{s(s - m_Z^2)} \right], \end{aligned} \quad (8.79)$$

where $x_W = \sin^2 \theta_W$ and $s = 4E^2$ is the square of the center-of-mass energy. Using $m = 100$ GeV and $s = (250 \text{ GeV})^2$ as an example, we find this cross section to be 0.79 pb.

In QCD, there are $q\bar{q}$ bound states which are bosons, and qqq bound states which are fermions. In QHD, there are only bound-state bosons, because the confining symmetry is $SU(2)_I$. Also, unlike baryon (or quark) number in QCD, there is no such thing as hemion number in QHD, because y is effectively \bar{x} . This explains why there are no stable analog fermion in QHD such as the proton in QCD.

8.11 Conclusions

Candidates for dark matter are often introduced in an *ad hoc* manner, because it is so easy to do. There are thus numerous claimants to the title. Is there a guiding principle? One such is supersymmetry, where the superpartners of the SM particles naturally belong to a dark sector. Another possible guiding principle proposed recently is to look for a dark symmetry embedded as a gauge symmetry in a unifying extension of the SM, such as $[SU(3)]^N$. In this paper, the alternative $[SU(3)]^4$ gauge model of leptonic color and dark matter is discussed in some detail. The dark global $U(1)$ symmetry is identified as generalized $B - L$ and the dark parity is $R_D = (-1)^{3B-3L+2j}$. The dark sector contains fermions (h, x, y, n) , scalars $[(\eta^0, \eta^-), \lambda^0]$, and vector gauge bosons W_R^\pm , where h is a dark quark of charge $-1/3$, x, y are hemions of charge $\pm 1/2$, and n is a dark neutral fermion. The dark matter of the Universe is presumably a neutral scalar dominated by the singlet λ^0 .

The absence of observations of new physics at the LHC is a possible indication that

fundamental new physics may not be accessible using the strong interaction, i.e. quarks and gluons. It is then natural to think about future e^-e^+ colliders. But is there some fundamental issue of theoretical physics which may only reveal itself there? and not at hadron colliders? The notion of leptonic color is such a possible answer. Our alternative $[SU(3)]^4$ model allows for the existence of new half-charged fermions (hemions) under a confining $SU(2)_l$ leptonic color symmetry, with masses below the TeV scale. It also predicts the $SU(2)_l$ confining scale to be 0.4 MeV, so that stickball bound states of the vector gauge stickons are formed. These new particles have no QCD interactions, but hemions have electroweak couplings, so they are accessible in a future e^-e^+ collider, as described in this paper.

Chapter 9

Conclusions

In the first section, well-motivated $U(1)$ gauge extensions were applied to the Standard Model in an effort to describe a variety of observations. In Chapter 2, this symmetry served as a generalized B-L symmetry that, though heavily restricted by FCNC, was able to recreate the best-fit CKM parameters. In Chapter 3, neutrino mass and dark matter were discussed in unison via a triplet model where the doubly charged triplet scalar had an unexplored collider signature. In Chapter 4, right-handed isospin inspired a $U(1)$ extension to only right-handed fields, which permitted the generation of all light fermion masses radiatively through dark matter.

In the second section, left-right models that linked normal matter symmetries with dark matter stability were explored. In Chapter 5, a consistent, gauged $U(1)$ was constructed to replace a global symmetry and stabilize dark matter in ALRM. Chapter 6 explored a particular quartification scheme in which the low-energy particle content featured leptonic-color bound states with stable glueball-like states and associated signatures. In

Chapter 7, the symmetry breaking pattern from quartification and trinification to ALRM were studied, revealing the possible low-energy content and dark matter symmetry based on the pattern of symmetry breaking. In Chapter 8, some of these ideas were combined to find a consistent model of $SU(3)_4$ unification that featured ALRM as a low-energy subgroup as well as an emergent symmetry for dark matter.

Bibliography

- [1] R. E. Marshak and R. N. Mohapatra, Phys. Lett. **91B**, 222 (1980).
- [2] X.-G. He, G. C. Joshi, H. Lew, and R. R. Volkas, Phys. Rev. **D43**, 22 (1991); **D44**, 2118 (1991).
- [3] E. Ma, D. P. Roy, and S. Roy, Phys. Lett. **B525**, 101 (2002).
- [4] W. Altmannshofer, S. Gori, M. Pospelov, and I. Yavin, Phys. Rev. **D89**, 095033 (2014).
- [5] J. Heeck, M. Holthausen, W. Rodejohann, and Y. Shimizu, Nucl. Phys. **B896**, 281 (2015).
- [6] E. Ma, Phys. Lett. **B433**, 74 (1998).
- [7] E. Ma and U. Sarkar, Phys. Lett. **B439**, 95 (1998).
- [8] E. Ma and D. P. Roy, Phys. Rev. **D58**, 095005 (1998).
- [9] X.-J. Bi, X.-G. He, E. Ma, and J. Zhang, Phys. Rev. **D81**, 063522 (2010).
- [10] H.-S. Lee and E. Ma, Phys. Lett. **B688**, 319 (2010).
- [11] J.-Y. Liu, Y. Tang, and Y.-L. Wu, J. Phys. **G39**, 055003 (2012).
- [12] A. Crivellin, G. D'Ambrosio, and J. Heeck, Phys. Rev. **D91**, 075006 (2015).
- [13] P. Fileviez Perez and M. Wise, Phys. Rev. **D82**, 011901 (2010); Erratum-ibid. **D82**, 079901 (2010).
- [14] C. Patrignani *et al.* (Particle Data Group), Chin. Phys. **C40**, 100001 (2016).
- [15] G. Aad *et al.*, (ATLAS Collaboration), Phys. Rev. **D90**, 052005 (2014).
- [16] S. Khachatryan *et al.*, (CMS Collaboration), JHEP **1504**, 025 (2015).
- [17] M. Antonelli *et al.*, Phys. Rept. **494**, 197 (2010).
- [18] E. Ma and B. Melic, Phys. Lett. **B725**, 402 (2013).

- [19] J. Liao, D. Marfatia, and K. Whisnant, JHEP **1409**, 013 (2014).
- [20] T. Hurth, F. Mahmoudi, and S. Neshatpour, Nucl. Phys. **B909**, 737 (2016).
- [21] S. Weinberg, Phys. Rev. Lett. **43**, 1566 (1979).
- [22] E. Ma, Phys. Rev. Lett. **81**, 1171 (1998).
- [23] E. Ma, Phys. Rev. **D73**, 077301 (2006).
- [24] E. Ma and D. Suematsu, Mod. Phys. Lett. **A24**, 583 (2009).
- [25] E. Ma, Phys. Rev. Lett. **115**, 011801 (2015).
- [26] Particle Data Group, K. A. Olive *et al.*, Chin. Phys. **C38**, 090001 (2014).
- [27] ATLAS Collaboration, G. Aad *et al.*, JHEP **1503**, 041 (2015).
- [28] S. Kanemura, M. Kikuchi, K. Yagyu, and H. Yokoya, Phys. Rev. **D90**, 115018 (2014).
- [29] S. Kanemura, M. Kikuchi, K. Yagyu, and H. Yokoya, Prog. Theor. Exp. Phys. (**2015**) 051B02.
- [30] CMS Collaboration, V. Khachatryan *et al.*, Eur. Phys. J. **C74**, 3036 (2014).
- [31] CMS Collaboration, S. Chatrchyan *et al.*, Phys. Rev. **D90**, 032006 (2014).
- [32] ATLAS Collaboration, G. Aad *et al.*, Phys. Rev. **D90**, 052001 (2014).
- [33] Alloul, Adam *et al.*, Comput.Phys.Commun. **185**, 2250 (2014).
- [34] J. Alwall *et al.*, J. High Energy Phys. **1106**, 128 (2011).
- [35] B. Dumont, B. Fuks, S. Kraml *et al.*, Eur.Phys.J. **C75** (2015) 2,56
- [36] L. Feng, S. Profumo, and L. Ubaldi, JHEP **1503**, 045 (2015).
- [37] G. Steigman, B. Dasgupta, and J. F. Beacom, Phys. Rev. **D86**, 023506 (2012).
- [38] D. N. Spergel and P. J. Steinhardt, Phys. Rev. Lett. **84**, 3760 (2000).
- [39] J. McDonald, Phys. Rev. Lett. **88**, 091304 (2002).
- [40] M. Markevitch *et al.*, Astrophys. J. **606**, 819 (2004).
- [41] C. Kouvaris, Phys. Rev. Lett. **108**, 191301 (2012).
- [42] M. Kaplinghat, T. Linden, and H.-B. Yu, Phys. Rev. Lett. **114**, 211303 (2015).
- [43] For a recent brief review, see for example S. Tulin, AIP Conf. Proc. **1604**, 121 (2014).
- [44] ATLAS Collaboration, ATLAS-CONF-2015-081.
- [45] E. Ma, Phys. Rev. Lett. **112**, 091801 (2014).

- [46] G. Aad *et al.* (ATLAS Collaboration), Phys. Rev. **D90**, 052005 (2014).
- [47] S. Khachatryan *et al.* (CMS Collaboration), JHEP **1504**, 025 (2015).
- [48] J. Ellis, S. A. R. Ellis, J. Quevillon, V. Sanz, and T. You, arXiv:1512.05327 [hep-ph].
- [49] Y. Hamada, H. Kawai, K. Kawana, and K. Tsumura, arXiv:1602.04170 [hep-ph].
- [50] N. G. Deshpande and E. Ma, Phys. Rev. **D18**, 2574 (1978).
- [51] R. Barbieri, L. J. Hall, and V. S. Rychkov, Phys. Rev. **D74**, 015007 (2006).
- [52] A. Arhrib, Y.-L. S. Tsai, Q. Yuan, and T.-C. Yuan, JCAP **1406**, 030 (2014).
- [53] A. Ilnicka, M. Krawczyk, and T. Robens, Phys. Rev. **D93**, 055026 (2016).
- [54] M. A. Diaz, B. Koch, and S. Urrutia-Quiroga, arXiv:1511.04429 [hep-ph].
- [55] S. Khalil, H.-S. Lee, and E. Ma, Phys. Rev. **D79**, 041701(R) (2009).
- [56] S. Khalil, H.-S. Lee, and E. Ma, Phys. Rev. **D81**, 051702(R) (2010).
- [57] S. Bhattacharya, E. Ma, and D. Wegman, Eur. Phys. J. **C74**, 2902 (2014).
- [58] Q.-H. Cao, E. Ma, J. Wudka, and C.-P. Yuan, arXiv:0711.3881 [hep-ph].
- [59] C. Kownacki and E. Ma, Phys. Lett. **B760**, 59 (2016).
- [60] S. Khachatryan *et al.* (CMS Collaboration), JHEP **1504**, 025 (2015).
- [61] G. Steigman, B. Dasgupta, and J. F. Beacom, Phys. Rev. **D86**, 023506 (2012).
- [62] D. S. Akerib *et al.* (LUX Collaboration), Phys. Rev. Lett. **118**, 021303 (2017).
- [63] G. Belanger, F. Boudjema, A. Pukhov, and A. Semenov, Comput. Phys. Commun. **180**, 747 (2009).
- [64] H. Ohki *et al.* (JLQCD Collaboration), Phys. Rev. **D78**, 054502 (2008).
- [65] The CMS Collaboration, CMS-PAS-SUS-16-036.
- [66] K. S. Babu, E. Ma, and S. Willenbrock, Phys. Rev. **D69**, 051301(R) (2004).
- [67] R. Foot and H. Lew, Phys. Rev. **D41**, 3502 (1990).
- [68] R. Foot, H. Lew, and R. R. Volkas, Phys. Rev. **D44**, 1531 (1991).
- [69] G. C. Joshi and R. R. Volkas, Phys. Rev. **D45**, 1711 (1992).
- [70] A. Soni and Y. Zhang, Phys. Rev. **D93**, 115025 (2016).
- [71] R. Foot, H. Lew, and R. R. Volkas, Phys. Rev. **D42**, 1851 (1991).
- [72] J. D. Clarke, R. Foot, and R. R. Volkas, Phys. Rev. **D85**, 074012 (2012).

- [73] K. S. Jeong and F. Takahashi, Phys. Lett. **B725**, 134 (2013).
- [74] K. M. Nollett and G. Steigman, Phys. Rev. **D91**, 083505 (2015).
- [75] P. A. R. Ade *et al.* (PLANCK Collaboration), Astron.Astrophys. **594**, A13 (2016).
- [76] E. D. Carlson, M. E. Machacek, and L. J. Hall, Astrophys. J. **398**, 43 (1992).
- [77] J. Baur, N. Palanque-Delabrouille, C. Yeche, C. Magneville, and M. Viel, JCAP **1608**, 012 (2016).
- [78] T. R. Slatyer and C.-L. Wu, arXiv:1610.06933v2 [astro-ph.CO].
- [79] Y. Mambrini, S. Profumo, and F. S. Queiroz, Phys. Lett. **B760**, 807 (2016).
- [80] A. De Rujula, H. Georgi, and S. L. Glashow, in *Fifth Workshop on Grand Unification*, edited by K. Kang, H. Fried, and P. Frampton (World Scientific, Singapore, 1984), p. 88.
- [81] K. S. Babu, X.-G. He, and S. Pakvasa, Phys. Rev. **D33**, 763 (1986).
- [82] C. Kownacki, E. Ma, N. Pollard, O. Popov, and M. Zakeri, Phys. Lett. **B769**, 267 (2017).
- [83] E. Ma, Phys. Rev. **D36**, 274 (1987).
- [84] K. S. Babu, X.-G. He, and E. Ma, Phys. Rev. **D36**, 878 (1987).
- [85] C. Kownacki, E. Ma, N. Pollard, O. Popov, and M. Zakeri, arXiv:1706.06501 [hep-ph].
- [86] D. London and J. L. Rosner, Phys. Rev. **D34**, 1530 (1986).
- [87] J. L. Diaz-Cruz and E. Ma, Phys. Lett. **B695**, 264 (2011).
- [88] S. Bhattacharya, J. L. Diaz-Cruz, E. Ma, and D. Wegman, Phys. Rev. **D85**, 055008 (2012).
- [89] S. Fraser, E. Ma, and M. Zakeri, Int. J. Mod. Phys. **A30**, 1550018 (2015).
- [90] S. M. Barr, Phys. Rev. **D85**, 013001 (2012).
- [91] E. Ma, Phys. Rev. **D88**, 117702 (2013).
- [92] E. Ma, M. Mondragon, and G. Zoupanos, JHEP **0412**, 026 (2004).
- [93] C. Kownacki, E. Ma, N. Pollard, O. Popov, and M. Zakeri, Phys. Lett. **B777**, 121 (2018).
- [94] E. Ma, Mod. Phys. Lett. **A20**, 1953 (2005).
- [95] E. Ma, Phys. Lett. **B593**, 198 (2004).

- [96] P. V. Dong, T. Huong, F. Queiroz, J. W. F. Valle, and C. A. Vaquera-Araujo, arXiv:1710.06951.
- [97] E. Ma, arXiv:1712.08994 [hep-ph].
- [98] M. Aaboud *et al.* (ATLAS Collaboration), JHEP **1710**, 182 (2017).
- [99] E. Aprile *et al.* (XENON Collaboration), Phys. Rev. Lett. **119**, 181301 (2017).